UNIVERSITI TEKNOLOGI MARA

PHYSICOCHEMICAL AND BIOCOMPATIBILITY CHARACTERISATION OF LYOPHILISED PLATELET-RICH FIBRIN FOR BONE TISSUE ENGINEERING

WAN NUR IRDINA BINTI RUSMAN

MSc

April 2026

UNIVERSITI TEKNOLOGI MARA

PHYSICOCHEMICAL AND BIOCOMPATIBILITY CHARACTERISATION OF LYOPHILISED PLATELET-RICH FIBRIN FOR BONE TISSUE ENGINEERING

WAN NUR IRDINA BINTI RUSMAN

Thesis submitted in fulfilment
of the requirements for the degree of
Master of Dental Science

Faculty of Dentistry

April 2026

CONFIRMATION BY PANEL OF EXAMINERS

I certify that a Panel of Examiners has met on 27th February 2026 to conduct the final examination of Wan Nur Irdina Binti Rusman on her Masters of Dental Science thesis entitled "Physicochemical and Biocompatibility Characterisation of Lyophilised Platelet-Rich Fibrin For Craniofacial Regeneration" in accordance with Universiti Teknologi MARA Act 1976 (Akta 173). The Panel of Examiner recommends that the student be awarded the relevant degree. The Panel of Examiners was as follows:

Indah Mohd Amin, PhD
Associate Professor
Faculty of Dentistry
Universiti Teknologi MARA
(Chairman)

Norhayati Liaqat Ali Khan, PhD
Senior Lecturer
Faculty of Dentistry
Universiti Teknologi MARA
(Internal Examiner)

Ahmad Dzulfikar Samsudin, PhD
Deputy Dean of Student Affairs & Alumni
Faculty of Dentistry
Universiti Sains Islam Malaysia
(External Examiner)

PROFESSOR DR HJH ZURAEDA IBRAHIM
Dean
Institute of Postgraduates Studies
Universiti Teknologi MARA

Date: April 2026

AUTHOR'S DECLARATION

I declare that the work in this thesis was carried out in accordance with the regulations of Universiti Teknologi MARA. It is original and is the results of my own work, unless otherwise indicated or acknowledged as referenced work. This thesis has not been submitted to any other academic institution or non-academic institution for any degree or qualification.

I, hereby, acknowledge that I have been supplied with the Academic Rules and Regulations for Post Graduate, Universiti Teknologi MARA, regulating the conduct of my study and research.

Name of Student	Wan Nur Irdina
Student ID. No.	2024597103
Programme	Master of Dental Science (DS750)
Faculty	Faculty of Dentistry
Thesis Title	Physicochemical and Biocompatibility Characterisation of Lyophilised Platelet-Rich Fibrin For Bone Tissue Engineering

Signature of Student .....

Date April 2026

ABSTRACT

The preservation and functional stability of platelet-rich fibrin (PRF) are critical for its translational use in craniofacial bone tissue engineering. Preservation methods for frozen PRF (FPRF) remain controversial; freeze-thaw cycles can compromise fibrin structure and diminish bioactivity. Lyophilisation presents an alternative strategy that may enhance storage stability, handling and clinical shelf life while maintaining microarchitecture and biological efficacy. This study aimed to evaluate and compare the physicochemical and biological properties of LyPRF and FPRF. PRF samples were prepared from venous blood obtained from healthy donors and processed into LyPRF and FPRF. Comprehensive physicochemical characterisation was conducted using scanning electron microscopy (SEM), energy-dispersive X-ray spectroscopy (EDX), Fourier-transform infrared spectroscopy (FTIR), and X-ray diffraction (XRD). The kinetic release pattern of Growth factor (PDGF-AB, PDGF-BB, and TGF-β1) were quantified via enzyme-linked immunosorbent assay (ELISA), while biocompatibility was assessed using the MTT assay on human gingival fibroblasts (HGFs). SEM analysis demonstrated a more porous and interconnected fibrin network in LyPRF compared to FPRF. EDX analysis revealed higher mineral retention in LyPRF, and both FTIR and XRD confirmed the preservation of fibrin-associated protein structures in both groups. Notably, LyPRF exhibited sustained release of growth factors and enhanced fibroblast metabolic activity over 72 hours relative to FPRF. The aforementioned results demonstrates LyPRF exceptional physicochemical and biocompatibility characteristics, establishing it as a promising biomaterial for craniofacial bone tissue engineering.

ACKNOWLEDGEMENT

First and foremost, I would like to express my deepest gratitude to Allah Almighty for His blessings, guidance, and strength throughout the course of my Master of Dental Science (MDSCs) journey. Without His grace and mercy, the successful completion of this thesis would not have been possible.

I wish to extend my heartfelt appreciation to my main supervisor, Dr. Nurul Aida Ngah, for her invaluable guidance, encouragement, and continuous support throughout this research. Her patience, insightful feedback, and dedication have been instrumental in shaping the direction and quality of this work. My sincere thanks also go to my co-supervisors, Prof. Dr. Siti Noor Fazliah Mohd Noor, Prof. Dr. Wong Tin Wui, and Dr. Nurul 'Izzah Mohd Sarmin, for their expert advice, constructive suggestions, and generous assistance that have greatly contributed to the completion of this study.

I am profoundly grateful to my family, colleagues, and friends for their unwavering support, motivation, and understanding throughout this journey. Their encouragement during moments of difficulty has been a source of strength and perseverance.

Finally, this thesis is lovingly dedicated to my beloved mother and stepfather, whose love, prayers, and sacrifices have been my greatest inspiration, and to the loving memory of my late father, whose vision and determination to educate me continue to guide my path. This achievement is a tribute to all of you. Alhamdulillah.

TABLE OF CONTENTS

LIST OF TABLES

LIST OF FIGURES

LIST OF SYMBOLS

Symbols

cm	Reciprocal Centimetres; measurement for wavenumber
co_2	Carbon Dioxid
H_20	Dihydrogen Ox
%	Percentage
º	Degree
°c	Degree Celsius
±	Plus or Minus
Å	Angstrom; unit of length
cm	Centimetre
9	Relative Centri
h	Hour
k	Thousand; 10^3
kV	Kilovolt
rag	Milligram
rain	Minute
rah	Millilitre
nm	Nanometre
	Probability; p -value

4+/"6	Picograms Per Millilitre
74"	Revolutions Per Minute
89	Weight
:	Theta; represent an angle
;"	Micrometre

LIST OF ABBREVIATIONS

Abbreviations

3D	Three-Dimensional
ABG	Alveolar Bone Grafting
ASA	American Society of Anaesthesiologists
BMPs	Bone Morphogenic Proteins
BTE	Bone Tissue Engineering
CLP	Cleft Lip and Palate
DMEM	Dulbecco's Modified Eagle Medium
DMSO	Dimethyl Sulfoxide
DNA	Deoxyribonucleic Acid
ECM	Extracellular Matrix
EDX	Energy Dispersive X-Ray Spectroscopy
ELISA	Enzyme-Linked Immunosorbent Assay
FBS	Foetal Bovine Serum
FESEM	Field Emission Scanning Electron Microscopy
FGFR2	Fibroblast Growth Factor Receptor 2
FPRF	Frozen Platelet-Rich Fibrin
FTIR	Fourier Transform Infrared Spectroscopy
HGF	Human Gingival Fibroblasts
IL-10	Interleukin-10

IL-6	Interleukin-6
LyPRF	Lyophilised Platelet-Rich Fibrin
MSCs	Mesenchymal Stem Cells
MTT	3-(4,5-Dimethylthiazol-2-yl)-2-5-Diphenyltetrazolium Bromide Assay
NSAIDs	Non-Steroidal Anti-Inflammatory Drugs
PCs	Platelet Concentrates
PDGF	Platelet-Derived Growth Factor
PDGF-AB	Platelet-Derived Growth Factor-AB
PDGF-BB	Platelet-Derived Growth Factor-BB
PRF	Platelet-Rich Fibrin
PRP	Platelet-Rich Plasma
RBC	Red Blood Cell
TGF- β	Transforming Growth Factor-β
TGF-β1	Transforming Growth Factor-β1
TNF-a	Tumour Necrosis Factor-Alpha
TWIST1	Twist Family bHLH Transcription Factor 1
VEGF	Vascular Endothelial Growth Factor
XRD	X-Ray Diffraction

CHAPTER 1
INTRODUCTION

1.1 Research Background

Craniofacial malformations encompass a broad spectrum of congenital or acquired abnormalities that affect the structure and function of facial bones. Genetic mutations, abnormalities during embryonic development, or external causes, such as trauma, inflammation, and illnesses, can cause these deformities. The most common congenital malformations are cleft lip and palate (CLP), craniosynostosis, and micrognathia that can significantly affect the patient's appearance and overall quality of life (Heydari et al., 2024). Craniofacial deformities present a significant clinical challenge encompassing a range of congenital and acquired conditions impacting both functional and aesthetic aspects of a patient's life. The prevalence of these deformities is rather high, affecting around 1 in 600–800 live births for conditions such as CLP and 1 in 2000–2500 live births for craniosynostosis. Current treatment approaches, including surgical correction such as alveolar bone grafting (ABG), often face limitations and challenges regarding effectiveness, patient-specific customisation, long-term outcomes, and donor-site morbidity (Kim & Kim, 2024; Vyas et al., 2020). Therefore, advances in genetic research, regenerative strategies, and biomaterials that can enhance tissue repair and reconstruction are essential for improving treatments of craniofacial malformations.

The aetiology of these conditions involves complex interactions among genetic and environmental factors. Mutations and variations of genes involved in craniofacial development have been implicated in the emergence of these deformities. The genes are integral to cellular processes, including cell proliferation, attachment, and differentiation. Whilst environmental risk factors play a critical role in modulating genetic susceptibility. Therefore, maternal smoking, alcohol consumption, use of certain drugs or medications, and nutritional deficiencies can disrupt normal craniofacial development and lead to craniofacial deformities (Heydari et al., 2024; Stanbouly et al., 2022). Additionally, epigenetic modifications involving changes in gene expression without altering DNA sequences play a significant role in both genetic

predispositions and environmental exposure. Therefore, advances in genetic research, surgical treatments, and regenerative medicine are essential for improving early detection and providing alternative treatments for craniofacial deformities.

A multidisciplinary team approach to treating craniofacial malformations aims to address both the functional impairments and aesthetic concerns associated with the condition. Surgical intervention is the primary treatment for craniofacial deformities, intending to restore normal body and soft tissue anatomy and function. Autologous ABG is the gold standard treatment for craniofacial malformations, particularly in the context of CLP, by targeting the restoration of alveolar bone continuity in the maxillary arch. For ABG, graft material is typically derived from the patient's bone from the iliac crest and transplanted into the alveolar cleft to stabilise the maxillary segments and provide support for subsequent orthodontic treatments. Additionally, successful alveolar cleft reconstruction has a significant impact on the patient's speech and mastication, alongside improving their facial aesthetics (Paradowska-Stolarz et al., 2022). Despite its widespread use and success, ABG presents several disadvantages and challenges. One significant drawback is the donor site morbidity associated with autologous bone grafts. It can lead to postoperative pain, gait abnormalities, intestinal herniation, infection, nerve damage, and growth retardation (Tonk et al., 2022).

Bone tissue engineering (BTE) offers an alternative treatment for craniofacial deformities, addressing the limitations of traditional approaches such as ABG incorporating autografts or allografts. BTE aims to overcome these issues by utilising a combination of biomaterials, stem cells, and growth factors to promote bone regeneration and integration. However, current biomaterials used for BTE, such as platelet-rich plasma (PRP) and platelet-rich fibrin (PRF), lack adequate biocompatibility and osteoinductivity and are constrained by short shelf life, making them less usable in long-term clinical settings (Arshad et al., 2021). These limitations highlight the necessity for innovative approaches, including enhanced biomaterials with a more consistent fabrication technique and methods to extend their shelf life. Addressing these challenges is essential for the advancement of BTE, especially for clinical applications.

Alternative treatments are being explored to address the limitations and challenges of traditional surgical interventions for craniofacial deformities such as ABG. One promising approach is the use of tissue engineering techniques, including the application of stem cells, growth factors, and scaffolds to promote bone tissue

regeneration. For instance, tissue engineering combines the use of biomaterials, cells, and growth factors to regenerate and repair damaged or missing tissues (Alonzo et al., 2021). The development of advanced biomaterials, such as scaffolds that offer structural support for the formation of tissues, and the incorporation of mesenchymal stem cells (MSCs) into the scaffolds enhances the process of tissue regeneration and integration. These scaffolds can be engineered to mimic the extracellular matrix of natural tissue, thereby facilitating cellular adhesion, proliferation, and differentiation (Almouemen et al., 2019; Bhushan et al., 2022). Despite this, several notable disadvantages, including the limited bioactivity of the synthetic scaffolds, hinder the clinical application of scaffolds for tissue engineering, affecting cell attachments, proliferation, and differentiation.

Therefore, to address the disadvantages of current scaffolds, growth factors are integrated to further enhance osteogenesis and angiogenesis, crucial for successful bone tissue repair. Using these new developments in tissue engineering could lead to more effective and less invasive treatments, lowering the need for autologous grafts and avoiding donor site morbidity (Bhushan et al., 2022; Grzelak et al., 2024; Ren et al., 2023). Platelet-rich fibrin (PRF), an autologous biomaterial derived from the patient's blood through a centrifugation protocol, is one of the most promising alternative biomaterials for bone tissue engineering. PRF is a fibrin matrix rich in platelets, leukocytes, and various growth factors that are vital in promoting cellular processes such as proliferation, differentiation, and angiogenesis (Jia et al., 2024; Kim & Kim, 2024). Unlike earlier platelet concentrates, PRF does not require anticoagulants or thrombin, preserving the natural healing properties of blood constituents. The fibrin network within PRF aids in cell migration and attachment, thereby facilitating the formation of new bone tissue. Additionally, its ability to release growth factors in a sustained manner ensures prolonged stimulation of the healing process, enhancing the integration and functionality of the engineered tissue (Park et al., 2024). PRF is predominantly used as a same-day treatment due to its inherent biological and structural properties. However, its restricted preservation capacities hinder its wider use in therapeutic applications.

To address this issue, PRF is lyophilised to enhance its stability, extend its shelf life, and facilitate its use in tissue engineering applications. This process effectively removes moisture from the PRF matrix through sublimation, which minimises enzymatic degradation and microbial contamination, thereby maintaining the

viability and functionality of the embedded growth factors (Li et al., 2014). The lyophilised PRF (LyPRF) retains its bioactivity, enabling a controlled release of growth factors upon rehydration, which is critical for promoting cell proliferation, differentiation, and tissue regeneration. Moreover, the dry, stable form of LyPRF is more manageable for clinical applications, as it can be easily stored at room temperature, increasing its shelf life and prolonging its usability. Furthermore, lyophilised PRF can be reconstituted with various carriers or combined with other biomaterials to create composite scaffolds, enhancing its versatility in tissue engineering (Andia et al., 2020; Dashore et al., 2021).

Therefore, this research aims to fabricate and characterise the physicochemical and biological properties of LyPRF. This study will assess the physicochemical and biocompatibility of LyPRF as a potential biomaterial for tissue engineering in clinical settings. Ultimately, this study seeks to contribute to the ongoing development of tissue engineering and improve patient quality of life by preventing invasive surgical procedures.

1.2 Problem Statement

PRF has emerged as a promising autologous biomaterial in BTE due to its biocompatibility, fibrin-based architecture, and intrinsic reservoir of bioactive growth factors that support angiogenesis, osteogenesis, and tissue regeneration. Despite these advantages, the clinical translation and widespread application of PRF remain constrained by its limited preservation stability and short shelf life. Conventional PRF must be prepared and applied immediately following centrifugation, as prolonged storage leads to rapid degradation of its fibrin network and a concomitant loss of biological activity. This requirement for immediate use significantly limits its practicality, reproducibility, and scalability in clinical settings, particularly for complex regenerative procedures that require pre-prepared, transportable, or storable biomaterials.

The inability to preserve PRF for extended periods restricts its versatility in clinical workflows and precludes its integration into tissue banking systems or off-the-shelf regenerative strategies. Consequently, there is a growing need for preservation approaches that can maintain the structural integrity and biological functionality of PRF

while improving its storage stability and handling characteristics. Lyophilisation, or freeze-drying, has been proposed as a promising preservation technique to address these limitations, as it removes water under low temperature and pressure conditions, thereby minimising structural and biochemical degradation. LyPRF has the potential to offer extended shelf life, ease of storage at ambient or controlled temperatures, and improved handling properties, while enabling rehydration prior to clinical application.

Furthermore, LyPRF may function as a stable reservoir for the sustained release of growth factors, a critical feature for promoting long-term tissue regeneration in BTE applications. The ability to preserve PRF in a dry, stable form also opens new opportunities for its use in tissue banking and regenerative medicine platforms, enhancing its clinical accessibility and translational potential. However, despite these anticipated advantages, the physicochemical and biological properties of LyPRF have not been comprehensively characterised. Concerns remain regarding whether the lyophilisation process alters the structural composition, chemical integrity, or biocompatibility of PRF, which are essential determinants of its regenerative efficacy.

Therefore, there is a clear knowledge gap in understanding the impact of lyophilisation on PRF and its suitability as a biomaterial for clinical bone tissue engineering applications. Addressing this gap is essential to validate LyPRF as a stable, safe, and effective alternative to conventional PRF. Accordingly, this study aims to fabricate and systematically characterise lyophilised platelet-rich fibrin by evaluating its physicochemical properties and biocompatibility, thereby assessing its potential as a preserved autologous biomaterial for bone tissue engineering and regenerative medicine.

1.3 Research Questions

a) What are the physicochemical characteristics of LyPRF in comparison with FPRF, as determined by X-ray diffraction (XRD), field emission scanning electron microscopy (FESEM), energy-dispersive X-ray spectroscopy (EDX), and Fourier-transform infrared spectroscopy (FTIR)?
b) What are the differences in the kinetic release patterns of platelet-derived growth factor AB (PDGF-AB), platelet-derived growth factor BB (PDGF-BB), and transforming growth factor-β1 (TGF-β1) between LyPRF and FPRF, as analysed using enzyme-linked immunosorbent assay (ELISA)?

c) Is lyophilised platelet-rich fibrin biocompatible with human gingival fibroblast (HGF), as evaluated through cytotoxicity testing using MTT assay?

1.4 Research Objectives

a) To characterise the physical and chemical properties of lyophilised platelet-rich fibrin, and frozen platelet-rich fibrin using x-ray diffraction (XRD), field emission scanning electron microscopy (FESEM), energy dispersive x-ray spectroscopy (EDX), and Fourier-transform infrared spectroscopy (FTIR).
b) To analyse and compare the kinetic release pattern of platelet-derived growth factor AB (PDGF-AB), platelet-derived growth factor BB (PDGF-BB), and transforming growth factor-β1 (TGF-β1) from lyophilised and frozen platelet-rich fibrin using enzyme-linked immunosorbent assay (ELISA).
c) To evaluate the biocompatibility of lyophilised platelet-rich fibrin, and frozen platelet-rich fibrin by conducting cytotoxicity testing (MTT Assay) using human gingival fibroblast (HGF) cell.

1.5 Significance of Study

The characterisation of lyophilised platelet-rich fibrin (LyPRF) aids in advancing its application in regenerative medicine, particularly in craniofacial and bone tissue engineering. Understanding its physical and chemical properties provides vital understanding into its structural stability, and bioactivity, which directly influence its therapeutic efficacy. The results of this research will contribute to the standardisation of PRF-based biomaterials, providing a scientific foundation for its use in tissue regeneration, and wound healing, in addition to facilitating its reproducibility in regenerative therapies.

1.6 Research Hypothesis

The hypothesis of this study is that lyophilisation enhances the physicochemical stability, biological reliability, and bioactivity of platelet-rich fibrin (PRF), positioning lyophilised PRF (LyPRF) as a superior alternative to frozen PRF (FPRF) for bone tissue engineering applications.

Specific hypothesis:

a) The physicochemical characteristics and chemical integrity of LyPRF, including its microstructural morphology and crystallinity shows significant difference in comparison to FPRF, as characterised by XRD, FESEM, EDX, and FTIR analyses.
b) LyPRF demonstrates increased sustained kinetic release pattern of key growth factors (PDGF-AB, PDGF-BB, and TGF-β1) compared to FPRF, indicating improved preservation of bioactive components.
c) LyPRF is expected to exhibit biocompatibility potential with HGF cells compared to FPRF, as assessed by the MTT assay, supporting its safety and suitability for bone tissue engineering and regenerative applications.

CHAPTER 2
LITERATURE REVIEW

A part of this chapter has been published online as an original research article in

Tissue Engineering Part B titled, “PHYSICOCHEMICAL AND BIOLOGICAL PROPERTIES OF LYOPHILISED PLATELET RICH FIBRIN: A SYSTEMATIC REVIEW”

A part of this chapter has been submitted online as an original research article in

Sains Malaysiana titled “STANDARDISING LYOPHILISED PLATELET-RICH FIBRIN PROTOCOLS FOR BONE TISSUE ENGINEERING: A SYSTEMATIC REVIEW”.

2.1 Craniofacial Deformities

2.1.1 Prevalence

Bone is a dynamic living tissue distinguished by its complex, highly vascularised hierarchical structure. This structure consists of a complex matrix of collagen fibres and mineral deposits, primarily hydroxyapatites (HA). Craniofacial deformities are among the most prevalent skeletal abnormalities that refers to a broad spectrum of congenital and acquired malformations that affect the structure and function of the skull and face. The degree and nature of these diseases can vary, ranging from minor abnormalities that may go unnoticed to serious deformities that can have a substantial impact on an individual's health and quality of life. These abnormalities are relatively common, with an approximate occurrence rate of 1 in 600–800 live births for diseases like CLP and 1 in 2000–2500 live births (Vyas *et al.*, 2020). The prevalence of these deformities can vary significantly across different populations due to genetic, environmental, and epigenetic factors. Advances in genetic screening and diagnostic imaging have improved early detection and classification rates of these malformations. Therefore, the development of multidisciplinary approaches involving surgery, orthodontics, speech therapy, and regenerative treatments has enhanced the management and outcomes for affected individuals (Heydari *et al.*, 2024).

2.1.2 Aetiology

The aetiology of craniofacial malformations is multifaceted and involves an array of genetic, environmental, and epigenetic factors such as congenital anomalies, trauma, oncological surgery, degenerative conditions, infections, tumour excision, or accidents (Dang *et al.*, 2018). One of the significant causes of this deformity is the mutations and variation of genes linked to the development of craniofacial features, including cells involved in cellular processes such as cell proliferation, growth, and differentiation. For instance, research has proven that the underlying causes of craniofacial deformities, such as Apert's and Crouzon's syndromes, stem from mutations in key regulatory genes, notably FGFR2 and TWIST1 (Vyas *et al.*, 2020). Environmental factors are also significant contributors to the development of craniofacial abnormalities. Maternal behaviours and health conditions, including smoking, alcohol use, utilisation of certain medications, and inadequate nutrition, are the primary influences on foetal craniofacial development. Therefore, the exertion of teratogenic effects and nutritional deficiencies disrupts normal craniofacial development, leading to conditions such as CLP (Heydari *et al.*, 2024). Additionally, epigenetic modifications, characterised by the alterations in gene expression without altering the DNA sequence, contribute another layer of complexity to the aetiology of craniofacial malformations. Epigenetic factors known as transgenerational epigenetic inheritance significantly influence the development process of craniofacial deformities. Therefore, understanding the etiological mechanisms underlying craniofacial malformations is crucial for the development of prevention strategies, early detection, and precise treatments to effectively manage these deformities (Stanbouly *et al.*, 2022).

2.1.3 Treatments

The management of craniofacial malformations requires a multidisciplinary approach that addresses both the functional impairments and aesthetic concerns associated with these deformities. Current treatment strategies integrate advanced surgical techniques, orthodontic interventions, and emerging regenerative therapies to restore form and function. Among these, surgical intervention remains the primary modality, with procedures tailored to the specific type and severity of the deformity.

Bone augmentation is frequently employed, utilising various biomaterials to facilitate osteointegration and restore structural integrity (Figure 2.1).

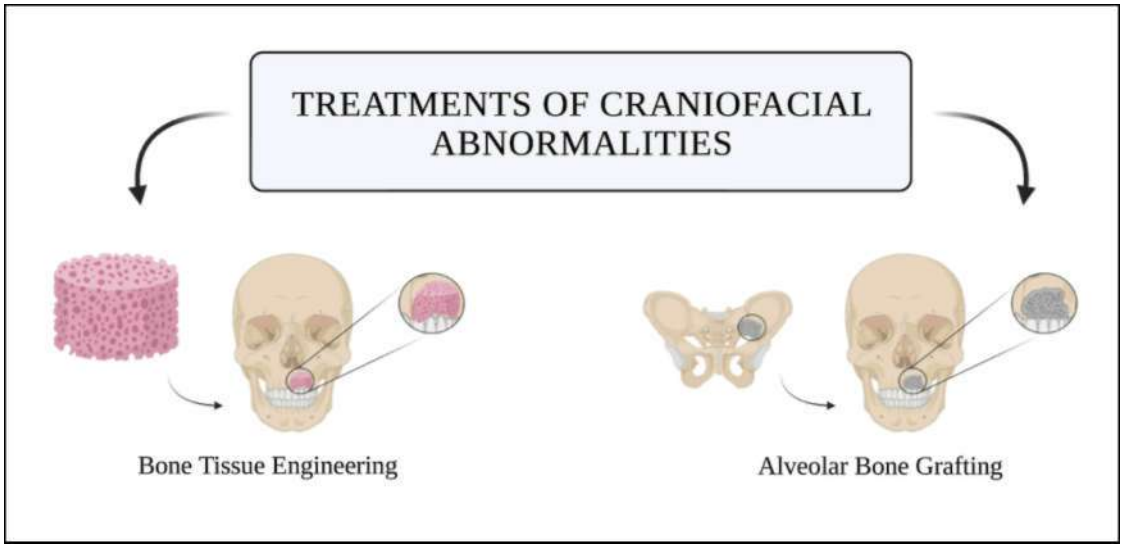

Figure 2.1 Overview of Common Treatment Approaches for Craniofacial Abnormalities.

One of the most widely practiced and effective surgical procedures is alveolar bone grafting (ABG), predominantly applied in the management of cleft lip and palate (CLP). The primary objective of ABG is to stabilise the maxillary segments and provide adequate support for subsequent orthodontic and implant procedures (Vuletic *et ah,* 2014). This procedure commonly utilises different types of bone grafts—such as autografts and allografts—to restore alveolar ridge continuity and support tooth eruption. Autogenous bone grafts (autografts), typically harvested from the patient's iliac crest, are considered the gold standard due to their superior osteogenic, osteoinductive, and osteoconductive properties, as well as their high biocompatibility and integration potential (Paradowska-Stolarz *et ah,* 2022).

Despite their clinical success, autografts present several disadvantages, including donor site morbidity, postoperative pain, gait disturbances, intestinal herniation, infection, nerve injury, growth retardation, and a limited supply of available graft material (Tonk *et ah,* 2022). Allogeneic bone grafts (allografts), sourced from human cadaveric donors, have been introduced to overcome the limitations of autografts by increasing material availability and eliminating donor site morbidity. While allografts exhibit favourable osteoconductive properties, they are associated with potential risks of immune rejection and disease transmission (Ferraz, 2023; Georgeanu

et al., 2023). Moreover, ABG generally lacks sufficient biological activity to promote optimal bone healing in craniofacial defects.

Therefore, existing therapeutic approaches for craniofacial deformities remain constrained by several inherent limitations, including variable clinical outcomes, the necessity for highly specialised surgical expertise, donor site morbidity, and the potential risks of immunological rejection and disease transmission. Consequently, recent advancements in regenerative medicine, genetic screening, and diagnostic imaging offer promising prospects for improving therapeutic efficacy, enabling earlier and more precise diagnosis and classification of congenital anomalies, and addressing the limitations of conventional treatment modalities (Heydari *et al.*, 2024).

2.2 Bone Tissue Engineering

2.2.1 Introduction

Bone is a living, adaptive tissue with a complex vascularised architecture made up of collagen fibers and hydroxyapatite minerals. It plays a crucial role in maintaining body structure, supporting weight, and facilitating movement through muscle attachment. However, when a defect surpasses the critical size threshold, natural regeneration becomes insufficient, requiring medical intervention.

2.2.2 Definition

Bone tissue engineering (BTE) has emerged as a promising alternative approach for the treatment of bone abnormalities, including craniofacial deformities. This multidisciplinary strategy aims to regenerate and repair damaged or diseased bone tissue by integrating principles of biology, materials science, and engineering. The primary objective of BTE is to construct a functional bone substitute through the combination of scaffolds, cells, and bioactive molecules. Achieving this requires a comprehensive understanding of bone architecture, mechanical properties, and tissue development processes.

Fundamentally, three components are necessary to execute this approach: scaffolds, cells, and signalling molecules (i.e., cytokines and growth factors). Alonzo et

al. (2021) conceptualised the integration of these three components as the BTE triad (Figure 2.2). Scaffolds act as a three-dimensional (3D) framework that facilitate cell attachment, proliferation, and differentiation, while mimicking the extracellular matrix (ECM) of natural bone. These scaffolds are designed to promote the production of bone matrix and tissue development by incorporating cells, particularly stem cells like mesenchymal stem cells (MSCs). Bioactive molecules, including growth factors and cytokines, are incorporated to enhance osteogenesis and modulate cellular activity (Almouemen *et al,* 2019; Bhushan *et al,* 2022).

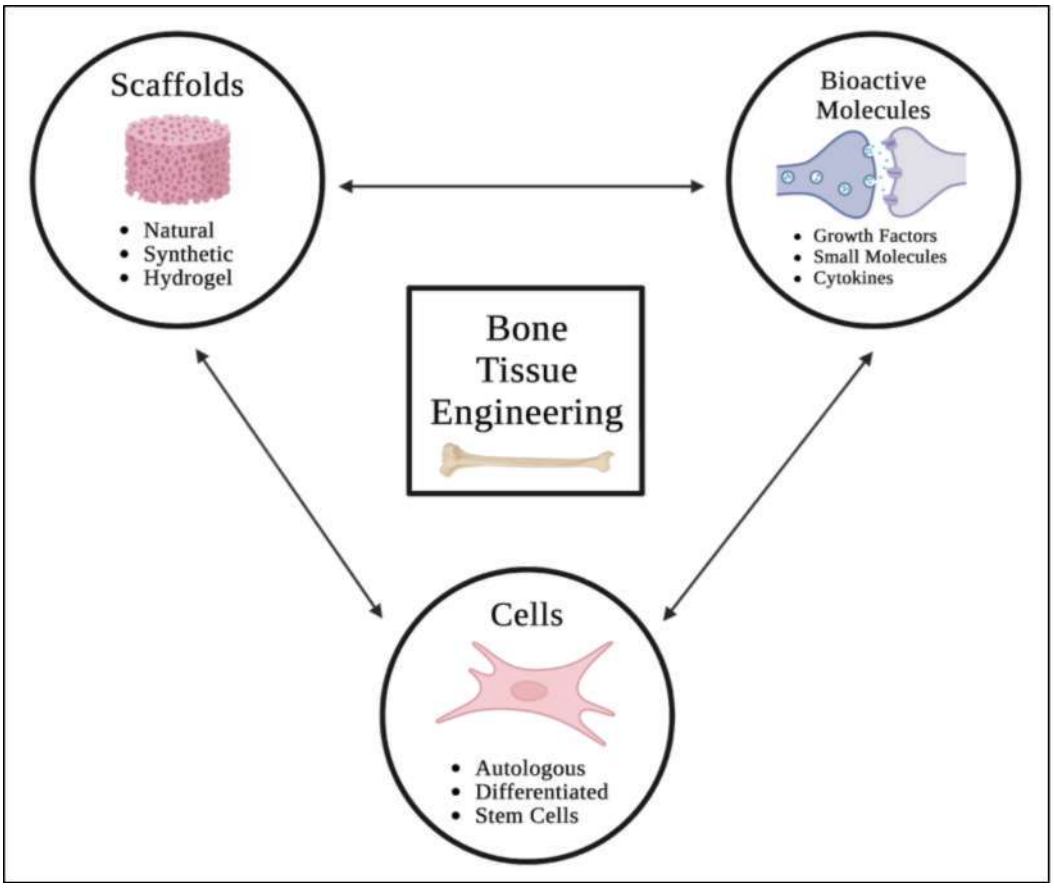

Figure 2.2 Bone Tissue Engineering Triad. The Three Factors That Need to Be Considered when Designing a Suitable Structure for Bone Tissue Engineering Applications.

Overall, BTE seeks to develop bioengineered bone grafts capable of integrating seamlessly with host tissue, restoring both the structural and functional properties of bone, and ultimately improving clinical outcomes in patients with bone deformities.

2.2.3 Scaffolds

Scaffold is a crucial element of the triad, serving as the foundational structure for the bone graft utilised in BTE. This three-dimensional (3D) structures are designed to mimic the extracellular matrix (ECM) of natural bone, providing both structural support and biological signals necessary for tissue development in BTE. Consequently, scaffolds are essential for the promotion of cell adhesion, proliferation, and differentiation, thereby facilitating the formation of novel tissues. Additionally, scaffolds are designed to possess specific characteristics, including porosity, mechanical strength, and degradation rates, that are compliant with the needs of the target tissue and enable successful interaction with its biological systems (Figure 2.3) (Almouemen *et al,* 2019; Bhushan *et al,* 2022).

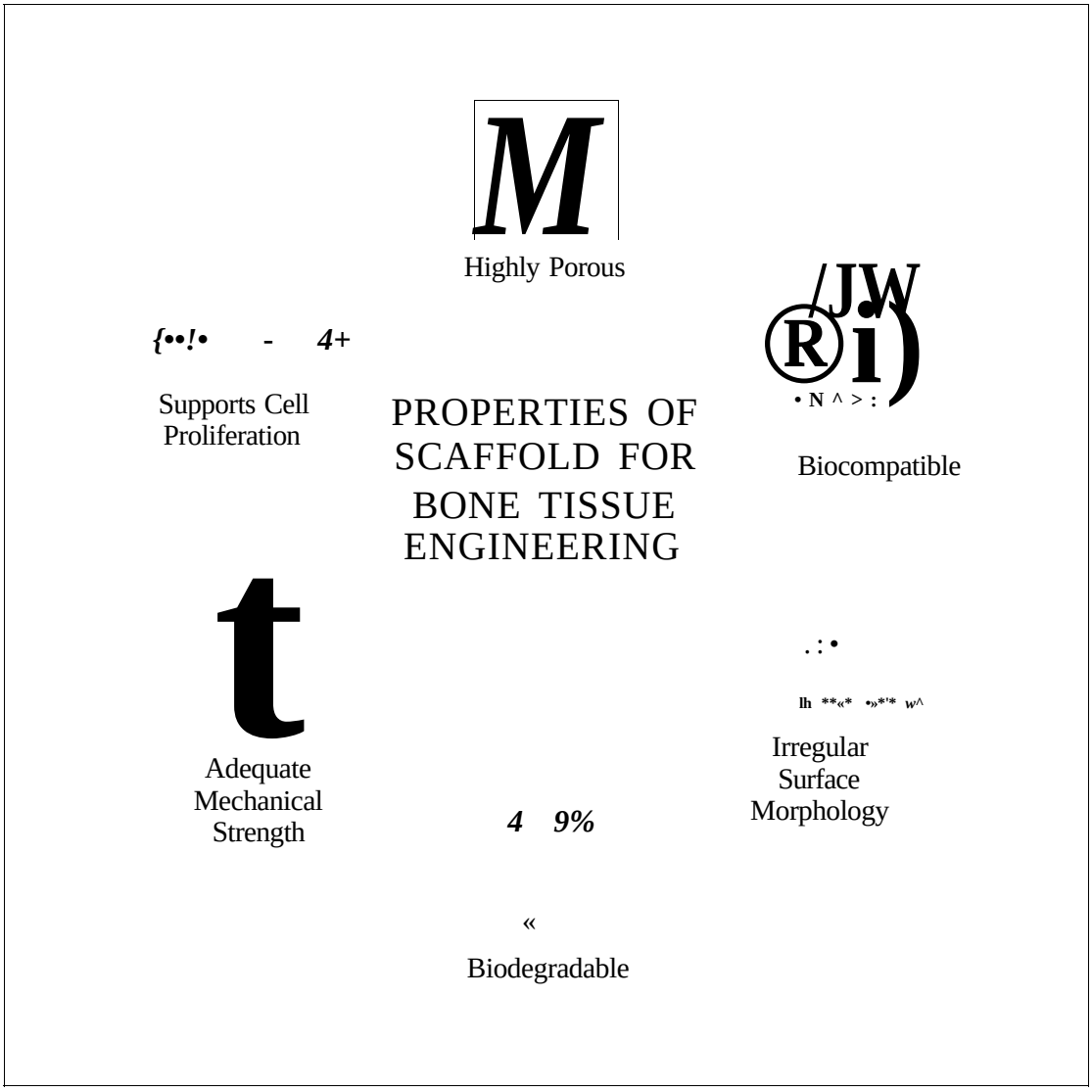

Figure 2.3 Essential Properties of Scaffolds for Optimal Bone Tissue Engineering.

These properties are critical for the proper ingrowth and vascularisation of tissue, thus ensuring that the engineered constructs are structurally solid, biologically active, and capable of integrating with the host tissue, thereby facilitating effective and long-lasting bone regeneration. The porosity of the scaffold is also essential, as it facilitates the diffusion of nutrients and waste products, while its mechanical properties must have comparable mechanical characteristics to the bone tissue. Furthermore, the scaffold's biodegradability is an important factor in ensuring that the resorption rate is concurrent with the rate of bone formation. This enables the osteoblasts to produce their own natural matrix structure and subsequently replace the patient's own tissue (Alonzo *et al.*, 2021). Additionally, bioactive molecules such as growth factors have the potential to alter scaffolds, thereby improving cell behaviour and tissue formation for clinical applications (Siqueira *et al.*, 2024).

2.2.4 Cells

Cells play a pivotal role in BTE as the fundamental biological component responsible for regenerating, repairing, and ensuring functional integration of bone tissue, ensuring its overall health and function. Different types of cells can be utilised to achieve suitable functionality of bone tissue, which can be derived into two main categories: undifferentiated cells (stem cells) and differentiated cells (Almouemen *et al.*, 2019). Osteogenic cells, such as osteoblasts, osteoclasts, and MSCs, are commonly utilised due to their inherent capacity to proliferate, differentiate, and produce bone matrix. MSCs are favoured for their multipotency and ability to differentiate into osteoblasts, the primary cells responsible for bone formation and resorption. This is accomplished by synthesising and secreting the organic matrix of bone, therefore regulating the mineral ions between the bone matrix and the extracellular space of the bone (Bhushan *et al.*, 2022; Stamnitz & Klimczak, 2021). These cells are often harvested from bone marrow, cultured in a laboratory, and seeded onto the scaffolds.

Moreover, cells are integral in the production of ECM, a complex network of proteins that provides structural and biochemical support to surrounding cells. ECM provides structural support for scaffold integration in BTE, facilitating cell adhesion and signalling, regulating cell behaviour, and acting as a reservoir for growth factors (Kargozar *et al.*, 2019). Additionally, the incorporation of growth factors such as bone

morphogenic proteins (BMPs), vascular endothelial growth factor (VEGF), and transforming growth factor beta (TGF-β) can enhance the osteogenic potential of these cells (Kargozar *et al.*, 2019; Stamnitz & Klimczak, 2021).

2.2.5 Bioactive Molecules

To facilitate effective bone regeneration in BTE, bioactive molecules are essential to coordinate the complex processes of bone regeneration, including cell proliferation, differentiation, and migration. Additionally, bioactive molecules are required to stimulate the processes of osteogenesis, angiogenesis, and ECM synthesis necessary for the formation of functional bone tissue. These bioactive molecules can be biochemical, such as growth factors and cytokines, or biophysical, including mechanical forces and electromagnetic fields (Bakhshandeh *et al.*, 2023; Dang *et al.*, 2018). Growth factors are the primary signal employed in bone tissue engineering. These are soluble proteins found in cells that attach to specific transmembrane receptors on target cells to regulate various cellular activities, such as proliferation, migration, and differentiation (Stone *et al.*, 2024).

Growth factors, such as bone morphogenetic proteins (BMPs), transforming growth factor beta (TGF-β), platelet-derived growth factor (PDGF), and vascular endothelial growth factor (VEGF), are crucial in stimulating the development of bone cells, the formation of new blood vessels, the creation of the ECM, and facilitating bone healing (Oliveira É *et al.*, 2021). BMPs, particularly BMP-2 and BMP-7, are effective growth factors used to stimulate the differentiation of MSCs into osteoblasts, thereby promoting the synthesis of bone matrix and facilitating new bone formation. TGF-β influences both the proliferation and differentiation of osteoblasts and enhances the structural integrity of the regenerating tissue (Xu *et al.*, 2018b). PDGF is a significant growth factor used in BTE to enhance crucial cellular processes necessary for bone repair, including cellular proliferation, migration, and extracellular matrix synthesis. The incorporation of PDGF into scaffolds creates a bioactive environment that closely mimics natural bone healing processes; therefore, it accelerates bone repair, improves the quality of regenerated bone, and ensures better integration with the host tissue (Sun *et al.*, 2020; Zhang *et al.*, 2018). The integration of these growth factors into scaffold

materials for BTE mimics the natural bone healing factor, thereby optimising the regenerative process and ensuring the formation of functional bone tissue.

2.3 Platelet Concentrate

2.3.1 Definition

Among the various biomaterials, recent research shows a focus on platelet concentrates (PC) as a biomaterial used to fabricate scaffolds due to its ability to deliver an abundance of bioactive molecules during bone regeneration alongside its osteoinductivity (Ngah *et al.*, 2021a). Platelet concentrates (PCs) are biologically active blood-derived products obtained from the patient's own blood, designed to enhance tissue repair and regeneration. These concentrates are prepared by centrifugation to separate the platelets from other blood components, thereby increasing the concentration of growth factors and cytokines. PCs are important in regenerative medicine, especially BTE, because they help with many physiological processes, such as cell growth, adhesion, differentiation, extracellular matrix production, and blood vessel formation. These processes aid in accelerating bone healing and improve the integration and functionality of engineered tissues. Additionally, the autologous nature of platelet concentrates reduces the risk of immunological responses and disease transmission, making them a safe and effective option for therapeutic applications (Oliveira É *et al.*, 2021; Stamnitz & Klimczak, 2021).

PCs are developed from the concept of isolating platelets from whole blood used in homeostasis and tissue repair to enhance healing processes in various medical and dental applications. The foundational understanding of PCs containing numerous growth factors and cytokines leads to the development of techniques to concentrate these cells from whole blood. These advancements lead to the development of platelet-rich plasma (PRP) and platelet-rich fibrin (PRF), characterised by their preparation methods, content, and intended clinical applications (Ngah *et al.*, 2021b).

2.3.2 Platelet-Rich Plasma

Platelet-rich plasma (PRP), introduced in the early 1980s as a significant advancement in the use of platelets for therapeutic purposes, is considered the first product derivative of PCs. PRP, a concentrated form of autologous blood plasma, contains a high concentration of platelets that aid in the body's innate healing mechanism. The clinical application of PRP was introduced by Marx in the 1990s by highlighting the efficacy of PRP in bone grafting and BTE (Marx *et al.*, 1998; Mościcka & Przylipiak, 2021).

Centrifuging a blood sample separates the plasma and platelets from other blood components to obtain PRP. The resulting product is enriched with growth factors and cytokines, including PDGF, TGF-β, and vascular endothelial growth factor (VEGF). These bioactive molecules are essential for cell proliferation, differentiation, and migration, thus enhancing tissue repair and regeneration (Asmundo *et al.*, 2024). The abundance of these bioactive molecules found in PRP leads to its various clinical applications, including BTE for craniofacial regeneration. Additionally, the autologous properties of PRP minimize the risks of immunological responses or disease transmission, ensuring a high level of biocompatibility for patients. However, PRP has several significant drawbacks that limit its clinical effectiveness and consistency. These drawbacks include its lack of a continuous release mechanism for growth factors, resulting in a rapid and short-lived biological impact that affects its therapeutic outcome. Another limitation of PRP is the addition of anticoagulants during its fabrication, thereby introducing risks of adverse reactions and further complicating the treatment process (Asmundo *et al.*, 2024; Grzelak *et al.*, 2024; Patel *et al.*, 2023). These limitations highlight the necessity for advancements that must be addressed to improve its bioactivity and provide a more precise and prolonged therapeutic impact in regenerative applications.

2.3.3 Platelet-Rich Fibrin

Platelet-rich fibrin (PRF) is a second-generation platelet concentrate (PC), and an advanced autologous biomaterial derived from a patient’s own blood. It is characterised by a dense fibrin matrix enriched with platelets and leukocytes, which

collectively enhance its regenerative potential. Developed by Choukroun et al. (2006), PRF was introduced to overcome the limitations of platelet-rich plasma (PRP), particularly its dependence on anticoagulants and rapid growth factor release (Choukroun *et al.*, 2006).

PRF has emerged as a highly suitable biomaterial for scaffold fabrication in bone tissue engineering (BTE) owing to its intrinsic biological composition and its ability to promote both bone and soft tissue regeneration. The fibrin network provides a natural three-dimensional (3D) scaffold that supports cellular attachment, migration, and proliferation while enabling the sustained release of growth factors crucial for tissue healing. Due to its autologous origin, ease of preparation, and regenerative efficacy, PRF has gained significant clinical popularity across dental and medical applications (Jia *et al.*, 2024; Roshan *et al.*, 2024). Consequently, numerous studies have explored its biological characteristics, therapeutic potential, and clinical outcomes in various craniofacial and dental procedures.

The regenerative capacity of PRF is largely attributed to its reservoir of bioactive molecules, particularly growth factors that stimulate cell proliferation, angiogenesis, and extracellular matrix synthesis. These biological processes collectively contribute to enhanced wound healing, osteogenesis, and soft tissue repair. A major advancement in PRF preparation is its simplified, single-step centrifugation process, which eliminates the need for anticoagulants and allows natural coagulation to form a stable fibrin matrix. This approach promotes a gradual and sustained release of growth factors while ensuring consistency in platelet and cytokine concentrations (Jia *et al.*, 2024; Wong *et al.*, 2023). The 3D architecture of PRF further facilitates controlled growth factor delivery, thereby improving its effectiveness in promoting bone regeneration and tissue repair.

Moreover, PRF's sustained release mechanism and absence of synthetic additives minimise the risk of adverse reactions, making it a safe and biocompatible biomaterial. It has demonstrated superior outcomes compared to PRP, particularly in bone regeneration, soft tissue healing, and implantology (Jia *et al.*, 2024; Park *et al.*, 2024; Roshan *et al.*, 2024). Despite these advantages, PRF presents certain limitations, notably its short shelf life and the necessity for immediate clinical use, as the fibrin matrix is prone to degradation over time. Therefore, continued advancements in biomaterial development for BTE are essential to address these challenges and improve the long-term applicability of PRF in regenerative therapies.

2.3.4 Frozen Platelet-Rich Fibrin

To maintain the use of PRF efficiently in BTE, a method of preserving PRF was developed by freezing it at -80°C. Fresh PRF required immediate post-preparation use; thereby, it poses complications for a standardised clinical use in regenerative medicine and limits scheduling alternatives for staged or multi-session treatments (Jia *et al.*, 2024). Consequently, frozen PRF enables its preservation and subsequent utilisation by decelerating its biological activities while maintaining the growth factors and the structural integrity of its fibrin matrix (Choukroun *et al.*, 2017). However, frozen PRF requires storage at a stable temperature of -80 °C, complicating its transportation. Additionally, meticulous thawing is crucial to prevent the degradation of growth factors and cellular elements. This limits the usability of frozen PRF, prompting further research (Banyatworakul *et al.*, 2021).

2.4 Lyophilised Platelet-Rich Fibrin

2.4.1 Definition

A recent advancement in the preservation of platelet-rich fibrin (PRF) involves its lyophilisation, leading to the development of lyophilised platelet-rich fibrin (LyPRF). Lyophilisation, or freeze-drying, removes moisture from the PRF through controlled freezing and sublimation, converting it into a dry, porous solid while maintaining its essential biological properties (Ngah *et al.*, 2021b).

Currently, LyPRF has gained popularity as an advanced PRF, undergoing a two-step process that involves centrifugation and lyophilisation of collected blood to increase the concentration of platelets and fibrin in PRF. The lyophilisation, or freeze-drying, process removes moisture from the biomaterial through freezing and sublimation, transforming the PRF into a dry, porous solid material. This process enhances its stability by preserving the structural integrity and bioactivity of the growth factors and cellular components. LyPRF's dried, solid form makes it easier to store and transport, thereby extending its shelf life (Grzelak *et al.*, 2024; Jia *et al.*, 2024).

LyPRF maintains the integrity of its growth factors and bioactive components and can be reconstituted when a suitable liquid is present, thereby preserving its regenerative properties. Additionally, the dry, powdery form of LyPRF enhances its biocompatibility, thereby easing its integration with other biomaterials to enhance its bioactivity processes. LyPRF's versatility enhances its functionality in tissue engineering and regenerative procedures by tailoring it to the patient's specific requirements for craniofacial regeneration. This is because the fibrin matrix of LyPRF acts as a natural scaffold that supports the biomaterial's integration with other biomaterials and the host tissue, facilitating more effective tissue repair and regeneration. Moreover, the extended shelf life, improved stability, versatility, and convenience of use provided by LyPRF optimise its effectiveness and applicability in BTE (Bhushan *et al.*, 2022; Grzelak *et al.*, 2024; Milano *et al.*, 2023).

2.4.2 Fabrication

The fabrication of LyPRF involves a systematic procedure that improves the stability and functionality of PRF for clinical application. Initially, venous blood is obtained from the patient without anticoagulant, lowering the risk of adverse reactions from foreign substances and increasing the biocompability of LyPRF. The collected blood sample is then subjected to centrifugation, separating the blood components into three distinct layers and concentrating platelets and fibrin within the PRF layer. Following the centrifugation, the PRF layer is extracted and prepared for lyophilisation by freezing the biomaterial at -80 and subsequently freeze-dried overnight at -51 . This procedure stabilises the biomaterial by removing its moisture through sublimation under reduced pressure, thereby enhancing its shelf life while preserving its bioactive components, including growth factors and cytokines. The lyophilised form of LyPRF can be reconstituted with a suitable liquid, making it easier to mix with other biomaterials and facilitating its application in various regenerative therapies such as tissue regeneration and wound healing. The fabrication process of LyPRF is crucial for ensuring its effectiveness and safety in promoting tissue repair and regeneration, as it overcomes the limitations of PRP and Fresh PRF (Andia *et al.*, 2020; Dashore *et al.*, 2021; Kardos *et al.*, 2018; Liu *et al.*, 2019a).

2.4.3 Standardised Fabrication of LyPRF

Following comprehensive searches employing a three-stage search methodology, the literature collected from the designated databases was integrated with the online search capabilities of Endnote literature management software. This process involved the removal of duplicates via the software's verification function, and a meticulous screening of titles and abstracts was conducted to assess the eligibility of the literature in accordance with the established inclusion and exclusion criteria. The collected material was published between 2019 and 2024, and any publications in languages other than English were excluded from consideration.

The electronic search across four databases initially yielded 3,047 records: SCOPUS (2,592), Web of Science (81), ScienceDirect (285), and PubMed (89). After removing 1,049 pre-2019 records and 401 duplicates, 1,597 records remained. Screening excluded 742 non-original articles and 48 non-English publications. Of the remaining records, 352 were retrieved for full-text review, while 455 were inaccessible. After applying inclusion and exclusion criteria, 337 articles were excluded for reasons such as lacking LyPRF focus or using other platelet concentrates. Ultimately, 15 in vitro studies on LyPRF were selected for data extraction.

The fifteen (15) included studies involve the extraction of PRF from various sources, differing amounts, centrifugation durations and speeds, as well as variability in the temperature and duration of lyophilisation. The details of the fabrication protocols carried by each literature are compiled and summarised in Table 2.1. Five (5) studies utilised human venous blood for the extraction of PRF, whereas four (4) studies employed blood taken from rabbits and three (3) studies used blood from rats for the blood collection methodology (Anaya-Sampayo *et al.*, 2024; Ngah *et al.*, 2024; Sui *et al.*, 2023b; Sun *et al.*, 2023b). The specified amount of blood collection was generally reported to be 10mL as evaluated in ten (10) studies, with two (2) studies collecting an amount of 14mL and one (1) with 12mL of blood collected (Anaya-Sampayo *et al.*, 2024; Gan *et al.*, 2023b; Warin *et al.*, 2022). In terms of centrifugation duration and speed, a number of nine (9) studies uses 3000 RPM for 10 minutes to separate the fibrin layer for collection (Gan *et al.*, 2023b; Liu *et al.*, 2022a; Ngah *et al.*, 2021a). The removed PRF clot was isolated for cryopreservation at -80 , as documented in thirteen (13) studies, typically for a duration of 24 hours (Sui *et al.*, 2023a; Wang *et al.*, 2019a).

However, three (3) studies reported to freeze the PRF clots for 30 minutes at the same temperature as previously mentioned (Liu *et al.*, 2022a; Ngah *et al.*, 2024). In regards of the lyophilisation process, it is typically freeze-dried at a temperature of -51 for a duration of 24 hours as recorded by six (6) studies (Liu *et al.*, 2022a; Liu *et al.*, 2019b; Ngah *et al.*, 2021a; Wang *et al.*, 2019a). However, one (1) study prolong the lyophilisation process to 48 hours at -80 and another study reported lyophilisation at a temperature of -60 for 4 hours (Nie *et al.*, 2020a; Wong *et al.*, 2021a). The finalized LyPRF product was thereafter stored correctly for analysis or integration into other biomaterials.

Table 2.1 Standardised Fabrication of LyPRF in The Included Journals.

Sample	Amount (mL)	Duration of Centrifugation (min)	Speed	Duration of Freezing (hrs)	Temperature Freezing	Duration of Lyophilisation (hrs)	Temperature Lyophilisation	Notes	References
Human	10	14	1500 RPM	NA	-80°C	24	-40°C	-	(Ansarizadeh *et al*, 2019)
Rabbits	5	10	3000 RPM	NA	-80°C	24	-51°C	-	(Liu *et al.*, 2019a)
Rabbits	10	10	3000 RPM	24	-80°C	24	-45°C	PRF Clot was compressed for 10s before lyophilisation	(Wang *et al.*, 2019b)
Rat	NA	10	3000 RPM	NA	-80°C	48	-80°C	-	(Nie *e*far/., 2020b)
Human	10	10	3000 RPM	0.5	-80°C	24	-51°C	-	(Ngah *et al.*, 2021a)
Rabbits	NA	NA	NA	24	-80°C	4	-60°C	Water was	(Wong *et al.*,

								added and immediately removed using paper tissues	2021b)
Human	10	10	3000 RPM	0.5	-80°C	24	-51°C	-	(Liu *et al.*, 2022b)
NA	10	10	3000 RPM	NA	-80°C	12	-51°C	-	*(Qimet al.*, 2022)
Labrador Retriever Dogs	10	14	lOOg	0.5	-80°C	24	-51°C	-	*(Warm et al.*, 2022)
Rat	NA	10	3000 RPM	24	-40°C	24	-50°C	PRF was compressed using forceps before centrifugation	*(Gmet al.*, 2023a)
Rat	5	10	3000	24	-80°C	24	NA	LyPRF was	*(Sm et al.*,

			RPM					grounded to powder	2023a)
Rabbits	20	10	1200g	NA	NA	NA	NA	PRF Clot was compressed for 10s before lyophilisation	(Sun. *et al.*, 2023)
Human	NA	12	2700 RPM	NA	-80°C	24	-51°C	-	(Anaya-Sampayo *et al*, 2024)
NA	NA	NA	NA	NA	NA	NA	NA	-	(Chuang *et al*, 2024)
Human	NA	10	3000 RPM	0.5	-80°C	24	-51°C	-	*(Ngah et al.*, 2024)

2.5 Physicochemical

The literature obtained from the designated databases was integrated with the online search capabilities of EndNote literature management software after comprehensive searches were conducted using a three-stage search methodology. During this process, the software's verification function was used to eliminate duplicates, and a meticulous review of titles and abstracts was conducted to evaluate the literature's eligibility in accordance with the established inclusion and exclusion criteria. Any publications in languages other than English were excluded from consideration, and the compiled material was published between 2019 and 2024.

Initially, 3047 publications were identified through the electronic search of the four databases that were examined: SCOPUS (2592), Web of Science (81), Science Direct (285), and PubMed (89). After eliminating 401 duplicates and excluding 1,049 publications prior to 2019, 1,597 articles are left for screening. The initial screening phase excluded 742 publications, which were categorised as reviews, meta-analyses, book chapters, books, editorials, and conference abstracts. Additionally, 48 publications were eliminated because of their publication in languages other than English. 352 of the 1597 literary works were deemed suitable for full-text retrieval; however, 455 were not effectively accessed. Consequently, the residual 352 pieces of literature were meticulously assessed for eligibility in accordance with the established inclusion and exclusion criteria. A total of 337 publications were excluded from the review for a variety of reasons, including the following: (i) the publications did not address the lyophilisation of PRF; (ii) the studies used other platelet concentrates instead of PRF; (iii) the publications lacked isolated analysis of LyPRF; and (iv) the publications exclusively conducted in vivo and/or clinical studies without including in vitro studies). In this systematic literature review, a total of 15 scholarly works that featured in vitro analyses of LyPRF were selected for data extraction and subsequent analysis after a comprehensive screening and evaluation phase.

The 15 included papers showcase diverse characterisation analyses undertaken to illustrate the structural and chemical potential of LyPRF in regenerative medicine (Table 2.2). Scanning Electron Microscopy (SEM) is the predominant analytical technique utilised in the literature to ascertain surface morphology, fibrin network, pore sizes, and cellular entrapment of biomaterials. The predominant results of this analysis

indicate an irregular and porous surface structure, as demonstrated by four (4) and five (5) studies, respectively. Additionally, the fibrin network of LyPRF was examined and shown to display an irregular configuration characterised by a three-dimensional (3D) structure with many trimolecular branch junctions, fibrin fibres, and fibrillae (Liu *et al.*, 2022a). In regard to the pore size measured, studies indicate a typically larger pore size in scaffolds with LyPRF and a homogeneous entrapment of cells and platelets (Anaya-Sampayo *et al.*, 2024).

Additionally, Fourier Transform Infrared Spectroscopy (FTIR) was implemented in two studies to evaluate any modifications in the chemical groups of the biomaterial subsequent to its incorporation with LyPRF. It was demonstrated that the FTIR peak consistently identifies peaks associated with Amide I, Amide II, and Amide III (Chuang *et al.*, 2024). The elemental composition of the biomaterial was determined using Energy Dispersive X-ray Spectroscopy (EDX) to support the physicochemical properties of LyPRF. In this review, a study that employed EDX identified the presence of carbon (C), sodium (Na), silicon (Si), chloride (Cl), potassium (K), nitrogen (N), oxygen (O), phosphorus (P), and calcium (Ca) in varying concentrations, thereby demonstrating its capacity to mimic the composition of bone tissue, including the presence of these elements in LyPRF (Anaya-Sampayo *et al.*, 2024).

Table 2.2 Physicochemical Characteristics of LyPRF in The Included Journals.

Scanning Electron Microscopy (SEM)				**Fourier Transform Infrared Spectroscopy (FTIR)**	**Energy Dispersive X-ray Spectroscopy (EDX)**	**References**
Arrangement	**Fibrin**	**Pore Size**	**Platelets**	**Bands (cm-1)**	**Elements**	
NA	NA	NA	NA	Amide I (1659), Amide II (1553), Amide III (1235)	NA	(Ansarizadeh *et al.*, 2019)
Porous Structure	Sponge fibrin-like appearance	NA	NA	NA	NA	(Liu *et al.*, 2019a)
Disordered	Three-dimensional network (trimolecular branch junctions, fibrin fibres, fibrillae)	NA	Present among the fibrin	NA	NA	(Wang *et al.*, 2019a)

Irregular and Porous	NA	1.51 ± 0.75	NA	NA	NA	(Nie *et al.*, 2020b)
Irregular	Dense 3D fibrin framework	NA	Cells embedded within the fibrous structure	NA	NA	(Ngah *et al.*, 2021a)
Porous Structure	Fibrous Network	NA	NA	NA	NA	(Wong *et al.*, 2021b)
Porous Structure	NA	NA	NA	NA	NA	(Liu *et al.*, 2022b)
Sponge-like microstructure	NA	NA	NA	NA	NA	(Qian *et al.*, 2022)
NA	NA	NA	NA	NA	NA	(Warin *et al.*, 2022)
Porous	NA	87.80 ±18.65	NA	NA	NA	(Gan *et al.*,

Structure		µm				2023b)
NA	NA	NA	NA	Amide I (1661), Amide II (1599)	NA	(Sui *et al.*, 2023a)
Irregular	Fibrin network with trimolecular branch junctions	NA	NA	NA	NA	(Sun *et al.*, 2023a)
NA	Porous Structure	NA	Small particles distributed homogeneously	NA	Carbon (C), Nitrogen(N), Oxygen (O), Phosphorus (P), Calcium (Ca)	(Anaya-Sampayo *et al.*, 2024)
NA	NA	NA	NA	Amide I (1650), and Amide II (1542)	NA	(Chuang *et al.*, 2024)
Irregular	Fibrin network with a condensed, inter-connected,	146 ± 23.69	Presence of cells and platelets	NA	Sodium (Na), Silicon (Si), Calcium (Ca), Phosphorus (P),	(Ngah *et al.*, 2024)

and densely packed framework	entangled in the fibrin network	Chloride (Cl), Potassium (K)

2.5.1 FESEM Analysis

Field Emission Scanning Electron Microscopy (FESEM), an advanced imaging technique, provides precise, high-resolution three-dimensional surface morphology for samples. FESEM utilises a field emission gun as the electron source that produces a narrower and more coherent electron beam, resulting in higher spatial resolution and greater depth of field. Pertaining to its high-resolution imaging capabilities, FESEM provides a comprehensive analysis of the microstructure and surface morphology of LyPRF by capturing images at the nanometre level. This is essential to acquire a comprehensive understanding of the surface morphology, microarchitecture, pore sizes, and fibrin matrix's integrity. Additionally, this analysis allows for the examination of the porous structure and fibre arrangement within the LyPRF, revealing the effects of the fibrin network on the distribution of platelets and growth factors. Moreover, FESEM enables the analysis of LyPRF porosity and surface characteristics that influence its integration with scaffolds for the use of BTE. This detailed morphological information is essential for optimising LyPRF's fabrication process, ensuring its effectiveness as a regenerative biomaterial, and improving its applications in tissue engineering for craniofacial regeneration (Orasugh *et al.*, 2020; Wong *et al.*, 2017).

2.5.2 EDX Analysis

Energy dispersive X-ray spectroscopy (EDX) is an analytical technique frequently used in conjunction with FESEM to provide comprehensive characterisation and elemental analysis of samples, such as LyPRF. EDX is the objective of this analysis is to identify and quantify the elemental composition of LyPRF. The functioning concept of EDX involves detecting the properties of the X-ray emitted from LyPRF when it is exposed to an electron beam. It allows for the accurate detection and measurement of elements found in the LyPRF matrix, including calcium and phosphorus. The distribution and concentration of elements detected from LyPRF provide information that aids in understanding its characteristics, safety, and efficacy for regenerative applications. Therefore, this analysis enables the evaluation of the quality and consistency of LyPRF preparation and assesses its potential for integration

with other biomaterials (Milano *et al.*, 2023; Scimeca *et al.*, 2018; Siqueira *et al.*, 2024; Wong *et al.*, 2017).

2.5.3 FTIR Analysis

Fourier-transform infrared spectroscopy (FTIR) is an analytical equipment used to identify and characterise the molecular composition and functional groups within a sample. This is achieved by measuring the absorption of infrared light by the sample based on its wavelength, resulting in a variety of distinctive absorption spectra. Therefore, FTIR provides a detailed analysis of the biomaterial and structural properties of LyPRF by examining the molecular composition and its functional groups. The primary functional groups detected by FTIR for this biomaterial are the amide I and amide II bands, which are used to determine the denaturation rate, the stability of the fibrin network, and the conformational composition of LyPRF. The amide I band reveals the C=O stretching vibrations of peptide bonds and helps identify changes in the secondary structure of fibrin proteins, including the presence of alpha-helices and beta-sheets. The amide II band correlates with N-H bending and C-N stretching, providing information on the hydrogen bonding and stability of the proteins in LyPRF. This analysis is crucial for ensuring that LyPRF maintains its effectiveness and suitability for BTE and wound healing (Khan *et al.*, 2024; Monaghan *et al.*, 2023; Usoltsev *et al.*, 2019).

2.5.4 XRD Analysis

A fundamental analysis method, X-ray diffraction (XRD), evaluates the crystalline structure of materials. The method involves directing X-rays at a sample that diffracts upon interaction with the periodic arrangement of atoms within the crystalline material. Therefore, XRD analysis of LyPRF allows for the investigation of its crystalline structure, phase composition, and the identification of any crystalline impurities that may be present in the biomaterial. The analysis of the crystalline salts or minerals that may have formed during the lyophilisation process is essential to evaluating LyPRF biocompatibility and performance in clinical applications such as BTE. Furthermore, changes in the diffraction patterns influence the stability of LyPRF

and indicate alterations in its structural properties, thereby disturbing cellular processes including cell attachment, proliferation, and tissue regeneration. Therefore, XRD analysis is crucial in ensuring the quality and effectiveness of LyPRF in craniofacial regeneration (Ali *et al.*, 2022; Shokouhinejad *et al.*, 2023).

2.6 Biological Analysis

The biological characterisation of LyPRF is crucial for assessing its cellular compatibility, bioactivity, and osteogenic potential in tissue engineering applications (Table 2.3). The Enzyme-linked Immunosorbent Assay (ELISA) is the primary technique utilised in the observed studies to quantify vital bioactive proteins, particularly growth factors including Platelet-Derived Growth Factor (PDGF), Transforming Growth Factor (TGF-β), and Vascular Endothelial Growth Factor (VEGF). The ELISA results showed a constant and gradual release of growth factors, demonstrating that LyPRF maintains the growth factor bioavailability required for bone tissue engineering. This is apparent since the kinetic release pattern of growth factors from the included studies revealed consistency throughout the analysis period (Liu *et al.*, 2022a; Warin *et al.*, 2023).

The LyPRF biocompatibility analysis was frequently conducted using the 3-(4, 5-dimethylthiazolyl-2)-2, 5-diphenyltetrazolium bromide (MTT) assay to determine cell proliferation. Ten (10) studies have reported that LyPRF statistically increases the proliferation of fibroblast cells, osteoblastic cell line MC3T3-E1, and bone marrow stromal cells (BMSCs) (Ansarizadeh *et al.*, 2019). Furthermore, a study conducted by Gan et al. employed the cell counting kit-8 to observe cell proliferation and reported that the addition of LyPRF to the scaffold significantly enhanced cell proliferation (Gan *et al.*, 2023b).The osteogenesis potential of the LyPRF was assessed in three (3) of the included studies using the alkaline phosphatase (ALP) activity assay. The osteogenic differentiation potential of LyPRF was reported to be improved by bone mesenchymal stem cells (BMSCs) (Wang *et al.*, 2019b). Moreover, the effectiveness of LyPRF in facilitating wound closure was evaluated through a scratch wound assay. Warin et al. reported that LyPRF enables the complete closure of wounds by fibroblast cells within 24 hours.

Table 2.3 Biological Characteristics of LyPRF in The Included Journals.

Kinetic Release of Growth Factor		**Cell Proliferation**		
Enzyme-linked Immunosorbent Assay (ELISA) kit		**Cell**	**3-(4, 5-dimethylthiazolyl-2)-2, 5-diphenyltetrazolium bromide (MTT Assay)**	**References**
Maximum	**Duration**		**Cell Proliferation / Viability**	
NA	NA	MSCs	LyPRF shows a significantly positive cell viability effect on the membrane	(Ansarizadeh *et al.*, 2019)
TGF-β1: 407.69 ng/l VEGF: 79.63 ng/l PDGF-AB: 525.74 ng/l	28 Days	BMSC	The addition of LyPRF shows a statistically increase in cell proliferation	(Liu *et al.*, 2019a)
PDGF-BB: 1380.9 pg/mL VEGF: 230.1 pg/mL TGF-β: 30.1 pg/mL FGF: 55.7 pg/mL	14 Days	BMSC	LyPRF has a significant, dose-dependent and durable stimulative effect on cell proliferation	(Wang *et al.*, 2019a)
NA	NA	MEC3T3-E1	LyPRF shows a higher cell proliferation potential	(Nie *et al,* 2020b)

PDGF-AB: 418.66 pg/mL	28 Days	NA	NA	(Ngah *et al.,* 2021a)
TGF-P: ~180 ng/mL IGF: -55 ng/mL VEGF: -300 ng/mL	10 Days	MEC3T3-E2	Cell Viability is significantly higher with the addition of LyPRF	(Wong *et al.,* 2021b)
TGF-pi: -13000 ng/L VEGF: -50 - 100 (Based on w/v) PDGF-AB: 3800 ng/L	28 Days	SHED	The addition of LyPRF shows significant improvement in cell proliferation	(Liu *et al.,* 2022b)
PDGF-AA: 10638.55 ±1577.43 pg/mL (total release)	21 Days	NA	NA	(Qian *et al.,* 2022)
TGF-pi: 2700 pg/mL VEGF: 1485.4 pg/mL PDGF-BB: 1601 pg/mL	3 Days	Fibroblast	Cell Proliferation of LyPRF is significantly higher compared to FPRF	(Warm *et al.,* 2022)
TGF-P: 7.31% ± 0.34% PDGF-AB: 7.36% ± 0.29%	21 Days	BMSC	NA	(Gan *et al.,* 2023b)

VEGF: -200 pg/ml PDGF: -80 pg/ml TGF: -510 pg/ml	35 Days	MC3T3-E1	Biomaterial shows significant proliferation after 3 days of culture	(Sui *et al.*, 2023a)
NA	NA	BMSC	NA	(Sun *et al.*, 2023a)
FGF: NA PDGF-BB: NA	7 Days	DSPSC and OB-DPSC	Presence of LyPRF demonstrate lower cytotoxicity and higher viability	(Anaya-Sampayo *et al.*, 2024)
NA	NA	NA	NA	(Chuang ^*a*/., 2024)
PDGF-AB: -4000 pg/ml	28 Days	MC3T3-E1	Presence of LyPRF demonstrates a significant increase in cell proliferation	(Ngah *era*/., 2024)

2.6.1 Kinetic Release Pattern of Growth Factor Analysis Using ELISA

The kinetic release pattern of growth factors in LyPRF significantly influences its therapeutic efficacy for bone regeneration, osteogenesis, angiogenesis, and extracellular matrix formation that are essential for BTE. This is because LyPRF is rich in growth factors such as PDGF, VEGF, and TGF-β that are essential in promoting bone regeneration and wound healing. The timing and intensity of cellular reactions are influenced by the kinetic release pattern of growth factors released from LyPRF. The kinetic release pattern is typically characterised by an initial burst release that stimulates the tissue with a high concentration of growth factors, followed by a sustained release that is crucial for tissue regeneration. The enzyme-linked immunosorbent assay (ELISA) measures this kinetic release pattern by using antibodies that specifically bind to the target molecules, allowing detection even at low concentrations. This is achieved by tracking the temporal release of growth factors of LyPRF, allowing an assessment of the bioavailability and stability of these molecules over time. This analysis is essential to understanding the preservation and release patterns of growth factors that influence the regenerative capacity of LyPRF. Therefore, a suitable kinetic release pattern of growth factors in LyPRF can be determined to optimise the therapeutic potential of LyPRF in BTE, ensuring the efficacy of LyPRF on long-term tissue healing and bone regeneration (Liu *et al.*, 2022b; Liu *et al.*, 2019a; Ngah *et al.*, 2021a).

2.6.2 Cytotoxicity Analysis Using MTT Assay

A cytotoxicity assay is an in vitro test used to evaluate the potential toxic effects of substances, such as LyPRF, on living cells by measuring whether the lyophilisation process, or any residual compounds associated with it, adversely affects cellular health, including cell damage or death. The cytotoxicity assay involves exposing cultured cells such as fibroblasts or osteoblasts to LyPRF. Colorimetric assays, particularly MTT assays, assess the viability of this test by monitoring its metabolic activity. Understanding the cytotoxicity of LyPRF is essential in determining the biocompatibility of LyPRF after lyophilisation and ensuring its safety for use in clinical applications such as wound healing and bone tissue engineering. Therefore, cytotoxicity

assays are a fundamental tool in assessing the suitability of LyPRF as a regenerative biomaterial for BTE (He *et al.*, 2020; Vijayan *et al.*, 2023).

CHAPTER 3
RESEARCH METHODOLOGY

3.1 Research Design

This study adopts a cross-sectional experimental research design to fabricate and characterise LyPRF and FPRF for potential application in BTE applications. The research design encompasses both physicochemical and biological characterisation to comprehensively evaluate and compare the properties of the two biomaterials. Venous blood samples were collected and processed to obtain PRF, which was subsequently subjected to two preservation techniques: freezing and lyophilisation. The lyophilisation process was conducted under controlled temperature and vacuum conditions to remove moisture and enhance the structural stability and shelf life of the material.

The physical and chemical properties of both LyPRF and FPRF were analysed using a combination of analytical techniques. X-ray diffraction (XRD) was employed to determine crystallinity and phase composition, field emission scanning electron microscopy (FESEM) to examine microstructural morphology, energy dispersive X-ray spectroscopy (EDX) to assess elemental composition, and Fourier-transform infrared spectroscopy (FTIR) to identify functional groups and chemical bonds. Collectively, these analyses provided a comprehensive understanding of the materials' microstructure, elemental distribution, and chemical stability.

To evaluate biological performance, the biocompatibility of LyPRF and FPRF was assessed using human gingival fibroblast (HGF) cells through a cytotoxicity assay (3-(4,5-dimethylthiazol-2-yl)-2,5-diphenyltetrazolium bromide, MTT assay). This assay determined the effects of both materials on cell viability and metabolic activity, providing insight into their safety and potential for clinical application. The experimental data were subsequently subjected to statistical analysis to compare the physicochemical properties and cytocompatibility of LyPRF and FPRF.

Overall, this research design integrates comprehensive material characterisation and biological evaluation to assess and validate LyPRF as a stable, biocompatible, and clinically applicable biomaterial for BTE.

3.2 Ethical Approval

Ethical approval for the research was obtained from University Teknologi MARA (UiTM) under the governance of UiTM Research and Innovation and University Research Committee (REC/08/2024 (PG/MR/378)).

3.3 Participant Recruitment

Human venous blood was taken from three healthy individuals with the purpose of FPRF and LyPRF fabrication for the study (Aizawa *et al.*, 2020; Ngah *et al.*, 2024). Participants were recruited based on the inclusion and exclusion criteria and given a detailed explanation of the research protocol, risks, expected benefits, and the future potential of its clinical use for the community, therefore, informed consent was obtained. The inclusion criteria included individuals in the age range of 20 to 30 years old, fit and healthy, non-smokers, and with no history of recent aspirin intake within 3 months or anticoagulant drugs (Nakajima *et al.*, 2024). The study excluded participants that do not meet the stated inclusion criteria, individuals with chronic illnesses, and participants taking anticoagulants, aspirin or NSAIDs (non-steroidal anti-inflammatory drugs) for the last 3 months. Table 3.1 summarises the inclusion and exclusion criteria applied in this study.

Table 3.1 Inclusion and Exclusion Criteria

Inclusion	**Exclusion**
Aged between 20 to 30 years old	Smokers
American Society of Anaesthesiologists (ASA) Class I Individuals	History of Recent Anticoagulant, Aspirin, or NSAIDs (Non-Steroidal Anti-Inflammatory Drugs) for the last 3 months.

3.4 Fabrication of LyPRF and FPRF

The fabrication protocol is illustrated in Figure 3.3. Venous blood was collected without anticoagulant into 10 mL vacuum-sealed tubes (Dr. Choukroun's Glass A-PRF Tubes; Process for PRF, Nice, France) and processed within 1 minute following Choukroun's protocol. Centrifugation was carried out at 3000rpm (approximately 400 x g) for 10 minutes using a standard tabletop centrifuge (Kubota Compact Tabletop Centrifuge, Model 2420; Kubota Corporation, Tokyo, Japan), resulting in the separation of three distinct layers: an upper acellular plasma layer, a middle PRF clot, and a lower red blood cell layer (Ngah *et ah,* 2021a).

The PRF layer, located between the plasma and red blood cell layers, was carefully extracted using sterile forceps, and any residual red blood cells were trimmed with sterile surgical scissors. The harvested PRF clots were measured, recorded, and initially stored at -80 °C in a biomedical freezer (SANYO MDF-U73VC VIP Series; Panasonic Healthcare, Japan). A portion of the samples was then lyophilised overnight at -51 °C using a freeze-dryer machine (Labconco FreeZone 2.5 Liter Benchtop Freeze Dryer) to produce LyPRF for subsequent physicochemical and biological analyses (Figure 3.1). Following lyophilisation, both the LyPRF samples and the remaining frozen PRF samples (FPRF) were stored at -20 °C in a biomedical freezer (SANYO MDF-U537; Panasonic Healthcare, Japan) until further analysis in this study.

Figure 3.1 Labconco FreeZone 2.5 Liter Benchtop Freeze Dryer

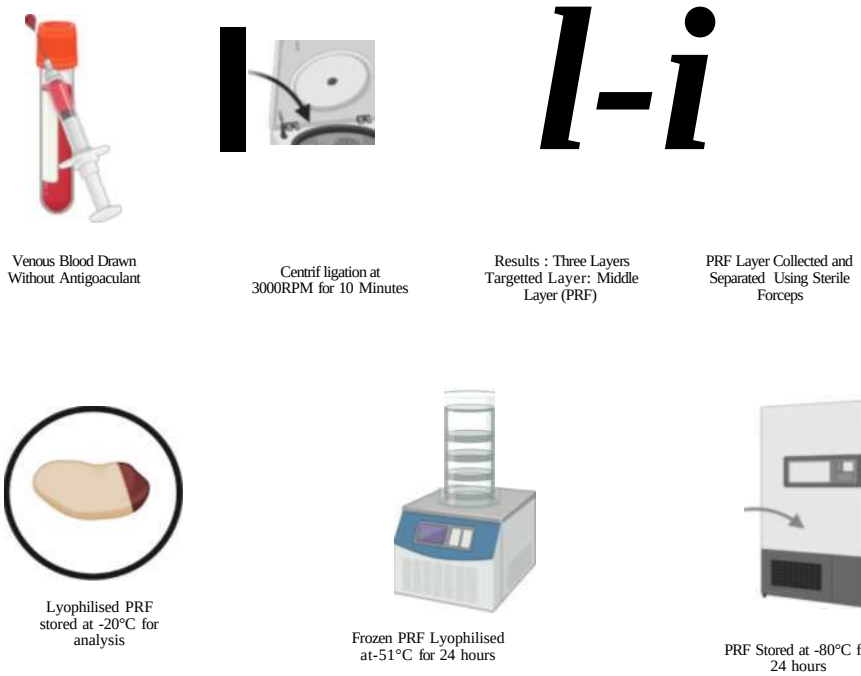

Figure 3.2 Schematic Representation of The Fabrication Protocol for LyPRF, Outlining Blood Collection, Centrifugation, Fibrin Clot Isolation, Freezing, and Lyophilisation Steps

Following the fabrication of LyPRF and FPRF, the resulting samples were carefully weighed to determine their initial mass prior to further physicochemical and biological analyses. Sample weights were measured using a calibrated analytical balance (GF3000, AND Instruments, Japan) with a readability of 0.1 mg to ensure high precision. Prior to weighing, the balance was levelled and tared to ensure accuracy, and the measurements were conducted under controlled environmental conditions to minimise measurement variability. After the weight of the samples was recorded, the mean weight was calculated to assess uniformity between preparations.

3.5 Scanning Electron Microscopy (SEM) Analysis

Lyophilised platelet-rich fibrin (LyPRF) samples were prepared for morphological observation using scanning electron microscopy (SEM). The samples were initially fixed in 2.5% glutaraldehyde (Sigma-Aldrich, USA) for 1 hour at room temperature to preserve their microstructural architecture. Subsequently, the samples were dehydrated through a graded ethanol series of 20%, 40%, 60%, and 80% (Merck,

Germany) for 10 minutes at each concentration. After dehydration, the samples were air-dried and sputter-coated with a thin layer of palladium (Quorum SC7620 SEM Sputter Coater) to improve electrical conductivity and imaging quality (Figure 3.4).

Figure 3.3 Quorum SC7620 SEM Sputter Coater

Field emission scanning electron microscopy (FESEM) imaging of LyPRF was performed using a Thermo Scientific Apreo 2S at magnifications of 200x, 600x, 1000x, and 1200x under an accelerating voltage of 5 kV. Complementary SEM analysis was carried out using a Hitachi TM3000 at similar magnifications and voltage settings (Figure 3.5). Both analyses were conducted to evaluate surface morphology, fibrin network organization, fibrin thickness, porosity, and interconnectivity. Identical sample preparation and imaging protocols were applied to FPRF samples, which served as the control group for comparative morphological assessment (Ngah *et ah*, 2021a; Wong *et ah*, 2017).

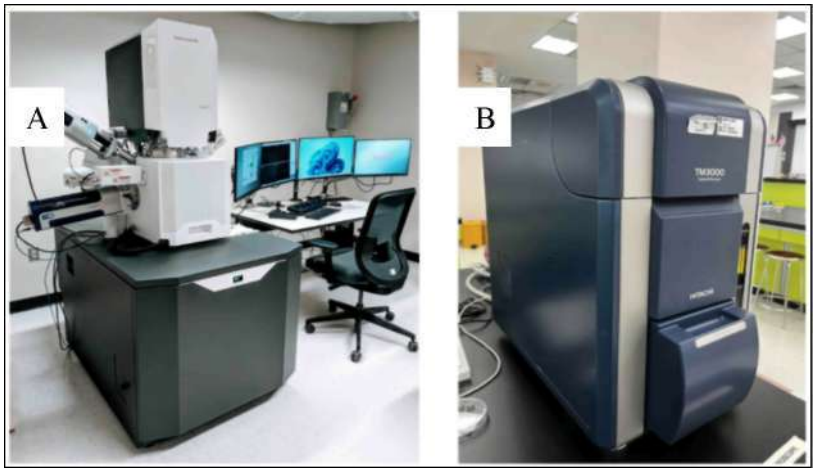

Figure 3.4 SEM analysis: (A) Thermo Scientific Apreo 2S and (B) Hitachi TM3000

3.6 Energy Dispersive X-ray (EDX) Analysis

Energy dispersive X-ray (EDX) analysis was performed to determine the elemental composition of LyPRF, with the same procedure applied to FPRF samples for comparative evaluation(Ngah *et ah,* 2024; Wong *et ah,* 2021b). The analysis was conducted using an EDX detector integrated with the FESEM system under high vacuum conditions and an accelerating voltage of 15kV to ensure optimal X-ray generation and detection. Spectra were collected from multiple regions of each sample to provide representative elemental profiling. Elements were identified based on their characteristic energy peaks, and their weight (%) and atomic (%) compositions were quantified using the system's software. Additionally, elemental mapping was performed to visualise the spatial distribution of major components, including carbon (C), oxygen (O), calcium (Ca), and phosphorus (P), within the fibrin matrix. Comparative analysis between LyPRF and FPRF was then conducted to assess compositional changes associated with the lyophilisation process.

3.7 Fourier Transform Infrared Spectroscopy (FTIR) Analysis

Fourier Transform Infrared Spectroscopy (FTIR) was employed to identify the functional molecular groups present in LyPRF and FPRF. Samples were trimmed to approximately 0.5 cm x 0.5 cm and directly placed on the sample stage of the FTIR Spectrometer (PerkinElmer Spectrum One FT-IR Spectrometer). Spectral acquisition was conducted according to the manufacturer's protocol (Haghparast-Kenarsari *et ah,*

2024). The characteristic absorption peaks associated with essential biochemical groups, such as amide I, amide II, amide III, hydroxyl, and carboxyl functional groups, were identified in the FTIR spectra that were generated. A comparative analysis was conducted using FPRF, which allowed for the assessment of the biochemical fidelity of LyPRF. This approach confirmed the retention of functional groups that are indicative of the integrity of the fibrin matrix and platelet-derived proteins (Xie *et al.*, 2019). FTIR analysis was conducted in triplicate to validate the consistency of the results.

3.8 X-Ray Diffraction (XRD) Analysis

X-ray diffraction (XRD) analysis was performed to investigate the crystallographic structure and phase composition of LyPRF and FPRF using a PANalytical X'Pert Pro system. Samples were carefully crushed to fit the XRD holder, ensuring a uniform and flat surface, and securely mounted with adhesive to prevent displacement during scanning. Measurements were carried out using Cu Kα radiation ($\lambda = 1.5406$ Å) at 45 kV and 40 mA. Scans were performed over a 2θ range of 5°–90° at a rate of 2°/min with a step size of 0.02°, and additional scans at 8°/min over 20°–70° were conducted to ensure detailed peak resolution. The resulting diffraction patterns were analysed to identify crystalline phases, semi-crystalline features, and potential impurities within the fibrin matrix (Sui *et al.*, 2023a). To ensure reproducibility and consistency, all analyses were performed in triplicate.

3.9 Kinetic Release Pattern of PDGF-AB, PDGF-BB, TGF-β1

The spatiotemporal release kinetics of selected growth factors from LyPRF and FPRF were quantified using an ELISA kit for PDGF-AB, PDGF-BB, and TGF-β1 (ELK Biotechnology Co., Ltd. ELISA Kits). PDGF-AB and TGF-β1 were the analytes that were specifically targeted. To produce the conditioned media, the initial weight of each sample was standardised using the average weight of intact LyPRF and FPRF clots. The samples were subsequently incubated in 6-well plates at 37°C under a humidified 5% CO atmosphere for 21 days in 4 mL of Dulbecco's Modified Eagle Medium (DMEM; low glucose with L-glutamine and sodium pyruvate; Biosera, France; Biosera, France). At predetermined intervals (days 1, 7, 14, and 21), the

conditioned media were collected and promptly replaced with an equivalent volume of fresh DMEM following each collection. All harvested media were stored at –80°C until they were subjected to additional analysis. The ELISA assay was performed in accordance with the manufacturer's instructions. A microplate reader (Synergy™ HTX, BioTek Instruments, USA) was employed to measure absorbance at 450 nm, with a reference wavelength of 540 nm. The results were reported as the mean ± standard deviation, and all measurements were performed in triplicate. The temporal release profiles of the growth factors were evaluated through statistical analysis (Xu *et al.*, 2018a).

3.10 MTT [3-(4,5-Dimethylthiazol-2-yl)-2-5-Diphenyltetrazolium Bromide] Assay

Human gingival fibroblasts (HGF) were used in this study to evaluate the proliferative response to lyophilised PRF (LyPRF) and frozen PRF (FPRF). The cells were cultivated in complete Dulbecco's Modified Eagle Medium (DMEM) supplemented with 10% foetal bovine serum (FBS) (Sigma-Aldrich, Merck KGaA, Germany) and 1% penicillin-streptomycin (Gibco™, Thermo Fisher Scientific, USA). The medium was refreshed every three days, and the cultures were maintained at 37 °C in a humidified incubator with 5% CO (Izumiya *et al.*, 2021). Cells from passages P3 to P10 were used for all experiments to ensure consistency. All instruments and consumables were sterilised using 70% ethanol (Chemiz®, Chemiz Sdn. Bhd., Malaysia) and exposed to ultraviolet light for 30 minutes. Media and reagents were pre-warmed in a 37°C water bath, and all procedures were conducted in a Class II biosafety cabinet (Esco Lifesciences Class II Biological Safety Cabinet) under sterile conditions.

LyPRF samples were pre-equilibrated in complete DMEM at 37°C with 5% CO prior to cell seeding. After equilibration, the LyPRF samples were retrieved for cell proliferation analysis (Huang *et al.*, 2020). The MTT assay was performed to evaluate cell proliferation at 24, 48, and 72 hours, in accordance with the manufacturer's guidelines. The wells were treated with MTT reagent at each time point, and the formazan crystals that were produced by metabolically active cells were dissolved in dimethyl sulfoxide (DMSO) (Sigma-Aldrich, Merck KGaA, Germany). Absorbance

was measured at 570 nm using a microplate spectrophotometer. The data were presented as the mean ± standard deviation, and all experiments were conducted in triplicate. To evaluate variations in cell proliferation over time and between groups, statistical analysis was implemented.

3.11 Statistical Analysis

Statistical analysis was performed to comprehensively evaluate the physical, structural, and biochemical properties of the fabricated FPRF and LyPRF samples. All quantitative data were expressed as mean ± standard deviation (SD) to represent data variability and ensure consistency across experimental assessments. Each experiment was performed at least twice, with samples prepared in triplicate (n = 3) for each volunteer at the designated intervals. Statistical analyses were conducted using GraphPad Prism software (GraphPad Prism 6, CA, USA), while schematic illustrations of the experimental workflow were generated using BioRender (BioRender.com).

The analysed parameters included physical measurements (weight and length), surface morphology and elemental composition (FESEM, EDX), structural characterisation (XRD), functional group identification (FTIR) and kinetic release pattern of growth factor (ELISA). Comparative analyses between FPRF and LyPRF groups were performed using either two-way analysis of variance (ANOVA) followed by Tukey's post hoc test or an unpaired *t*-test, depending on the dataset. Two-way ANOVA was applied to the MTT assay, ELISA kinetic release profiles, and SEM-based cell entrapment analysis, while unpaired *t*-tests were used for fibrin network thickness and porosity measurements obtained from SEM analysis. A p-value < 0.05 was considered statistically significant.

CHAPTER 4
RESULTS

4.1 Fabrication of Lyophilised Platelet Rich Fibrin and Frozen Platelet Rich Fibrin

Following venous blood collection and immediate centrifugation, the middle PRF layer was carefully extracted using a sterile forceps, together with a thin portion of the underlying red blood cell (RBC) layer (Choukroun *et ah,* 2017). The isolated fraction corresponded to the fibrin-rich clot, presenting as a yellowish structure consistent with previously described PRF morphology as illustrated in (Figures 4.1 A and 4. IB). To preserve the PRF for further analysis and applications, the clots were subjected to a two-step preservation process involving initial freezing followed by lyophilisation (Figure 4.1C and 4. ID).

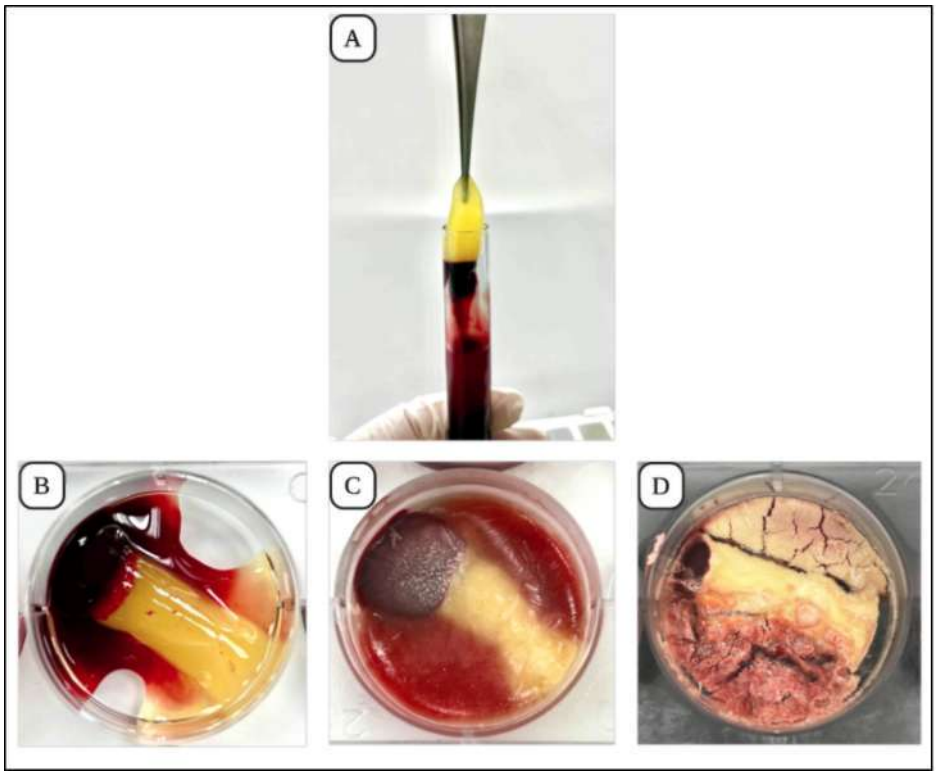

Figure 4.1 Fabrication of Platelet-Rich Fibrin. (A) Isolated PRF Matrix Fraction. (B) Fresh PRF. (C) Frozen PRF. (D) Lyophilised PRF

The weight of the observed PRF and LyPRF from the four samples were measured and shown in (Table 4.1). The FPRF had a mean weight of 1.11 ± 0.34 mg, and its mean length was reported as 3.18 ± 0.34 cm, whereas the mean weight for LyPRF was 0.14 ± 0.07 mg, and the mean length was 2.73 ± 0.26 cm. It was observed that weight loss of LyPRF in comparison to FPRF was approximately 87%. Additionally, the mean percentage of difference in length of the two sample phases were observed to be 14%. Statistical analysis revealed a significant reduction in the weight of LyPRF compared to FPRF ($P < 0.05$). In contrast, no statistically significant difference was observed in sample length between the two groups ($P > 0.05$) (Figure 4.2 and 4.3) display the physical and morphological differences between FPRF and LyPRF.

Table 4.1 Comparative Weight and Length of FPRF and LyPRF.

		Sample A	**Sample B**	**Sample C**	**Sample D**	**Mean ± SD**	*Statistics" (df)*	*P-Value"*
Weight (mg)	LyPRF	0.12	0.08	0.24	0.13	0.14 ± 0.07	0.0096	**"
	FPRF	1.00	0.76	1.58	1.10	1.11 ± 0.34		
Length (cm)	LyPRF	2.50	3.10	2.70	2.60	2.73 ± 0.26	0.0843	***ns*[c]
	FPRF	2.70	3.50	3.20	3.30	3.18 ± 0.34		

[a] Unpaired t-test

[b] The mean weight of the samples is significantly different by post-hoc test (Welch's t-test)

[b] The mean length of the samples is not significantly different by post-hoc test (Welch's t-test)

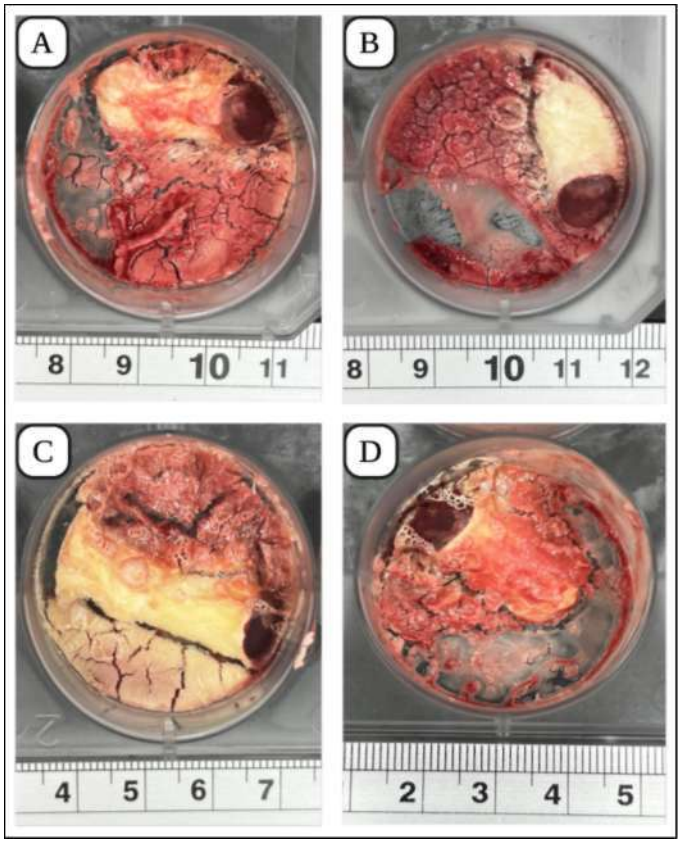

Figure 4.2 Lyophilised PRF (A, B, C, D) display variations in the size and shape

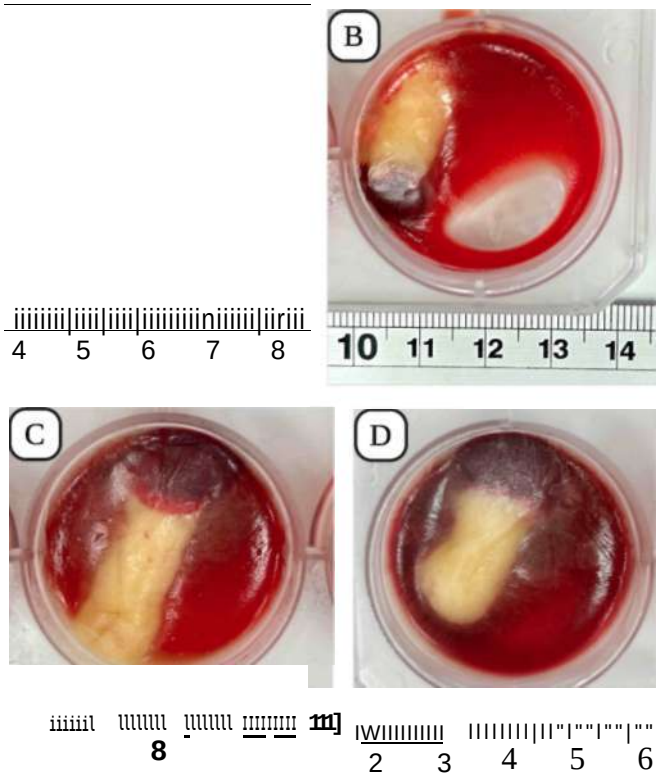

Figure 4.3 Frozen PRF (A, B, C, D) Display Variations in The Size and Shape

4.2 Microstructure of LyPRF and FPRF Analysed using FESEM

4.2.1 Surface Morphology

The surface morphology of LyPRF and FPRF observed using FESEM were revealed to have distinct differences. LyPRF exhibited a highly porous, sponge-like architecture with rough surface morphology and visible pores (Figure 4.4). In contrast, FPRF showed an irregular fibrin matrix with fewer visible pores and smoother surface features, reflecting its hydrated, gel-like state (Figure 4.5).

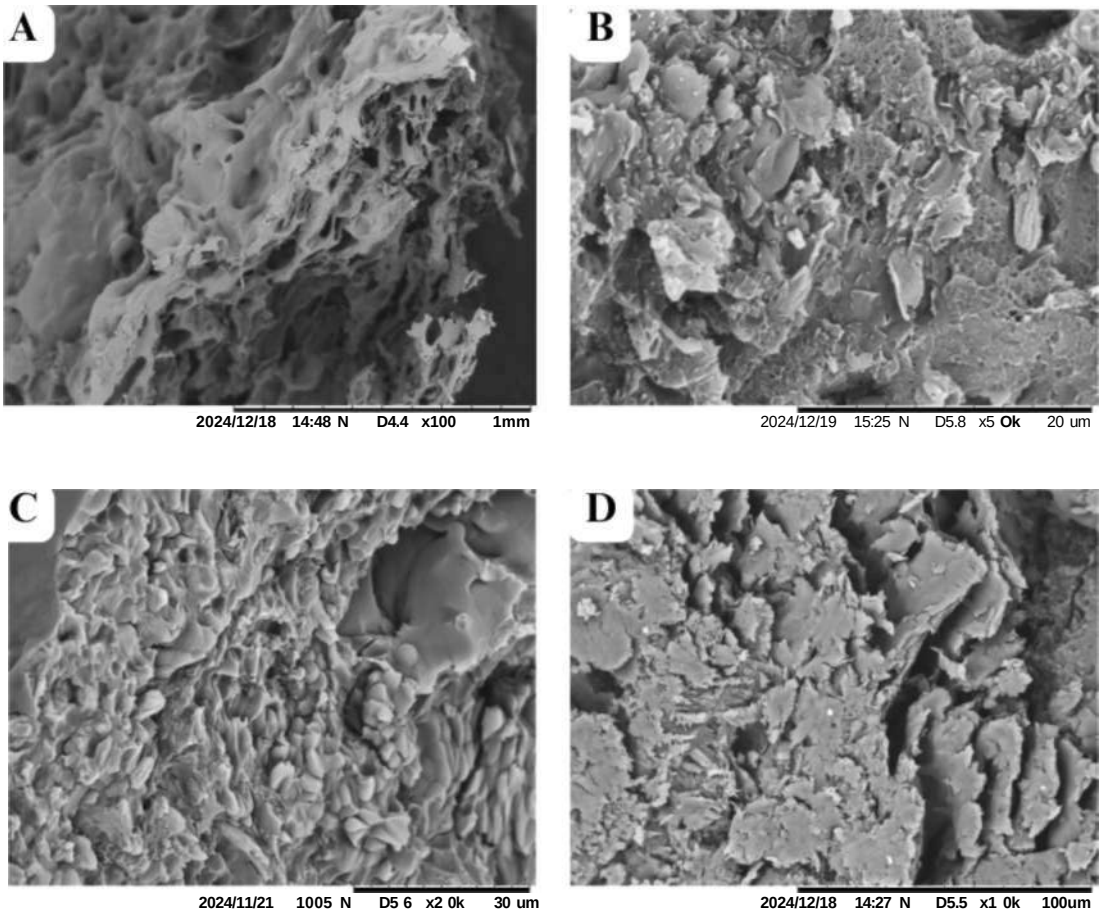

Figure 4.4 Representative SEM Micrographs of The Microstructure of LyPRF Showing its Porous Surface Morphology. SEM Scale bar: (A) 1mm, (B) 20um, (C) 30um, (D) lOOum.

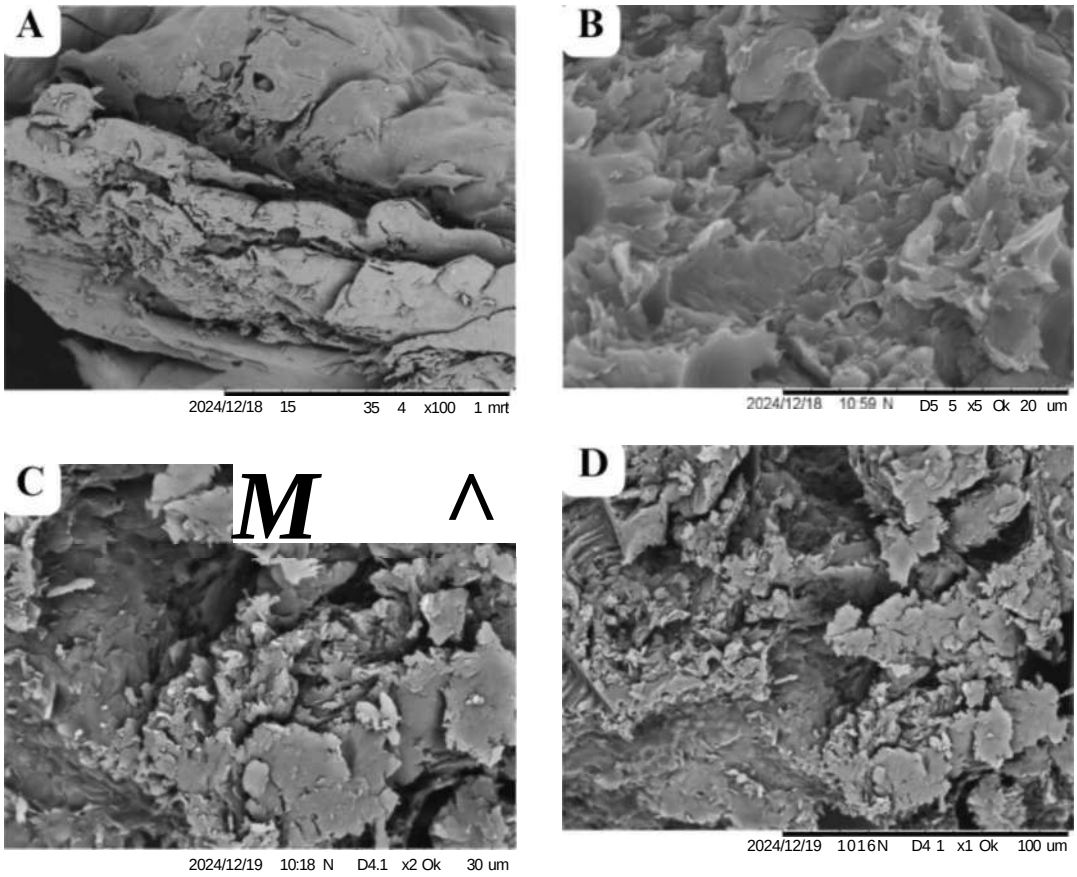

Figure 4.5 Representative SEM Micrographs of The Microstructure of FPRF Showing Its Loose Surface Morphology. SEM Scale bar: (A) 1mm, (B) 20um, (C) 30um, (D) lOOum.

4.2.2 Porosity

Cross-sectional analysis of the porous microstructure in LyPRF and FPRF revealed clear differences in pore morphology and distribution, as summarised in (Table 4.2) and illustrated in (Figures 4.6 and 4.7). LyPRF exhibited larger and more heterogeneous pores, with a mean pore size of 97.85 ± 58.06 µm. In contrast, FPRF demonstrated comparatively smaller pore dimensions, with a mean pore size of 54.79 ± 54.67 µm. However, the difference in mean pore sizes between LyPRF and FPRF is not statistically significant (P>0.05). Qualitative microstructural evaluation further revealed that LyPRF possessed a more interconnected pore network, whereas FPRF primarily exhibited isolated, concave depressions with limited interconnectivity. Collectively, these observations suggest that although LyPRF demonstrates a more favourable and interconnected pore architecture, the quantitative differences in pore size did not reach statistical significance.

Table 4.2 Mean Pore Size, P-value, and Statistical Comparison Between LyPRF and FPRF.

	Mean Pore Size (± SD)	*Statistics*[11] **(df)**	*P - value"*
LyPRF	97.85 ± 58.06 µm	0.0287	*[b]
FPRF	54.79 ± 54.67 µm		

[a] Unpaired t-test

[b] The mean pore size of the samples is significantly different by post-hoc test (Welch's t-test)

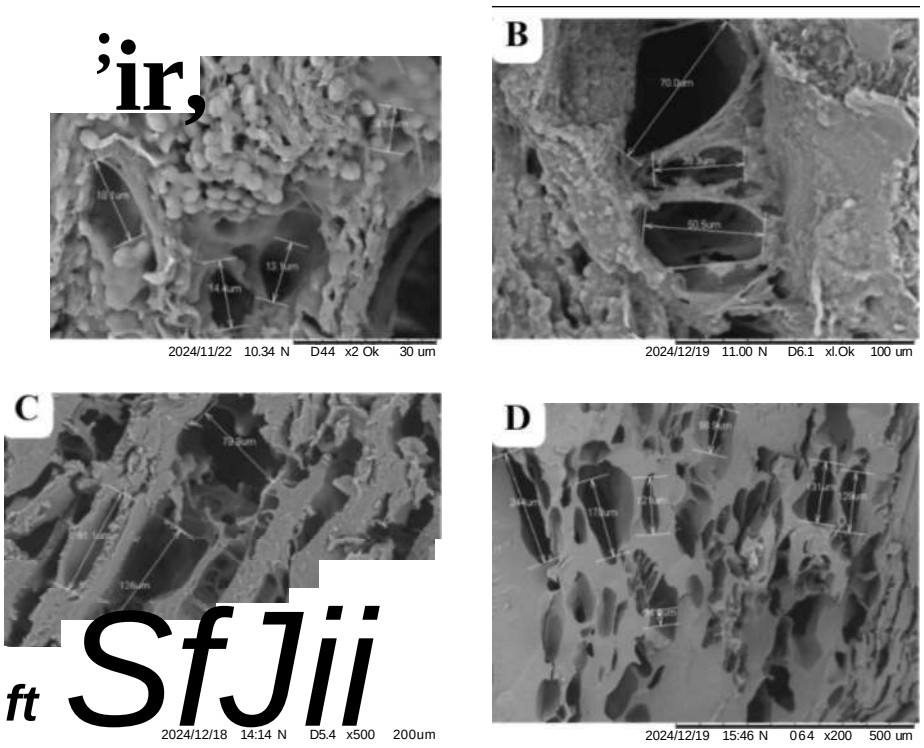

Figure 4.6Cross-Sections of LyPRF Demonstrating Its Porosity and Measurements of The Mixture of Different Pore Sizes. SEM Scale Bar: (A) 30um, (B) lOOum, (C) 200um, (D) 500um.

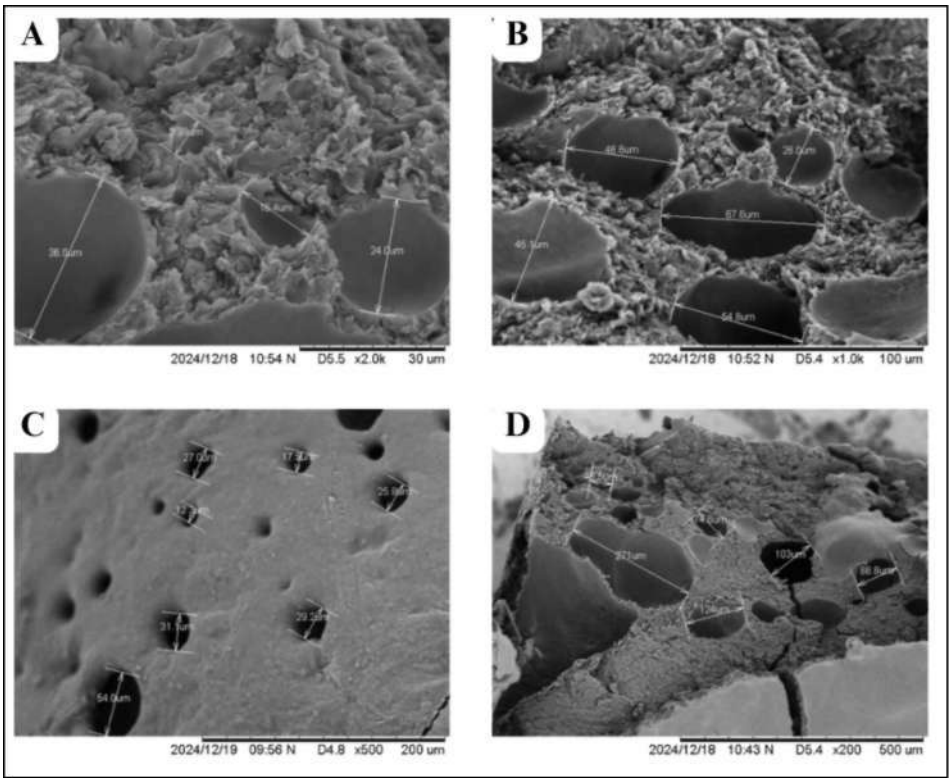

Figure 4.7Cross-Sections of FPRF Demonstrating Its Porosity and Measurements of The Mixture of Different Pore Sizes. SEM Scale Bar: (A) 30um, (B) lOOum, (C) 200um, (D) 500um.

4.2.3 Fibrin Network

FESEM analysis revealed that LyPRF exhibited a more established 3D fibrin framework in the cross-sectional view compared to FPRF. This observation was supported by fibrin thickness distribution analysis derived from SEM measurements, which demonstrated that LyPRF possessed a broader range of fibrin network sizes from 0.5 to 3.5 µm, whereas FPRF exhibited a narrower distribution limited to 0.0 to 2.0 µm, as summarised in (Table 4.3). Quantitative comparison of mean fibrin network thickness further indicated that LyPRF had significantly larger fibrin structures (1.278 ± 0.491 µm) compared to FPRF (0.561 ± 0.305 µm) (Table 4.4). The disparity between fibrin thickness of LyPRF and FPRF is statistically significant (P<0.005) as illustrated in figure 4.8 and 4.9. Morphologically, the fibrin network in LyPRF appeared as a densely well-distributed, interconnected mesh with uniform porosity and clearly distinguishable fibrin strands. In contrast, FPRF exhibited a more compact and less defined fibrin architecture, characterised by loosely packed fibres and reduced interconnectivity, likely attributable to its hydrated and frozen state.

Table 4.3. Frequency Distribution of The Fibrin Networks in LyPRF and FPRF.

Bin ***(fim)***	**LyPRF**	**FPRF**
0.0 - 0.5	0	151
0.5 - 1.0	89	119
1.0 - 1.5	138	29
1.5 - 2.0	39	1
2.0 - 2.5	24	0
2.5 - 3.0	8	0
3.0 - 3.5	2	0
Total Value	**300**	**300**

Table 4.4 Mean Fibrin Network Size and Corresponding P-value for LyPRF and FPRF.

	Mean Fibrin Size (± SD)	*Statistics"* **(df)**	*P - Value"*
LyPRF	1.278 ± 0.491	0.0059	**[b]
FPRF	0.561 + 0.305		

[a] Unpaired t-test

[b] The mean fibrin size of the samples is significantly different by post-hoc test (Welch's t-test)

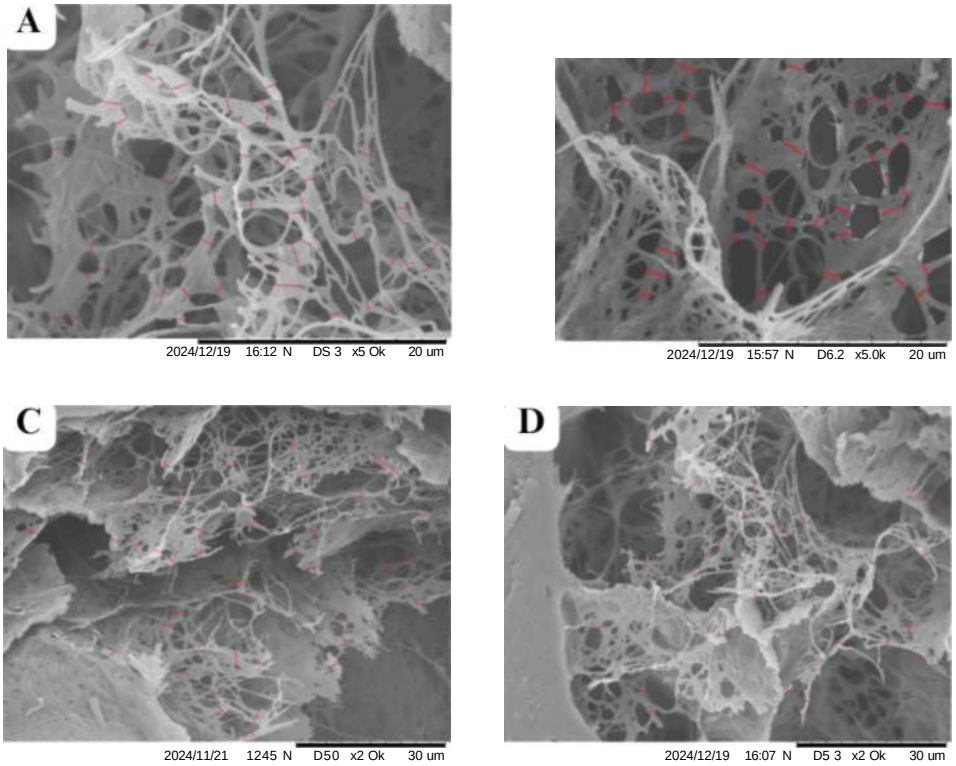

Figure 4.8Microstructure of LyPRF Showing a Porous and Loosely Arranged Fibrin Network. SEM Scale Bar: (A) 20um, (B) 20um, (C) 30um, (D) 30um.

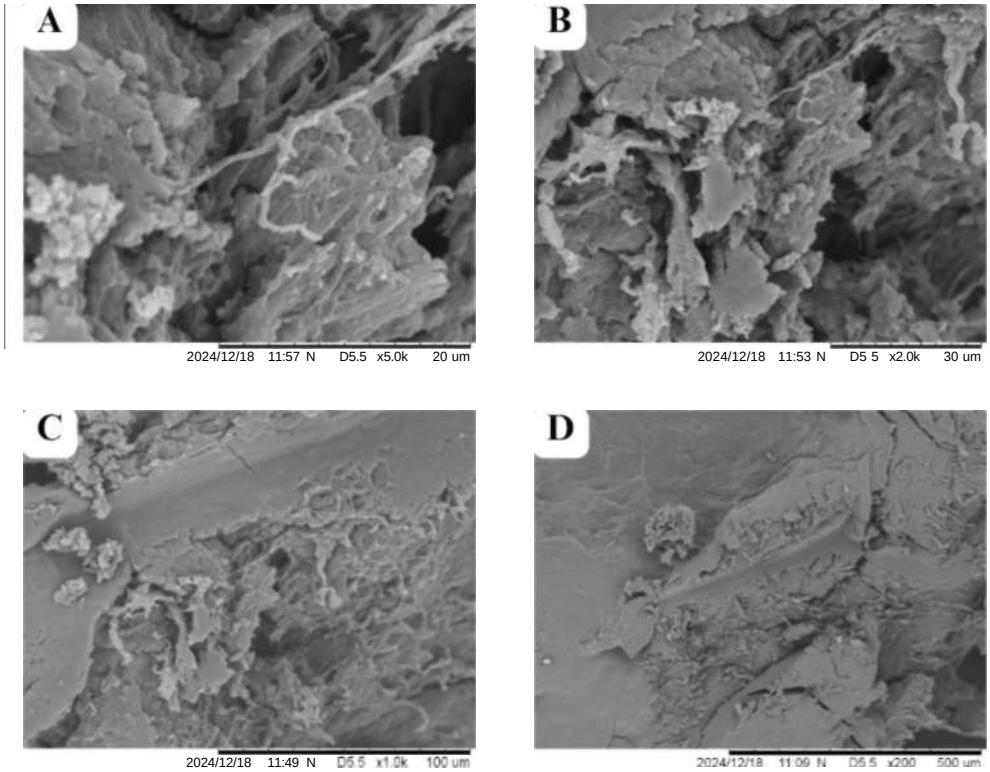

Figure 4.9Microstructure of FPRF Displaying a Compact and Less Defined Fibrin Network. SEM Scale Bar: (A) 20um, (B) 20um, (C) 30um, (D) 30um.

4.2.4 Cell Entrapment

Analysis of cell entrapment, including platelets (~2-4 µm) and leukocytes (~6-15 µm), within LyPRF and FPRF revealed notable differences in both distribution and density, with mean values reported in (Table 4.5) and representative images shown in (Figures 4.10 and 4.11). LyPRF demonstrated a higher concentration of entrapped cells, with both platelets and leukocytes clearly visualised throughout its porous, interconnected fibrin matrix. In contrast, FPRF showed sparse cellular components, predominantly localised near the surface, with fewer cells embedded within its dense fibrin network. Notably, leukocytes in FPRF were not clearly observable under SEM, in contrast to LyPRF where they were readily visualised. Quantitatively, the mean platelet size in LyPRF was 3.852 µm ± 0.422 µm and the mean leukocyte size was 6.076 µm ± 0.490 µm, while the platelets observed in FPRF measured 2.034 µm ± 1.060 µm. The analysis revealed statistically significant differences between LyPRF platelets and LyPRF leukocytes ($p < 0.005$), as well as between LyPRF platelets and FPRF platelets ($p < 0.005$). A more pronounced difference was observed between LyPRF leukocytes and FPRF platelets ($p < 0.0001$), indicating distinct cellular distributions and preservation profiles between LyPRF and FPRF. Overall, these findings highlight the differences in cell sizes, allowing more accurate quantification in LyPRF compared to FPRF. Therefore, these findings indicate that LyPRF provides superior quantification and quality of cellular components, due to its interconnected porous structure compared to FPRF.

Table 4.5 Observed Sizes of Platelets and Leukocytes in LyPRF and FPRF.

		Mean Cell Size (± SD)	*Statistics*[11] **(df)**	*P - Value"*
Platelets	**LyPRF**	3.852 µm ± 0.422 µm	0.0081	**[b]
	FPRF	2.034 µm ± 1.060 µm		
Leukocytes	**LyPRF**	6.076 µm ± 0.490 µm		
	FPRF			

[a] Two-Way ANOVA test

[b] The mean cell size of the samples is significantly different by post-hoc test (Turkey's test)

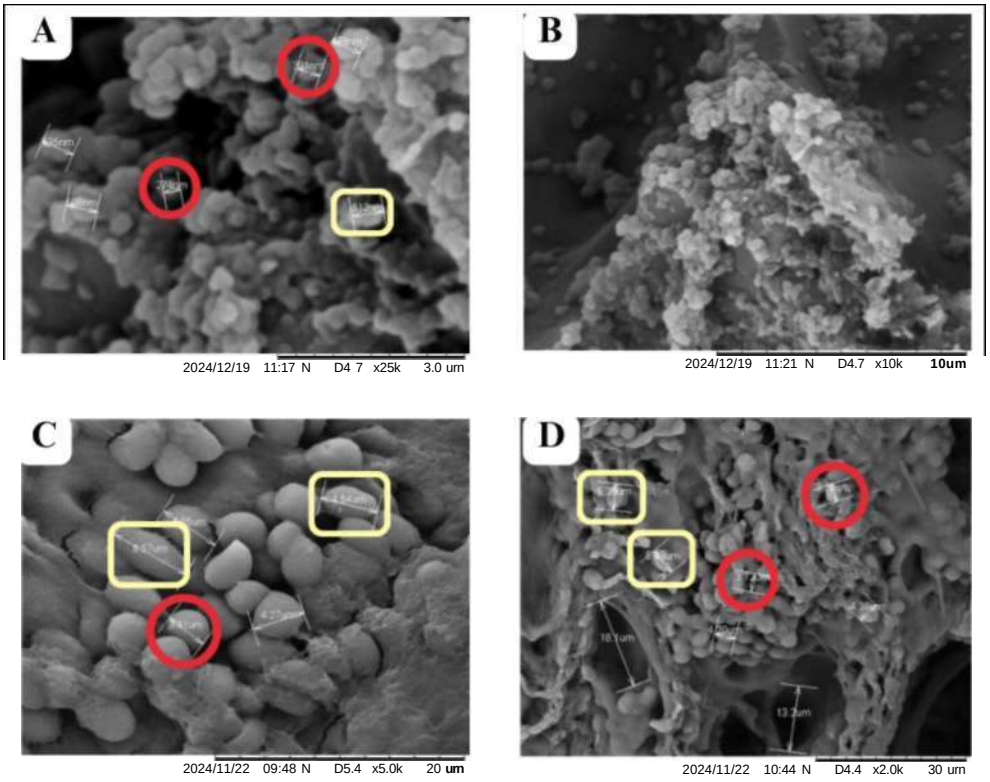

Figure 4.10 SEM Micrographs of LyPRF Showing Cells Within a Porous Fibrin Matrix. Red Circles: Platelets; Yellow Squares: Leukocytes. SEM Scale Bar: (A) 3.0um, (B) lOum, (C) 20um, (D) 30um.

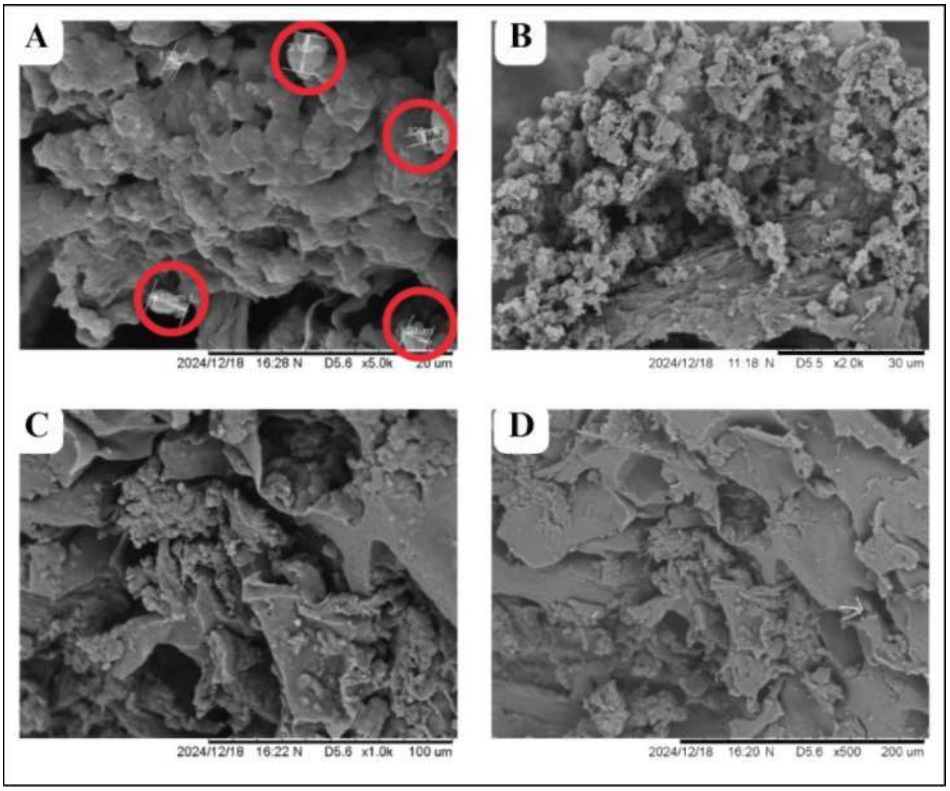

Figure 4.11 SEM Micrographs of FPRF Showing Cells Within a Porous Fibrin Matrix. Red Circles: Platelets. SEM Scale Bar: (A) 20um, (B) 30um, (C) lOOum, (D) 200um.

4.3 Energy Dispersive X-Ray Spectroscopy (EDX) Analysis

An EDX analysis was performed to ascertain the confirmation of PRF's elemental composition in both samples. The analysis revealed that LyPRF and FPRF contained a predominant number of essential elements that are frequently found in biological tissue, including carbon (C), oxygen (O), calcium (Ca), and phosphorus (P) (Figure 4.12). In LyPRF, carbon constituted 69.95 wt%, followed by nitrogen at 17.38 wt% and oxygen at 7.27 wt%. Comparatively lower values were observed in FPRF, with carbon, nitrogen, and oxygen accounting for 68.94 wt%, 16.38 wt%, and 6.65 wt%, respectively. Furthermore, trace amounts of calcium and phosphorus were detected in both groups, with a higher phosphorus content observed in LyPRF and a higher calcium content observed in FPRF. In FPRF, calcium and phosphorus were recorded at 0.28 wt% and 0.74 wt%, respectively, whereas LyPRF exhibited 1.19 wt% phosphorus and 0.08 wt% calcium.

Additionally, magnesium (Mg), zinc (Zn), silicon (Si), copper (Cu), and iron (Fe), were identified in trace amounts in both LyPRF and FPRF, with slight variations between the two biomaterials. The presence of these elements, along with other minor constituents, is illustrated in (Figure 4.12). Overall, LyPRF exhibited a higher relative abundance of elemental components compared to FPRF. Both samples were predominantly composed of organic elements (C, N, O), while mineral-associated elements, including Ca, P, Mg, Zn, Fe, Si, and Cu, were detected in trace amounts. Therefore, the presence of these elements may contribute to better bioactivity and cellular interactions of the biomaterial.

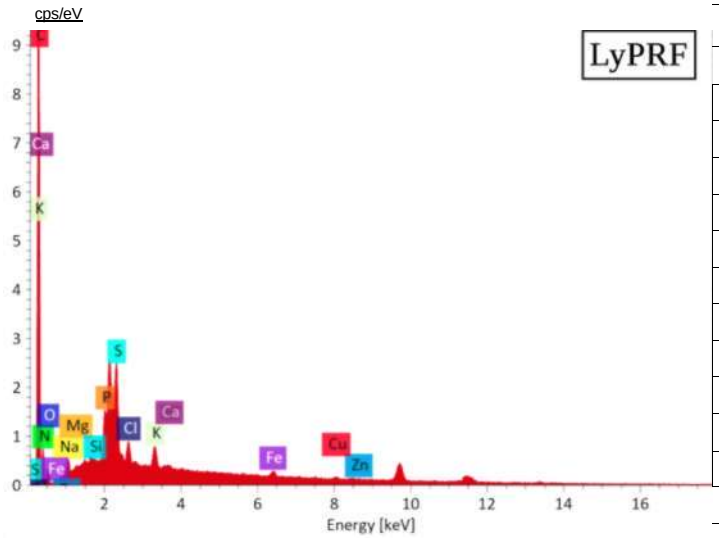

Element	Mass Norm (%)
Carbon (C)	69.95
Nitrogen (N)	17.38
Oxygen(O)	**7.27**
Sulphur (S)	1.97
Sodium (Na)	-
Chlorine (CI)	0.46
Phosphorus (P)	**1.19**
Potassium (K)	0.46
Iron (l-'e)	0.25
Calcium (Ca)	0.08
Zinc (Zn)	0.12
Copper (Cu)	0.12
Silicon (Si)	0.04
Magnesium (Mg)	0.04

FPRF

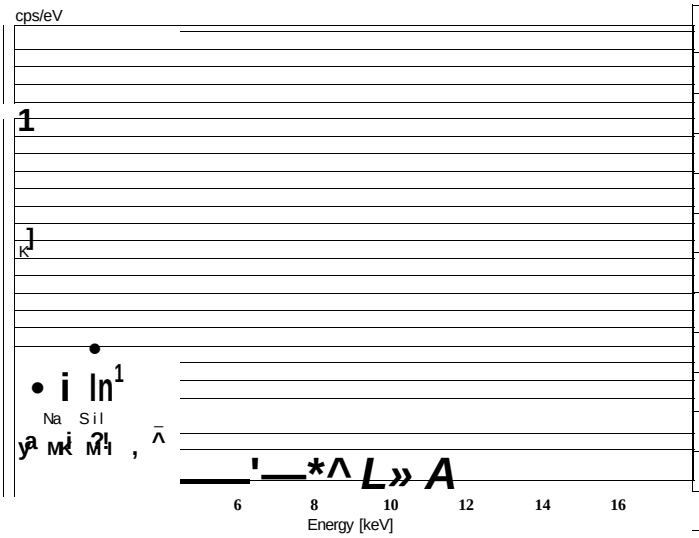

Element	Mass Norm (%)
Carbon (C)	68.94
Nitrogen (N)	16.38
Oxygen (0)	6.65
Sulphur (S)	2.48
Sodium (Na)	**1.31**
Chlorine (CI)	**1.95**
Phosphorus(P)	**0.74**
Potassium (K)	0.38
Iron (Fe)	0.45
Calcium (Ca)	0.28
Zinc (Zn)	0.20
Copper (Cu)	0.16
Silicon (Si)	0.04
Magnesium (Mg)	0.03

Figure 4.12 EDX Analysis of Samples (A) LyPRF, and (B) FPRF, Presenting FESEM Micrograph, and Corresponding Elemental Spectra

4.4 Fourier-Transform Infrared Spectroscopy (FTIR) Analysis

FTIR spectroscopy was conducted to assess the preservation of key biochemical components in LyPRF and FPRF, with particular emphasis on amide I, amide II, O-H, and N-H functional groups. The FTIR spectra of both LyPRF and FPRF, recorded over the range of 4000-650 cm^{-1}, are presented in (Figure 4.13). Both samples displayed characteristic absorption bands corresponding to amide I (-1650 cm^{1}) and amide II (-1540 cm^{1}), indicating the retention of protein secondary structures following the respective preservation processes. In addition, a broad absorption band observed at approximately -3300 $cirr^{1}$ in both groups was attributed to O-H and N-H stretching vibrations, reflecting the presence of hydrogen bonding within the protein matrix. Collectively, these results confirm that the essential protein-related biochemical features of PRF were well preserved in both lyophilised and frozen forms, demonstrating that neither preservation method caused significant alterations to the molecular integrity of the fibrin-based matrix.

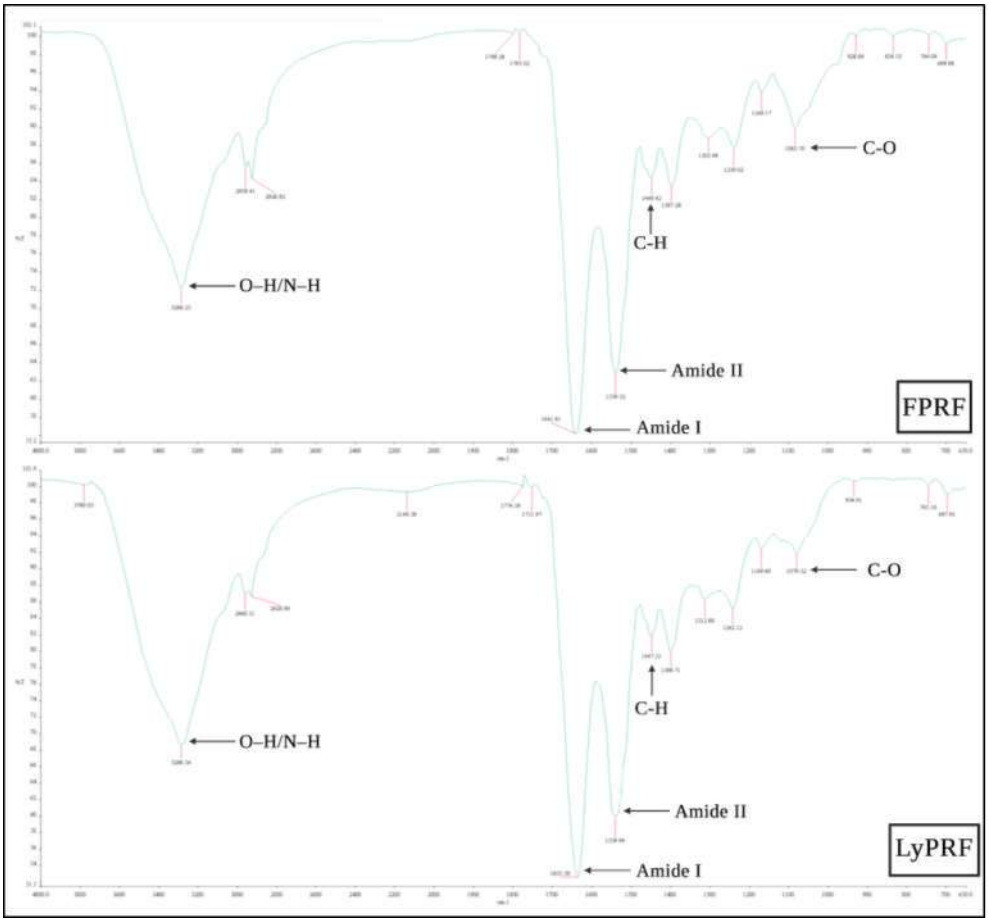

Figure 4.13 FTIR Spectra of (A) FPRF, and (B) LyPRF, Indicating Characteristic

Peaks Corresponding to O-H/N-H Stretching, Amide I, and Amide II Bands

4.5 X-Ray Diffraction

The XRD analysis was performed to examine the crystalline characteristics of LyPRF and FPRF samples (Figure 4.14). All samples exhibited broad diffraction patterns, indicating a largely amorphous structure consistent with fibrin-based biomaterials. A notable diffraction peak was observed in the range of 30°-31° (29) across both LyPRF and FPRF, suggesting the presence of crystalline calcium phosphate phases. LyPRF generally display a more prominent peak intensity in this region in comparison to FPRF. Additional minor peaks were detected at lower intensities, but no other major diffraction peaks were observed. These results confirm the presence of limited crystalline content, with LyPRF samples exhibiting slightly higher peak intensities than FPRF.

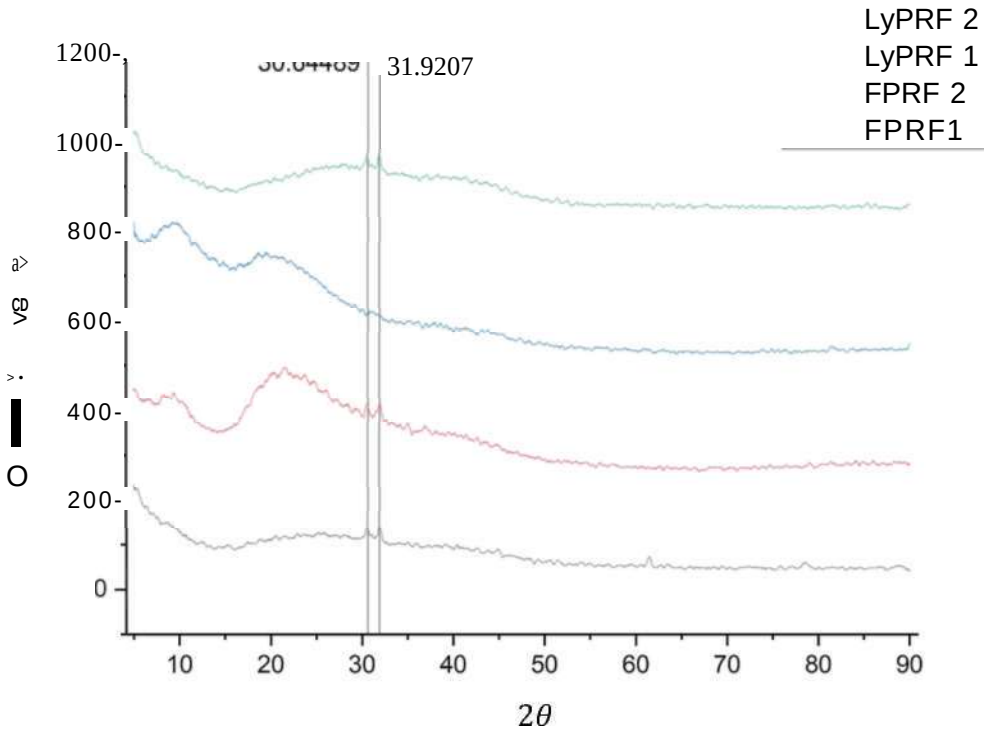

Figure 4.14 XRD Patterns of Samples FPRF and LyPRF, Illustrating the Crystalline Phases and Comparing the Diffraction Peaks Associated with Their Structural Composition

4.6 Enzyme-Linked Immunosorbent Assay (ELISA)

4.6.1 Kinetic Release Pattern of PDGF-AB, PDGF-BB, and TGF-β1

The kinetic release patterns of PDGF-AB, PDGF-BB, and TGF-β1 from LyPRF and FPRF were quantitatively evaluated over a 21-day period utilising a commercial ELISA assay technique. The calibration data for each growth factor are presented in Figure 4.15 as bar graphs, illustrating the relationship between optical density and concentration and ensuring accurate quantification across the measured range. Notably, PDGF-AB and PDGF-BB exhibited a characteristic biphasic kinetic release pattern released in two stages. This is defined by initial rapid initial burst phase, where a substantial amount of the growth factor is rapidly liberated from the PRF matrix. This is followed by a second, slower sustained phase, during which the remaining growth factors are gradually released as the fibrin network continues to degrade. This two-stage release pattern reflects the combined influence of surface-associated release and deeper matrix-controlled release mechanism. In contrast, TGF-β1 demonstrated a distinctly different release profile, characterised by a single early peak followed by a gradual, continuous decline with no subsequent secondary peaks.

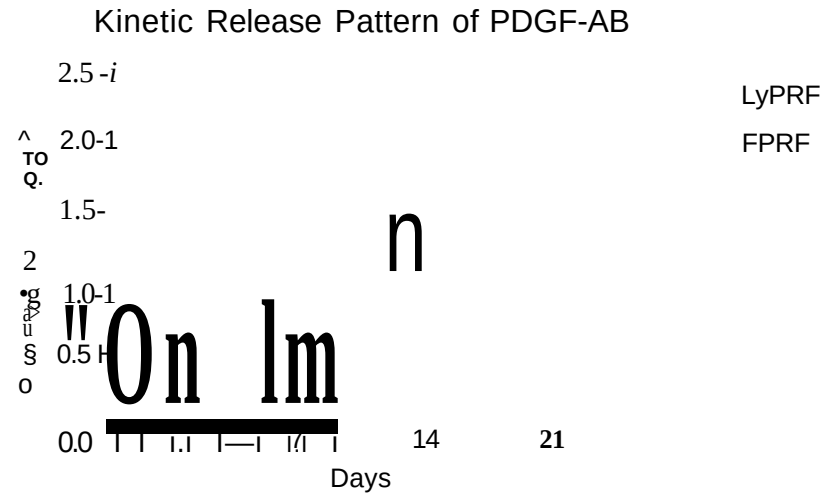

ure 4.15 Kinetic Release Pattern of PDGF-AB, PDGF-BB, and TGF-P, from FPRF and LyPRF over 21 days

The concentrations of PDGF-AB analysed and reported in (Table 4.6) demonstrated a distinct biphasic release pattern in both LyPRF and FPRF. This pattern was characterised by an initial burst release within the first 24 hours, followed by a continuous and sustained release phase up to day 14. Notably, LyPRF exhibited a higher initial PDGF-AB release (1.045 ± 0.682 pg/ml) compared to FPRF (0.761 ± 0.475 pg/ml), suggesting that the lyophilisation process facilitates sustained release of bioactive molecules. The peak release occurred on day 14, with LyPRF reaching 1.562 ± 0.487 pg/ml and FPRF attaining 1.019 ± 0.482 pg/ml. Overall, the extended-release profile observed in LyPRF indicates enhanced molecular stability and sustained matrix integrity following lyophilisation, thereby supporting prolonged bioavailability of PDGF-AB.

Table 4.6 Kinetic Release Pattern of PDGF-AB.

Days	**LyPRF (pg/ml)**	**FPRF (pg/ml)**	*Statistics*[11] **(df)**	*P - value"*
1	1.045 ± 0.682	0.761 ± 0.474	0.4286	*ns*[b]
7	0.986 ± 0.529	0.528 ± 0.209		
14	1.562 ± 0.487	1.019 ± 0.482		
21	0.621 ±0.853	0.820 ± 1.066		

[a] Two-Way ANOVA test
[b] The mean interaction of the samples is not significantly different by post-hoc test (Turkey's test)

Similarly, PDGF-BB exhibited a comparable biphasic release profile, as reported in (Table 4.7), characterised by a pronounced initial surge on day 1 followed by a gradual and sustained increase up to day 14. At the early time point, LyPRF demonstrated a higher release of PDGF-BB (97.41 ± 62.28 pg/ml) compared to FPRF (65.78 ± 49.65 pg/ml), indicating more effective preservation and subsequent release of growth factors in the lyophilised form. The maximal PDGF-BB release was observed on day 14, with LyPRF reaching 153.26 ± 42.25 pg/ml, in contrast to 85.74 ± 47.88 pg/ml for FPRF.

Table 4.7 Kinetic Release Pattern of PDGF-BB.

Days	LyPRF (pg/ml)	FPRF (pg/ml)	*Statistics*[a]	(df)	*P - value*[a]
1	97.407 ±62.277	65.778 ±49.648	0.3764		*ns*[b]
7	94.296 ± 58.003	38.444 ± 20.240			
14	153.259 ±42.244	85.741 ±47.877			
21	47.963 ±89.520	63.407 ± 108.001			

[a] Two-Way ANOVA test
[b] The mean interaction of the samples is not significantly different by post-hoc test (Turkey's test)

Conversely, as presented in (Table 4.8), TGF-β1 exhibited a distinct release profile compared to PDGF-AB and PDGF-BB, with the highest kinetic release observed on day 1 for both LyPRF and FPRF. During this initial phase, LyPRF demonstrated a substantially higher release of TGF-β1 (165.72 ± 201.04 pg/ml) compared to FPRF (55.94 ± 113.05 pg/ml), which is consistent with the early release of TGF-β1 associated with the fibrin surface and platelet membranes. Following this peak, TGF-β1 levels in both preparations declined sharply, reaching undetectable levels in FPRF by day 14, while LyPRF retained a minimal residual concentration (3.389 ± 71.207 pg/ml) at the same time.

Table 4.8 Kinetic Release Pattern of TGF-B1.

Days	LyPRF (pg/ml)	FPRF (pg/ml)	*Statistics*[a]	(df)	*P - value*[a]
1	165.722 ±201.041	55.945 ±113.052	0.0513		*ns*[b]
7	115.167 ± 164.704	-76.167 ±26.965			
14	3.389 ± 71.207	-70.000 ±44.531			
21	-72.444 ± 30.348	-71.889 ±69.661			

[a] Two-Way ANOVA test
[b] The mean interaction of the samples is not significantly different by post-hoc test (Turkey's test)

Overall, the kinetic release pattern analysis indicates that LyPRF demonstrated a trend towards a more prolonged and quantitatively higher release of PDGF-AB and PDGF-BB compared to FPRF, while also maintaining detectable levels of TGF-β1 beyond the acute release phase. Nevertheless, statistical analysis revealed that these differences were not significant ($P > 0.05$) Although the observed release profiles suggest enhanced growth factor retention and sustained release behaviour in LyPRF, these trends should be interpreted with caution. Collectively, the findings suggest that LyPRF shows potential as a biomaterial for sustained growth factor release for BTE.

4.6.2 Cumulative Release Pattern of PDGF-AB, PDGF-BB, and TGF-pi

The cumulative release profiles of PDGF-AB, PDGF-BB, and TGF-pi from LyPRF and FPRF were quantified over 21 days using ELISA assay. All growth factors exhibited a time-dependent increase in concentration, demonstrating sustained release behaviour throughout the analysis period (Figure 4.16). In general, LyPRF consistently showed higher cumulative release levels compared to FPRF, suggesting enhanced long-term availability of growth factors. The statistical analysis, performed using Tukey's post hoc test, is presented in (Table 4.9).

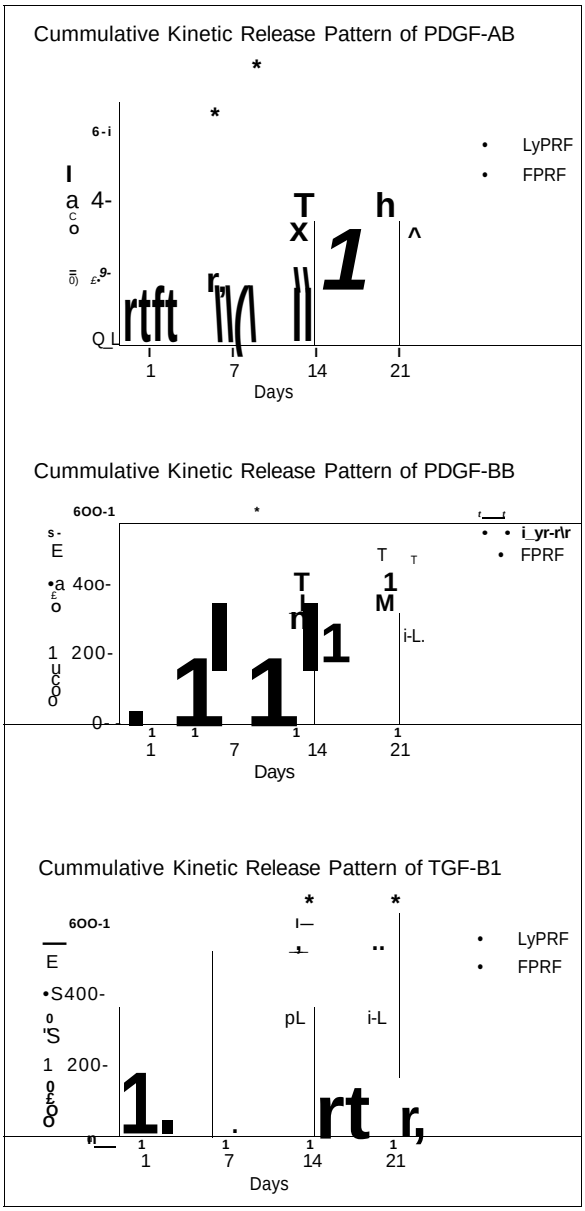

Figure 4.16 Cummulative release pattern of PDGF-AB, PDGF-BB, and TGF-P from FPRF and LyPRF over 21 days

Table 4.9 Multiple Comparison Turkey Post-Hoc for LyPRF vs FPRF.

Time	**Comparison**	*Statistics*[11] **(df)**	*P-value"*
Day 1	PDGF-AB	0.7536	*ns*[b]
	PDGF-BB	0.7223	*ns*[b]
	TGF-B1	0.4315	*ns*[b]
Day 7	PDGF-AB	0.4163	*ns*[b]
	PDGF-BB	03319	*ns*[b]
	TGF-B1	0.0687	*ns*[b]
Day 14	PDGF-AB	0.1675	*ns*[b]
	PDGF-BB	0.0953	*ns*[b]
	TGF-B1	0.0453	*[c]
Day 21	PDGF-AB	0.2392	*ns*[b]
	PDGF-BB	0.1235	*ns*[b]
	TGF-B1	0.0453	*[c]

a Two-Way ANOVA test and Turkey's post-hoc analysis

PDGF-AB exhibited a gradual cumulative release over the 21-day period. LyPRF released 1.045 pg/mL on day 1, increasing steadily to 2.031 pg/mL, 3.593 pg/mL, and 4.214 pg/mL on days 7, 14, and 21, respectively. In contrast, FPRF displayed lower release values at all time points, beginning at 0.761 pg/mL on day 1 and rising to 1.289 pg/mL, 2.308 pg/mL, and 3.128 pg/mL on the corresponding days. Although LyPRF consistently showed higher PDGF-AB release, the differences were not statistically significant at any time point ($P > 0.05$).

The release profile of PDGF-BB followed a similar cumulative trend but with substantially higher absolute concentrations. LyPRF increased from 97.407 pg/mL on day 1 to 191.703 pg/mL on day 7, reaching 344.962 pg/mL and 392.925 pg/mL on days 14 and 21, respectively. FPRF exhibited a slower cumulative progression, releasing 65.778 pg/mL, 104.222 pg/mL, 189.963 pg/mL, and 253.370 pg/mL at the corresponding time points. Although LyPRF demonstrated higher cumulative PDGF-BB release, these differences were not statistically significant at any time point ($P > 0.05$). The gradual slope after day 14 suggests a sustained late-phase release, consistent with prolonged bioactivity potential.

TGF-β1 exhibited a distinct release pattern, characterised by a rapid early release followed by plateauing. LyPRF released 165.722 pg/mL on day 1, rising to 280.889 pg/mL on day 7 and stabilising at approximately 284.278 pg/mL on days 14 and 21. In contrast, FPRF showed markedly lower and largely unchanging concentrations, remaining around 55.944 pg/mL across all time points. While differences in TGF-β1 release were not statistically significant on days 1 and 7 ($P > 0.05$), LyPRF exhibited significantly higher release compared to FPRF on days 14 and 21 ($P < 0.05$). The extended release from LyPRF suggests that lyophilisation preserved latent TGF-β1 stores within the fibrin mesh, allowing slow enzymatic degradation and diffusion throughout the incubation period.

Collectively, these data indicate that lyophilisation modifies the release kinetics of key growth factors by attenuating premature diffusion and prolonging late-phase availability. Among the examined growth factors, PDGF-BB showed the highest cumulative release, followed by TGF-β1 and PDGF-AB.

4.7 MTT Assay (3-(4,5-dimethylthiazol-2-yl)-2,5-diphenyltetrazolium bromide)

The biocompatibility analysis conducted on HGF using MTT assay demonstrates the cell proliferation trends for LyPRF, FPRF, and the medium as an additional control group over 24, 48 and 72 hours is presented in (Table 4.10) and illustrated in (Figure 4.17). At 24 hours, both LyPRF (0.656 ± 0.079) and FPRF (0.713 ± 0.065) demonstrated higher metabolic activity compared to the control group (0.538 ± 0.012). Statistical analysis of the MTT assay data (Table 4.11) showed that FPRF induced significantly higher cell proliferation compared with the control group ($p < 0.005$). In contrast, no statistically significant differences were observed between LyPRF and FPRF ($p > 0.05$) or between LyPRF and the control group ($p > 0.05$).

Table 4.10 Descriptive Analysis of Cell Proliferation of HGF Over Time.

	24 Hours	48 Hours	72 Hours
Lyophilised Platelet-Rich Fibrin (LyPRF)	0.656 + 0.079	0.672 + 0.094	0.737 + 0.065
Frozen Platelet-Rich Fibrin (FPRF)	0.713 + 0.065	0.750 + 0.029	0.562 + 0.050
Control	0.538 + 0.012	0.583 + 0.032	0.441 + 0.035

Table 4.11 Multiple Comparison Turkey Post-Hot for HGF Proliferation.

Time	Comparison	P-value	Significance
24 Hours	LyPRF vs FPRF	0.4705	ns
	LyPRF vs Control	0.0590	ns
	FPRF vs Control	0.0068	**
48 Hours	LyPRF vs FPRF	0.2717	ns
	LyPRF vs Control	0.2184	ns
	FPRF vs Control	0.0041	**
72 Hours	LyPRF vs FPRF	0.0043	**
	LyPRF vs Control	0.0004	***
	FPRF vs Control	0.0189	*

[a] Two-Way ANOVA test and Turkey's post-hoc analysis

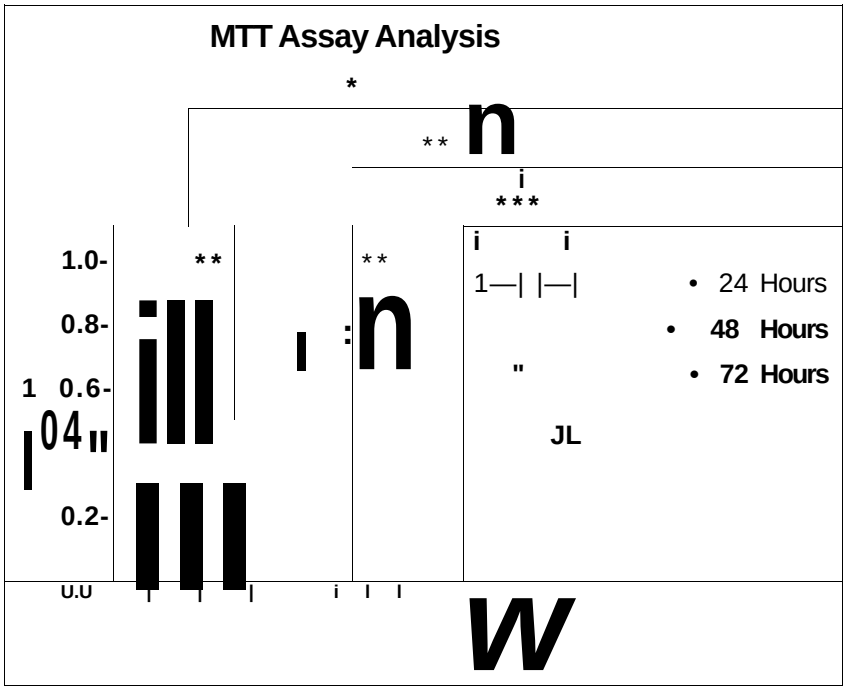

Figure 4.17 Biocompatibility Evaluation by MTT Assay on Human Gingival Fibroblasts (HGF) Exposed to FPRF and LyPRF

A similar trend was observed at 48 hours, with LyPRF maintaining a moderate proliferation rate (0.672 ± 0.094), and FPRF exhibiting the highest cell proliferation (0.750 ± 0.029), where both biomaterials exceeding the control group (0.583 ± 0.032). Statistical analysis at this time point revealed a significant difference between FPRF and the control group ($p < 0.005$). In contrast, no statistically significant differences were observed for comparisons involving LyPRF, including LyPRF versus FPRF and LyPRF versus the control group ($p > 0.05$).

In contrast, the observed cell proliferation results at 72 hours demonstrated LyPRF having the highest proliferation rate (0.737 ± 0.065), which is notably higher than both FPRF (0.562 ± 0.050) and the control group (0.441 ± 0.035). Statistical analysis demonstrated that LyPRF exhibited significantly higher cell proliferation compared with both FPRF ($p < 0.005$) and the control group ($p < 0.0005$). Although FPRF showed a reduction in proliferative activity at this time point, it remained significantly greater than the control ($p < 0.05$).

Overall, the MTT analysis exhibited higher proliferation for both LyPRF and FPRF in comparison to the control throughout all time points. Moreover, the analysis demonstrates FPRF supported stronger early-stage cell proliferation, particularly during the initial 24 and 48 hours. In contrast, LyPRF provided a more favourable microenvironment for sustained cellular growth over time, as it demonstrates the highest metabolic activity at 72 hours. This sustained proliferative response highlights the potential of LyPRF to support longer-term cellular viability and growth, that are advantageous for tissue regeneration applications.

CHAPTER 5
DISCUSSION

5.1 Participant Recruitment

The participant recruitment was conducted using a standardised protocol of predetermined criteria, in accordance with previously established literatures (Nakajima *et al.*, 2024; Ngah *et al.*, 2021a). The selection process was designed to ensure that all recruited participants met the physiological and health requirements necessary to produce reproducible and biologically consistent platelet concentrate-based material. By adhering to these standards, the study ensured methodological consistency and standardisation throughout the experimental procedures.

The number of participants in this study is consistent with previous reports, as similar studies involving autologous biomaterials have employed a limited number of participants (Anaya-Sampayo *et al.*, 2024; Liu *et al.*, 2022b; Ngah *et al.*, 2021a). This is aimed to enhance the reproducibility of the fabricated biomaterials while minimising biological variability that may arise during preparation. It also ensures that the comparative analysis of FPRF and LyPRF characteristics remains consistent and scientifically valid for bone tissue engineering applications. To provide a reliable baseline for tissue regeneration, participants were selected from a homogeneous group of healthy young adults aged between 20 and 30 years. This age range was chosen because it represents the optimal physiological window for platelet activity, fibrinogen concentration, and leukocyte function. Restricting recruitment to this demographic helps to eliminate age-related variations in coagulation dynamics, fibrin network density, and growth factor release, which could otherwise introduce confounding effect (Yajamanya *et al.*, 2016). This is because the differences in platelet activity, fibrin polymerisation rates, and the baseline concentration of bioactive molecules tend to fluctuate across different age groups. This variability influences the biomaterial-related outcomes through its clot formation, structural integrity, and the subsequent kinetic release pattern of key regenerative signals, including growth factors (Calciolari *et al.*, 2025; Piplani *et al.*, 2025). By narrowing the age range of participants, the study

minimises physiological heterogeneity and enhances the reliability and internal validity of the comparative analyses between LyPRF and FPRF.

Another significant criteria that were taken into consideration in this study are the lifestyle and health of the participants. This is because the biological composition and regenerative potential of the biomaterial are directly influenced by the lifestyle and health of an individual. Therefore, non-smokers were an important criteria of the participants recruited, as smoking has been documented to impair platelet aggregation, vascular function, and angiogenesis, thereby compromising the biological activity of PRF in this study (Srirangarajan *et al.*, 2021). Furthermore, to prevent pathological changes in blood composition that could potentially impact the fibrin structure and growth factor retention of the sample in this study, individuals with chronic systemic illnesses were excluded. Additionally, participants who had taken aspirin or NSAIDS medications within the three months prior of the blood collection were excluded, as these medications are known to interfere with platelet activity and fibrin polymerisation of PRF (Mahmoodabadi *et al.*, 2023).

Overall, the implementation of strict inclusion and exclusion criteria based on previous protocol in literature ensured that all participants represented a healthy physiological baseline, thereby strengthening the internal validity of the study. This careful selection process minimised donor-related variability and provided a consistent foundation for subsequent physicochemical and biological analyses of FPRF and LyPRF.

5.2 Fabrication of LyPRF and FPRF

This study highlights the fabrication of both FPRF and LyPRF using previously established protocols by Liu et al. (2022) and Ngah et al. (2024), with minor modifications tailored, specifically designed to accommodate the intended application. The methodological reproducibility and comparability with previous findings are ensured by the implementation of an established fabrication protocol while enabling the optimisation of this biomaterial for bone tissue engineering purposes.

PRF was fabricated through the standard centrifugation technique without the use of anticoagulant which enables the natural activation of the coagulant cascade from the biomaterial. This process allows platelets and leukocytes to become entrapped

within a dense fibrin matrix, forming a biologically active clot capable of sustaining growth factor release. This technique reflects the original protocol introduced by Choukroun et al (2006), which describes PRF as an autologous biomaterial derived from venous blood without the addition of anticoagulant agents. This further enhances the functionality of this biomaterial due to its simplicity and biocompatibility, ensuring its safety and clinical practicality, specifically in craniofacial regeneration.

To produce FPRF, the freshly prepared biomaterial was subjected to a freezing protocol, aiming to preserve its structural integrity and biological components by stabilising the fibrin matrix. This procedure offers an innovative approach to prolong the clinical shelf life of PRF and preserves its bioactive potential for physicochemical analysis and BTE applications (Liu *et al.*, 2024a). However, FPRF introduces a different set of limitations. While its prolonged clinical shelf life is advantageous, the biomaterial requires highly specific storage conditions, particularly continuous maintenance at ultra-low temperatures (–80 °C). This requirement increases logistical complexity and operational cost. Furthermore, transportation becomes challenging, as the biomaterial must remain strictly within the ultra-low temperature range throughout transit to ensure preservation of its physicochemical properties and biological functionality (Palanques-Pastor *et al.*, 2025).

To address these limitations, LyPRF was developed with the aim of improving storage stability, enhancing transportability, and clinical half-life. Therefore, it enables the potential of using LyPRF as a tissue bank biomaterial. LyPRF is produced by lyophilising FPRF under controlled low-temperature and low-pressure conditions, a process that removes moisture from the biomaterial while preserving its structural and biological integrity (Bhambere *et al.*, 2015). Lyophilisation stabilises the fibrin matrix and prevents the degradation of the embedded cellular components and growth factors in the biomaterial. Therefore, the bioactivity of the bio scaffold can be preserved over extended periods without dependence on continuous low-temperature storage conditions. This improvement enhances the clinical half-life, storage capability and transportation requirements of LyPRF. Furthermore, this method increases the versatility of LyPRF as a readily available, off-the-shelf product for BTE and regenerative applications, particularly in craniofacial regeneration (Jia *et al.*, 2024; Liu *et al.*, 2022b).

As evident by the analysis conducted, LyPRF retains the essential physical characteristics of fresh PRF, such as its dry, sponge-like morphology and porous fibrin

network. The preservation of these characteristics indicates that the structural framework of the fibrin matrix remains largely intact despite the lyophilisation process, thereby maintaining its functional role as a bio scaffold for BTE (Krishani *et al.*, 2023). Nevertheless, some observable changes in the physical dimensions of the PRF matrix were detected following lyophilisation. LyPRF demonstrated a substantial reduction in both weight and length compared to FPRF, primarily attributed to the complete removal of moisture during the sublimation stage of the lyophilisation process (Ngah *et al.*, 2021a). This transformation produces a lightweight scaffold, enhancing the handling and storage potential of the biomaterial while maintaining a stable, sponge-like texture suitable for BTE applications. The porous, compressible nature of this sponge-like structure facilitates the integration of LyPRF with other biomaterials commonly used in BTE, thereby broadening its versatility in composite scaffold fabrication (Li *et al.*, 2024a; Lutzweiler *et al.*, 2020).

From a clinical standpoint, these changes are advantageous for future clinical application, as the resulting biomaterial is easier to handle, and transportable, exhibiting an improved storage capability. This innovation reduces the fabrication, storage, and transportation constraints commonly associated with PRF-based materials and facilitate wider clinical usability. Consequently, LyPRF presents a potential solution as a clinically versatile and shelf-stable biomaterial, aligning with the growing demand for personalised medicine, and platelet-based scaffolds in BTE (Huang *et al.*, 2025b; Pardeshi *et al.*, 2023).

5.3 Microstructure of LyPRF and FPRF Analysed using FESEM

The analysis of the microstructure of LyPRF and FPRF using FESEM provides an in-depth visual evaluation of the morphological characteristics that are fundamental to the biological performance of the biomaterials. Through FESEM imaging, the fibrin architecture of both LyPRF and FPRF can be observed clearly, revealing a dense and interconnected porous network that serves as a natural scaffold for cellular interaction during tissue regeneration. This fibrous matrix is essential in supporting key cellular functions including cell proliferation, adhesion, and migration, which are vital for BTE (Wong *et al.*, 2017). In addition, the visible porosity and fibrillar arrangement of these biomaterials facilitate the entrapment and gradual release of bioactive materials such as

platelets, leukocytes, and growth factors, thereby establishing a sustained biological microenvironment conducive to wound healing and osteogenic activity (Sun *et al.*, 2023a). During the dehydration process achieved through lyophilisation, LyPRF demonstrated the abundance of dense fibrin structure of fresh PRF and FPRF while introducing subtle morphological alterations. These structural changes potentially enhance the stability and handling properties of the biomaterial without compromising its cellular activities including cell proliferation, migration and adhesion. Moreover, we speculate that the porous microstructure of both LyPRF and FPRF promotes vascular ingrowth, facilitates cell attachment and proliferation, and supports efficient nutrient diffusion and waste removal critical in regeneration process (Anaya-Sampayo *et al.*, 2024). Overall, the FESEM analysis demonstrated that LyPRF preserves the essential microarchitectural required to function as an effective bio scaffold, despite undergoing lyophilisation process.

5.3.1 Surface Morphology

The analysis of the surface morphology of both LyPRF and FPRF highlights distinct structural differences that may significantly influence key biological responses, particularly craniofacial regeneration. FESEM imaging revealed distinct surface morphological differences between the two biomaterials, demonstrating the differential effects of the lyophilisation and freezing processes towards PRF structure. LyPRF exhibited a rough and irregular surface microarchitecture, which enhances its functional suitability as a bio scaffold by providing a larger surface area for cellular attachment and proliferation. This topographical advantage supports more efficient adhesion of osteogenic and endothelial cells to the fibrin matrix, thereby promoting favourable cellular responses essential for bone tissue regeneration. The interconnected porous structure also facilitates cellular migration that are essential for neovascularisation and new tissue formation within bone defects (Abbasi *et al.*, 2020; Sun *et al.*, 2023a).

Moreover, the surface irregularities and micro-roughness observed in LyPRF contribute to the enhanced protein adsorption, a critical factor in the integrin-mediated signalling pathways, thus aiding in mediating cell adhesion. Abbasi et al discovered that proteins such as fibronectin and vitronectin, when adsorbed onto the rough surface, function as bioactive anchors that facilitates the binding of osteoblasts and fibroblasts,

thereby promoting rapid cell proliferation and matrix synthesis (Hamraoui, 2025). The increase surface roughness also provides microenvironments that promotes platelet adhesion and activation, sustaining the localised release of essential growth factors such as PDGF, VEGF, and TGF-β. The synergistic effect of these growth factors is essential for the effective regeneration of craniofacial bone tissue, considering this process promotes angiogenesis, collagen synthesis, and osteoblastic differentiation (Aghali, 2021).

In contrast, the FPRF samples demonstrated a comparatively smoother and homogenous appearance compared to LyPRF. We speculate this material demonstrates less favourable environment for cellular attachment and proliferation (Jia *et al.*, 2024). Moreover, the number of active binding sites accessible for cell adhesion is reduced in correlation to the decreased roughness of its surface morphology, thus potentially limiting cell migration and subsequent regenerative mechanisms. In addition, it was demonstrated that the loose architecture of FPRF allows for a faster diffusion and release of growth factors, resulting a shortened duration of biological activity (Ngah *et al.*, 2021a). Therefore, the FPRF retaining the smoother morphology of FPRF compromises the sustained release and spatial distribution of bioactive molecules, thereby restricting its long-term regenerative efficacy compared to LyPRF.

These finding collectively indicates that the surface morphology of LyPRF demonstrate a distinct functional advantage over FPRF. The rough surface morphology of LyPRF mimics natural ECM, providing a 3D framework that facilitates cellular interactions and promotes tissue regeneration (Liu *et al.*, 2024b). Furthermore, the sponge-like microstructure of LyPRF enhances its capacity to retain and gradually release bioactive factors, resulting in a sustained stimulatory microenvironment that promotes osteogenesis and angiogenesis over time. This is particularly advantages for BTE applications, where prolonged signalling and cellular integration are required for craniofacial regeneration (Sun *et al.*, 2023a). Therefore, it is evident that lyophilisation produces a spongier and more roughened surface in LyPRF, while simultaneously extending its shelf life. This enhancement improves the biomaterial's suitability for transportation and long-term storage without compromising its capacity to support essential cellular activities.

5.3.2 Pore Sizes

The porosity of a biomaterial refers to the presence of interconnected pores or void spaces within its structure, which plays a fundamental role in BTE. The pores are essential for the formation of new regenerative tissue by supporting essential physiological processes, including nutrient and oxygen diffusion, waste removal, cellular migration, proliferation, and vascularisation. These regenerative functions are attributed to the inherently high porosity of PRF-based materials, as reported in previous literature (Altalbawy *et al.*, 2025; de Lima Barbosa *et al.*, 2023) . The interconnected, tunnel-like porous morphology within the fibrin matrix facilitates efficient nutrient and waste exchange. In addition, it provides pathways for cell migration and vascularisation, thereby creating a microenvironment conducive to sustained tissue regeneration (Lutzweiler *et al.*, 2020; Wong *et al.*, 2021b) . Therefore, the porous biomaterial enhances mechanical interlocking between the scaffold and the native bone and improves its overall stability as a bio scaffold. This properties is further supported by adequate pore interconnectivity, which facilitates communication between microenvironments within the biomaterial, enabling synchronised cellular signalling and matrix remodelling essential for effective tissue regeneration. (Hasan *et al.*, 2025; Karageorgiou & Kaplan, 2005). The porosity demonstrated by both LyPRF and FPRF represents one of the most critical morphological parameters influencing their cellular efficacy. This physical characteristic facilitates key cell activities, including migration, proliferation, differentiation, and vascularisation. The efficacy of this process is dependent on the degree of porosity, pore size distribution, and the extent of interconnectivity within the fibrin matrix (Khan *et al.*, 2025).

Based on the FESEM analysis conducted in this study, LyPRF exhibited significantly higher porosity compared to FPRF, with pore sizes ranging from 40 to 250 ;" and a mean pore diameter of 104.6 ; " . These values is within the optimal pore size range of 100 to 200 ; " , that has been reported in previous studies as ideal for facilitating osteoconduction and angiogenesis (Gan *et al.*, 2023a). Pore sizes within this range support the migration of osteogenic cells, endothelial cells, and mesenchymal stem cells (MSCs), thereby promoting concurrent bone matrix deposition and vascularisation essential for tissue regeneration (Jasmine *et al.*, 2021). The larger pore sizes observed in LyPRF reflect the structural modifications caused by the

lyophilisation process by removing water content while preserving the fundamental integrity of the biomaterial. Previous studies have similarly reported a maximum pore size of approximately 250 μm, which Anaya-Sampayo et al. and Wong et al. have speculated is optimal for promoting angiogenesis (Anaya-Sampayo *et al.*, 2024; Wong *et al.*, 2021b). The microarchitecture observed is characterised by a sponge-like framework with interconnected pores, capable of maintaining mechanical stability while simultaneously facilitating extensive cellular migration, thereby supporting tissue regeneration. Therefore, this enhanced porosity provides multiple pathways for cell migration and integration for leukocytes and platelets within the biomaterial, contributing to prolonged growth factor release and modulation of the inflammatory phase during early healing (Altalbawy *et al.*, 2025; Anaya-Sampayo *et al.*, 2024).

In contrast, FPRF exhibit a loose and less porous biomaterial, with an average pore size of approximately 48.2 ; " . Although isolated larger pores up to 121 ;" were occasionally identified, these appeared irregular and concave, indicating a limited level of interconnectivity and restricted pathways for cellular migration. These smaller pore sizes restrict oxygen and nutrient diffusion, thus compromising cellular activities and reduce the overall regenerative efficacy of this biomaterial (Abbasi *et al.*, 2020). Additionally, the limited porosity of FPRF contributes to a more rapid release of entrapped growth factors, thereby reducing the duration of bioactivity at the defect site and diminishing its regenerative potential compared to LyPRF. This observation has been documented and discussed in previous studies by Jia et al. and Ngah et al (Jia *et al.*, 2024; Ngah *et al.*, 2021a).

Therefore, the bigger pore sizes observed in LyPRF presents significant advantages for BTE. The interconnected porous structure facilitates early-stage cellular migration and provides sufficient space for ECM deposition and mineralisation during later phases of healing. This interconnectivity is critical for angiogenesis, ensuring an adequate blood supply to support cell viability, growth, and integration of the newly formed bone tissue (Feng *et al.*, 2023). Furthermore, the presence of larger pores in LyPRF supports the cellular migration of macrophages and MSCs, which play an essential role in modulating inflammation and promoting tissue regeneration. Collectively, these microstructural features demonstrate that the lyophilisation process prolongs the shelf life of PRF in addition to enhance its structural characteristics, thus make it comparable to the porous architecture of native bone ECM (Jia *et al.*, 2024; Narayanaswamy *et al.*, 2023). Therefore, the FESEM analysis confirms that LyPRF is

a more promising biomaterial for BTE application, due to its favourable porous characteristics.

5.3.3 Fibrin Network

The architecture of the fibrin network is a critical determinant of the physicochemical and biological performance of LyPRF and FPRF in BTE. This fibrous matrix acts as a natural derived bio scaffold that replicates the organisational and biochemical characteristics of natural ECM, thereby providing structural framework that facilitates essential cellular activities such as cell adhesion, migration, proliferation, and differentiation (Aazmi *et al.*, 2024). This structural matrix is formed through the polymerisation of fibrinogen under the catalytic action of thrombin, resulting in the formation of fibrin glycoproteins essential for the activation and stabilisation of blood coagulation cascade. This process results in a 3D fibrous network capable of entrapping biological components, including platelets, leukocytes, and growth factors. The entrapment of these bioactive components within the fibrin matrix contributes to the formation of a mechanically stable bio scaffold and enables a sustained and controlled release of growth factors such as PDGF, TGF- β, and VEGF. These growth factor molecules are crucial in promoting angiogenesis, osteogenic differentiation, and facilitating ECM deposition, thereby enhancing the overall effectiveness of the biomaterials for tissue regeneration (Jia *et al.*, 2024). Moreover, the architecture of the fibrin network is essential in modulating the biological performance of both LyPRF and FPRF, directly influencing its degradation kinetics and regenerative efficacy. This is because fibrin network represents the primary structural framework of these biomaterials. Therefore, the density and organisation of this physical characteristic determine the rate of degradation, the sustained release of growth factors, and the overall potential to support cellular activities necessary for tissue regeneration (Li *et al.*, 2024a).

The analysis conducted by FESEM in this study demonstrate distinct morphological differences between LyPRF and FPRF in terms of fibrin network organisation. LyPRF exhibits a heterogenous, 3D fibrin matrix characterised by the densely packed, irregularly oriented fibrin fibers, and trimolecular junctions, forming a sponge-like microarchitecture. This structural pattern is consistent with the fibrin

network analysis reported by Sun et al and Wang et al (Sun *et al.*, 2025; Wang *et al.*, 2019b). Therefore, it is speculated to be advantageous for promoting cellular activities including cell attachment, migration, and vascularisation, thereby creating a favourable environment that supports both osteogenic and angiogenic activities (Wang *et al.*, 2024). The presence of fine fibrillae and inter-fibrillar matrix in LyPRF further enhances the permeability and surface area of LyPRF, which are critical for the sustained release of nutrients and bioactive molecules. Thus, it contributes to a more gradual and extended release of growth factors, supporting a continuous cellular signalling throughout the phases of BTE (Wong *et al.*, 2021b).

In contrast, FPRF displayed a less organised fibrin matrix, with reduced quantity of pore interconnectivity and a lower fiber density, resulting to a loose and less porous microarchitecture. Therefore, it disrupts effective cellular migration and nutrient transport, leading to a limited internal cellular activity of the biomaterial. As reported by previous literatures, the loose fibrin arrangement of FPRF facilitates a rapid release of growth factors. Despite its advantage during early inflammatory phase of healing, the biomaterial's sustained bioactivity gradually diminishes, thereby limiting its long-term regenerative potential (Orasugh *et al.*, 2020). The limited duration of growth factor signalling in FPRF is primarily due to the rapid release of these bioactive molecules, resulting from the less dense fibrin matrix's ineffective binding and retention capacity. This rapid initial burst leads to quick depletion or degradation of growth factors, producing a short effective half-life and preventing the sustained, sequential signalling necessary throughout the healing process. Consequently, both osteogenesis and angiogenesis are impaired, resulting in insufficient or delayed healing, and disrupts the tissue regeneration process (Abbasi *et al.*, 2020; Wang *et al.*, 2017). Therefore, it is speculated that the relatively lower fibrin density and reduced structural integrity in FPRF create a less favourable microenvironment for tissue regeneration. In contrast, the denser, sponge-like fibrin matrix of LyPRF provides an improved growth factor retention that preserves their bioactivity and supports the prolonged cellular activity required for successful tissue regeneration.

In addition to enabling the sustained and controlled release of bioactive molecules, previous studies indicate that the dense fibrin network of LyPRF slows the kinetic degradation of the biomaterial. This is because its compact structure reduces the diffusion and activity of fibrinolytic enzymes such as plasmin, which are responsible for fibrin breakdown (Li *et al.*, 2024a; Risman *et al.*, 2022). In contrast, the less compact

fibrin architecture of FPRF results to a faster enzymatic diffusion and activity. Consequently, FPRF undergoes a more rapid degradation, therefore, with its inherently faster growth factor release, it limits the biomaterial's ability to provide prolonged regenerative signalling beyond the early stages of healing. Conversely, the compact fibrin structure of LyPRF supports a more gradual degradation profile and sustained release of growth factors, thereby promoting continuous tissue regeneration throughout the entire healing process.

Collectively, the FESEM analysis indicates that the fibrin network microarchitecture of LyPRF is highly advantageous for BTE applications. Its dense, highly interconnected, and irregular fibrin network forms a 3D framework that closely mimics the structural organisation of natural ECM. This configuration enhances critical cellular activities such as adhesion, migration, and proliferation, while providing structural support for angiogenesis and facilitates efficient diffusion of nutrients and oxygen essential for tissue regeneration. Moreover, the irregular and dense fibrin network promotes the gradual and sustained release of growth factors, ensuring continuous stimulation of osteogenesis and vascularisation throughout the healing process. (Liu *et al.*, 2019a; Wang *et al.*, 2019a). In contrast, the less compact fibrin network observed in FPRF exhibits limited interconnectivity, thus restricting cellular activity, particularly cell migration. In addition, the loose fibrous structure accelerates the release of growth factors and reduces its regenerative potential. Overall, these findings suggest that the lyophilisation process preserves the intrinsic fibrin framework of PRF and enhances its regenerative functionality, establishing LyPRF as a structurally and functionally superior biomaterial for BTE applications.

5.3.4 Cell Entrapment

Cellular entrapment within the fibrin network is a fundamental characteristic that contributes to the biological efficacy of PRF-derived biomaterials in BTE. The fibrin matrix forms a 3D microarchitecture that facilitates cellular entrapment and regulates essential biological processes throughout the different phases of tissue regeneration. In particular, the integration of leukocytes and platelets within the fibrin network is crucial in modulating early inflammatory response, sustain the controlled release of growth factors, and promotes subsequent tissue repair and regeneration

(Zapata-Sifuentes *et al.*, 2024). The complementary role of these two cell types is essential for a successful tissue regeneration outcome.

Leukocytes are essential for immunomodulation by regulating the inflammatory phase of tissue regeneration through the secretion of cytokines, thereby coordinating the transition from inflammation to tissue repair. In addition, these cells contribute to antimicrobial defence by releasing antimicrobial peptides that aids in preventing infection at the implantation site (Mariano *et al.*, 2022; Moon *et al.*, 2023). Conversely, platelets serve as natural reservoirs of growth factors, gradually releasing the signalling molecules during fibrin degradation to promote angiogenesis, osteoblast proliferation and ECM synthesis (Jia *et al.*, 2024). Therefore, the synergistic interaction between leukocytes and platelets within the fibrin matrix supports a balanced healing microenvironment, thereby enhancing tissue regeneration for BTE applications (Huang *et al.*, 2025b; Jia *et al.*, 2024). The analysis of LyPRF and FPRF revealed clusters of leukocytes and platelets entrapped within the fibrin network. This identification is supported by the observed cell sizes, with smaller cells measuring approximately 2–3 ;" corresponding to platelets, and larger cells measuring 7–15 ;" consistent with leukocytes (Handtke & Thiele, 2020). The morphology of these cellular clusters aligns with previously reported findings, indicating that both biomaterials retain their biological integrity and remain suitable for BTE applications (Biswas *et al.*, 2023; Ngah *et al.*, 2024). The presence of these cellular components within the fibrin matrix is biologically significant because of its direct influence on the biomaterial's regenerative capability and overall suitability for BTE applications.

The presence of leukocytes, which were prominently observed in LyPRF compared to FPRF, emphasises its crucial role in immunomodulation by regulating the inflammatory phase of tissue regeneration. These regulations were mediated through the controlled release of cytokines, such as interleukin-6 (IL-6), interleukin-10 (IL-10), and tumour necrosis factor-alpha (TNF-α), thus preventing chronic inflammatory responses during tissue repair and remodelling. Furthermore, according to Sindhusha et al, leukocytes contribute to antimicrobial defence by secreting antimicrobial peptides and generating reactive oxygen species, thereby limiting infection at the surgical site (Sindhusha & Ramamurthy, 2023). These coordinated mechanisms suppress microbial proliferation and reduce the risk of post-implantation infection, ensuring a microbiologically regulated regenerative environment essential for successful bone tissue engineering applications (Mariano *et al.*, 2022; Warin *et al.*, 2023). Additionally,

the entrapped leukocytes act as a primary defensive barrier by actively phagocytosing and eliminating bacteria, further strengthening the biomaterial's antimicrobial function throughout the healing process (Feng *et al.*, 2020).

In addition to leukocytes, platelets entrapped within the fibrin matrix act as natural reservoirs for key growth factors, including PDGF, TGF-β, and VEGF. These bioactive molecules play crucial roles in promoting angiogenesis, stimulating osteoblast proliferation, and facilitating ECM synthesis (Wu *et al.*, 2022; Zhang *et al.*, 2024). To ensure the gradual release of these bioactive molecules, a slowed degradation process is required to ensure a prolonged regenerative signalling, and continuous osteogenesis and vascularisation at the defect site. Furthermore, the cooperative presence of leukocytes and platelets within the fibrin matrix establishes a synergistic microenvironment that integrates inflammatory modulation, antimicrobial defence, and growth factor–mediated tissue repair (Sui *et al.*, 2023a).

With these information, FESEM analysis revealed distinct differences in the distribution and density of entrapped cells between LyPRF and FPRF. LyPRF was observed to have a higher concentration and visualisation of both leukocytes and platelets distributed throughout its interconnected fibrin network. The cells appeared more uniformly dispersed and deeply integrated within the fibrin matrix, indicating successful migration into the internal 3D network. This finding suggests that the lyophilisation process preserves the cellular integrity of PRF and facilitates homogeneous cell entrapment within the fibrin architecture (Sun. *et al.*, 2023).

In contrast, FPRF exhibited fewer visible cells, which were predominantly localised near the surface layer. This reduction in cellular distribution is attributable to the nucleation and growth of ice crystals within the fibrin matrix during freezing, resulting in structural disruption and partial collapse of the fibrin network. Such alterations reduce the matrix's ability to uniformly entrap platelets and leukocytes throughout its structure (Dao *et al.*, 2022). In addition, ice crystal expansion may compromise cellular integrity, thereby contributing to reduced cell viability (Farag *et al.*, 2024). These effects collectively indicate limited cellular migration and sparse cell distribution within the inner regions of FPRF, ultimately diminishing its biological efficacy and restricting its regenerative potential. Consequently, FPRF demonstrates less efficient and less stable cell entrapment compared with matrices in which fibrin architecture is better preserved.

These findings demonstrate that LyPRF enhances the preservation and stabilization of cellular components within the PRF matrix, resulting in more efficient and uniform cellular entrapment compared to FPRF. The cellular entrapment observed in LyPRF facilitates immunomodulation, and promote prolonged tissue regeneration (Hasan *et al.*, 2025). Therefore, LyPRF exhibits a greater potential as a biomaterial for BTE due to its enhanced ability to entrap and stabilise key cellular components, including leukocytes and platelets, within its fibrin architecture. This enhanced cellular entrapment is collectively achieved by the combined physical characteristics of LyPRF, including surface morphology, pore sizes, and fibrin network. Thus, this physical characteristic contributes to a more favourable biological response and improves the tissue regeneration outcomes for BTE applications.

5.4 Elemental Composition of LyPRF and FPRF Analysed using EDX

The elemental composition obtained by EDX analysis provides an important understanding of the intrinsic elemental characteristics of LyPRF and FPRF, particularly in relation to their effectiveness for BTE. The analysis demonstrates the abundance of elemental composition that contributes to the biochemical stability and biocompatibility of LyPRF and FPRF. Notably, the predominance of organic elements reflects a composition that mimics the ECM environment of natural bone tissue, thereby facilitating optimal cell-matrix interactions. Consequently, this composition enhances the regenerative potential of the biomaterials for BTE applications (Liu *et al.*, 2024b). The analysis conducted revealed that both LyPRF and FPRF are predominantly composed of carbon (C) and oxygen (O). These elements form the fundamental basis for identifying the organic framework of fibrin matrix. Their high abundance reflects the protein-rich fibrin microarchitecture that constitute the primary structural component of the scaffold, essential for supporting cellular adhesion and ECM formations (Anaya-Sampayo *et al.*, 2024; Zhao *et al.*, 2024). Specifically, the presence of carbon corresponds to the organic content of natural bone tissue, including proteins and amino acid residues. Conversely, the presence of oxygen is associated with peptide bonds and glycoproteins that contributes to the biomaterial's molecular architecture. Collectively, this organic composition closely mimics the biochemical environment of

natural bone tissue, thereby supporting favourable cell-matrix interactions and enhances the regenerative potential of both LyPRF and FPRF (Huang *et al.*, 2025a).

In addition to carbon and oxygen, LyPRF and FPRF demonstrate the presence of calcium (Ca) and phosphorus (P), elements fundamental to bone mineralisation and apatite formation. Calcium acts as a key structural ion that facilitates the nucleation and growth of hydroxyapatite ($Ca_{10}(PO_4)_6(OH)_2$), while phosphorus functions as a complementary anionic component that stabilises the crystalline lattice of bone minerals (Pandey *et al.*, 2021; Serna & Bergwitz, 2020). The detection of these elements, even in trace amounts, indicates the intrinsic osteoconductive potential of PRF-based biomaterials, including both LyPRF and FPRF, and reflects their ability to preserve the elemental composition characteristic of fresh PRF. Based on the analysis conducted, LyPRF exhibited a relatively higher phosphorus content compared to FPRF, indicating an enhanced capacity to support mineral deposition and bone-matrix integration (Hughes *et al.*, 2019). In contrast, the concentration of calcium in LyPRF was slightly lower compared to FPRF. This reduction is advantageous as the kinetic release pattern of growth factors is dependent on both intracellular and extracellular calcium ions concentration. Therefore, lower calcium concentration influences the slower and controlled release pattern of growth factors, thereby prolonging its availability (Martineau *et al.*, 2004; Zhang *et al.*, 2022). This finding is speculated to be due to the lyophilisation process effectively preserves the ionic and protein constituents of LyPRF, thereby maintaining its elemental characteristics tissue regeneration (Dias *et al.*, 2020).

In addition to the major elements, the retention of trace bioactive elements such as magnesium (Mg), zinc (Zn), silicon (Si), copper (Cu), and iron (Fe) further reflects the multifunctionality of LyPRF and FPRF in regenerative potential (Anaya-Sampayo *et al.*, 2024; Ngah *et al.*, 2024). These trace elements exhibit distinct but complementary biological functions that collectively regulate bone tissue metabolism, matrix mineralisation, and cellular activities essential for effective tissue regeneration. Magnesium promotes osteoblast proliferation and activates alkaline phosphate, thereby facilitating fibrin matrix mineralisation and stabilises bone crystal formation (Gaßling *et al.*, 2013). Zinc modulates osteogenic differentiation and collagen synthesis through the regulation of osteoblast-specific transcription factors, such as Runx2, while exerting antioxidant and antimicrobial effects (Molenda & Kolmas, 2023). In addition, silicon is essential during the early phases of osteogenesis and angiogenesis by enhancing collagen crosslinking and stimulating osteoblast differentiation (Götz *et al.*, 2019).

While, copper contributes to angiogenesis by functioning as a cofactor for lysyl oxidase, an enzyme responsible for collagen and elastin crosslinking, which supports neovascularisation and matrix maturation (Diao *et al.*, 2024). Furthermore, iron is essential for oxygen metabolism, serving as a vital component of haemoproteins that sustain cellular respiration and promote tissue vitality throughout the healing process (Obeagu, 2025a).

Therefore, the interaction of these trace elements with the organic and inorganic constituents of LyPRF and FPRF emphasises their essential contribution to the biochemical and regenerative functions of the biomaterial for BTE (Dias *et al.*, 2020; Scimeca *et al.*, 2018). The EDX findings indicate that LyPRF demonstrates superior retention of essential elemental components, along with a higher abundance of trace elements, compared to FPRF. This enriched elemental composition contributes to the enhanced overall bioactivity of LyPRF. In particular, the relatively higher phosphorus and trace ion content in this biomaterial improves its mineral deposition, strengthens its biological interactions, and increases the regenerative potential of LyPRF. Therefore, these compositional advantages enhance osteoconductivity, promote angiogenesis, and facilitate biomaterial-tissue integration, thereby reinforcing LyPRF's potential as an innovative and versatile biomaterial for BTE applications.

5.5 Functional Group of LyPRF and FPRF Analysed using FTIR

The functional group analysis of LyPRF and FPRF using FTIR spectroscopy demonstrates similar peaks mimicking previous analysis of PRF reported by Ngah et al and Wijayanti et al. These analysis aids in the preservation of biochemical integrity and structural stability within the protein matrix of the biomaterial. The preservations of the functional groups are a fundamental influence on the biological functionality and regenerative potential of both LyPRF and FPRF (Ngah *et al.*, 2024; Wijayanti *et al.*, 2025). Detailed FTIR spectral evaluation revealed distinct vibrational bands corresponding to characteristic functional groups within the fibrin structure, confirming the preservation of key molecular bonds and secondary protein conformations. These findings provide a comprehensive understanding of the molecular interactions that are essential for the bioactivity and overall regenerative performance of the biomaterial, thereby emphasises its suitability for BTE applications.

The FTIR spectra of both LyPRF and FPRF demonstrate characteristic amide I (~1650 cm $^{-1}$) and amide II (~1540 cm $^{-1}$) absorption bands, confirming the preservation of the fibrin protein's secondary structural components, predominantly α-helices and β-sheets (Usoltsev *et al.*, 2019). This finding aligns with the analysis reported by Boskey et al., indicating that the FTIR spectra of both LyPRF and FPRF share key compositional features with natural bone. Such spectral similarity suggests that these PRF-derived matrices possess biochemical characteristics conducive to bone tissue engineering applications (Boskey & Pleshko Camacho, 2007). Therefore, this structural retention is essential to represent the maintenance of the intrinsic fibrin microarchitecture of PRF responsible for biomaterial's viscoelastic and mechanical stability. Specifically, the amide I band primarily represents the C=O (carbonyl group) stretching vibration of the protein polypeptide backbone. This signal is crucial for determining protein conformation and structural integrity, which influences the biomechanical properties and biological function of the PRF scaffold in promoting tissue regeneration (Baronio & Barth, 2020). In contrast, the amide II band originates from N–H bending and C–N stretching vibrations of the peptide bond, providing complementary information to the amide I band regarding the overall protein structure and composition. Collectively, these bands reflect the preservation of the fibrin network's molecular organisation and help explain the scaffold's regenerative potential (Chatterley *et al.*, 2022).

Furthermore, evident by previous studies by Kim et al, the preservation of functional group in the biomaterial aids in its capability to maintain the biological functionality of its protein contents, thereby facilitating cellular adhesion, proliferation, and differentiation (Kim *et al.*, 2021). In addition, the integrity of the fibrin network regulates enzymatic activity, and enables the controlled release of key growth factors, including PDGF, TGF- β, and VEGF, serving as essential regulators of angiogenesis, osteogenesis, and ECM formation during tissue regeneration (Li *et al.*, 2024a).

Moreover, the broad absorption band observed at ~3300 cm $^{-1}$ corresponds to O-H and N-H stretching vibrations, indicating the presence of extensive hydrogen bonding networks within the fibrin matrix. These hydrogen bonds are essential in maintaining the biomaterial's hydration state, biocompatibility, and molecular cohesion under physiological conditions. These characteristics are necessary for the biomaterial to integrate successfully with host tissues (Jarvis, 2023). In addition, the absorption peaks detected at ~1440 cm $^{-1}$ and 1080 cm $^{-1}$ corresponds to C-H bending and C-O stretching

vibrations respectively. These bands indicate the presence of carbohydrate and lipid residues within the fibrin matrix. These biochemical components aid in improving interfacial interactions between cells and the biomaterial, thereby enhancing cellular adhesion and metabolic activity essential for osteogenic differentiation during tissue regeneration.

Based on the observed FTIR spectral profile, both LyPRF and FPRF demonstrate the preservation of fundamental biochemical features of PRF through their ability to maintain the core structural and molecular integrity of fresh PRF matrix. However, subtle comparable spectral characteristics in peak intensities are apparent between the two biomaterials. These subtle variations suggest that lyophilisation process induces minor conformational modifications within the fibrin network, improving the chemical stability and degradation behaviour of LyPRF. These characteristics enhances the biomaterial's ability to sustain growth factor release over time, thus supporting prolonged cellular activity and ECM mineralisation compared to FPRF. Moreover, these structural modifications contribute to the improved handling characteristics and storage stability of LyPRF.

The FTIR analysis demonstrates that LyPRF preserves the fundamental functional groups of PRF, including its secondary protein structure and hydrogen-bonding framework. This preservation is achieved through the lyophilisation process, which removes water under low temperature and vacuum conditions. By eliminating water, lyophilisation prevents hydrolytic and enzymatic reactions that can denature proteins, while the low-temperature environment minimises thermal stress, stabilising the fibrin network and protecting both the protein structure and bioactive molecules from degradation (Abbasi *et al.*, 2020). These characteristics collectively reinforce LyPRF's potential as a durable, biocompatible, and effective biomaterial for BTE applications, capable of supporting long-term cellular viability and facilitating efficient tissue regeneration (Khan *et al.*, 2024; Monaghan *et al.*, 2023).

5.6 Crystallographic Characterisation of LyPRF and FPRF Analysed using XRD

The crystallographic characterisation of LyPRF and FPRF using XRD emphasises the predominance of amorphous structural features, consistent with the intrinsic nature of fibrin-based matrices. In contrast to conventional crystalline biomaterials, such as synthetic polymers, fibrin lacks the highly ordered internal atomic arrangement and long-range structural periodicity (Bayer, 2022). The observed diffraction patterns in both biomaterials confirm the extensive crystallisation does not occur during the fabrication method of both LyPRF and FPRF, thereby maintaining the physiological properties of the native fibrin scaffold.

Notably, a distinct diffraction peak observed at approximately 30°–31° (2θ) indicates the presence of calcium phosphate phases within the matrix. This characteristic is significant to BTE applications because calcium phosphate ($\#W_{\$}(Y\$_{(})_{\#}$) serves as of nucleation sites for hydroxyapatite formation, thereby facilitating osteoconduction, and promotes bone tissue mineralisation (Jeong *et al.*, 2019). The presence of $\#W_{\$}(Y\$_{(})_{\#}$ in LyPRF highlights its biomimetic properties, reflecting the mineral composition of natural craniofacial bone. Comparative analysis demonstrates that LyPRF exhibits higher peak intensity to FPRF, indicating an enhanced retention and stabilisation of the mineral-associated crystalline domains. This enhanced mineral preservation results from the lyophilisation process, effectively removing water while preserving the integrity of the fibrin-mineral composite, thereby ensuring both the mechanical stability and biofunctional properties of the biomaterial (Sui *et al.*, 2023a).

The synergistic coordination of predominantly amorphous fibrin network with stabilised mineral compositions in LyPRF presents a dual advantage for tissue regeneration applications. The amorphous fibrin network ensures mechanical flexibility and preserves the bioactive microenvironment necessary for cellular attachment, and proliferation. Furthermore, the mineral components enhance the biomaterial's osteoconductive potential, promoting mineral deposition and accelerating bone matrix maturation (Sindhi *et al.*, 2025). These amorphous characteristics emphasises the suitability of LyPRF as a biologically active biomaterial, capable of supporting both the biochemical and structural requirements essential for effective tissue healing BTE.

5.7 Kinetic Release Pattern of Growth Factors from LyPRF and FPRF Analysed using ELISA

Platelet-derived growth factors (PDGF-AB and PDGF-BB) and transforming growth factor beta 1 (TGF-β1) represents major growth factor released from both LyPRF and FPRF, essential for tissue regeneration in BTE applications. The kinetic release pattern of these growth factors exhibits a characteristic biphasic pattern, consisting of an initial burst followed by a sustained, gradual release phase. This spatiotemporal pattern is critically aligned with the sequential stages of tissue healing, reinforcing the ability of these biomaterials to provide molecular cues to coordinate tissue regeneration (Zhang *et al.*, 2018). Furthermore, the sustained presence of growth factors creates a continuous stimulatory environment that supports essential cellular activities, including cell proliferation, migration, adhesion, and vascularisation which are critical for effective tissue regeneration. Based on the ELISA analysis conducted, LyPRF exhibited higher and more prolonged growth factor release due to the lyophilisation process that stabilises its fibrin matrix, thus enhances its regenerative potential compared to FPRF (Ngah *et al.*, 2021a). Therefore, it emphasises the translational significance of LyPRF in BTE applications.

5.7.1 Platelet Derived Growth Factor-AB (PDGF-AB)

Platelet-derived growth factor-AB (PDGF-AB) is a key growth factor that regulates cellular activities, including cell migration, proliferation and ECM formation throughout tissue regeneration. It functions as a chemotactic and mitogenic signal for regenerative processes such as angiogenesis, osteogenesis, and tissue regeneration. The analysis revealed that LyPRF demonstrates a significantly higher release during the initial stage and leads to a greater cumulative release of PDGF-AB for 21 days compared to FPRF, emphasising its potential to enhance early angiogenesis and cellular migration (Obeagu, 2025b).

During the inflammatory phase, PDGF-AB functions as a potent chemotactic signal, attracting macrophages, MSCs, and endothelial cells essential for initiating bone regeneration. This effect is achieved through the coordinated roles of key cellular components, whereby macrophages regulate cytokine signalling, MSCs promote

osteogenic differentiation, and endothelial cells facilitate neovascularisation (Romero-López *et al.*, 2020). The observed sustained release of PDGF-AB from LyPRF up to day 14 corresponds with the proliferative phase of tissue healing, during which the growth factor stimulates fibroblast and osteoblast proliferation, and facilitate ECM synthesis. This extended bioavailability ensures a continued anabolic stimulus essential for forming a well-vascularised and mechanically competent tissue fibrin matrix (Xu *et al.*, 2018b).

During the remodelling phase, the sustained release of PDGF-AB from LyPRF supports the maturation and stabilisation of newly formed bone by promoting angiogenesis, collagen deposition, and extracellular matrix remodelling (Alizadeh *et al.*, 2023). In contrast, FPRF exhibits a lower and shorter PDGF-AB release, limiting its regenerative potential due to reduced cellular stimulation during healing. The sustained release of growth factors observed in LyPRF is attributed to the stabilisation of its fibrin network achieved through lyophilisation. By removing water under low temperature and vacuum conditions, lyophilisation preserves the structural integrity of the fibrin matrix and protects the embedded growth factor reservoirs from hydrolytic and enzymatic degradation. This prevents premature breakdown of the growth factors, allowing their gradual and controlled release, which is essential for maintaining bioactivity and supporting effective tissue regeneration (Liu *et al.*, 2022b).

The kinetic release pattern analysis in this study emphasis that LyPRF functions as an effective autologous reservoir, providing a sustained release of growth factors compared to FPRF. By delivering both an early burst and prolonged bioactivity, LyPRF supports the sequential phases of tissue regeneration, including the stimulation of cellular proliferation, migration, and extracellular matrix deposition, ultimately facilitating effective tissue repair. This controlled and sustained release profile underscores the potential of LyPRF as a suitable and reliable biomaterial for bone tissue engineering, particularly in craniofacial regenerative applications.

5.7.2 Platelet-Derived Growth Factor-BB (PDGF-BB)

Platelet-derived growth factor-BB (PDGF-BB) on the other hand, is a key proliferative and chemotactic growth factor that is essential in angiogenesis, osteogenesis, and fibroblast proliferation during tissue regeneration. This growth factor

is consistently recognised as a fundamental growth factor in PRF-based biomaterials (Mihaylova *et al.*, 2018). This is because, PDGF-BB plays a crucial role in regulating cell proliferation, migration, and ECM synthesis. The kinetic release pattern of PDGF-BB observed from both LyPRF and FPRF exhibited a distinct biphasic kinetic pattern, characterised by an initial burst release followed by a secondary peak at day 14. Although levels decline after day 14, they remain consistent throughout day 21, demonstrating a sustained release of growth factor. Therefore, this kinetic release pattern indicates that PDGF-BB contributes to both the early inflammatory and proliferative phases of tissue healing and sustain its activity into the later remodelling phases of tissue regeneration, reflecting its various involvement in regulating tissue regeneration (Paek *et al.*, 2020).

The coordinated release of PDGF-BB and PDGF-AB ensures complementary and synergistic signalling dynamics that enhance cellular proliferation, angiogenesis, and vascular stabilisation. In the inflammatory phase, both PDGF-AB and PDGF-BB function synergistically to aid cellular migration of macrophages, MSCs, and endothelial cells to the defect site, initiating tissue regeneration. PDGF-BB provides a strong chemotactic and proliferative signal, thus facilitating cell proliferation and migration (Mihaylova *et al.*, 2018). In addition, this growth factor promotes neovascularisation and the establishment of nutrient-rich microenvironment, supporting subsequent osteogenic activity. The early burst observed at day 1 corresponds with the acute inflammatory phase, while the secondary release peak at day 14 corresponds with a sustained regenerative signalling phase that aligns with the ECM formation and early bone tissue regeneration.

During the proliferative phase, the presence of PDGF-BB stimulates tissue formation, fibroblast proliferation, and ECM deposition. It promotes the differentiation of MSCs toward the osteoblastic lineage and enhances the synthesis of collagen and non-collagenous fibrin matrix, thereby accelerating new bone formation (Liu *et al.*, 2018). The sustained bioavailability observed in LyPRF throughout the observed duration, ensures prolonged stimulation of these cellular processes, advantageous for successful continuous tissue regeneration. Moreover, the angiogenic effects of PDGF-BB facilitates the coupling of vascular and bone tissue regeneration for BTE applications.

According to previous literature, the sustained presence of PDGF-BB during the remodelling phase supports the maturation and mineralisation of the newly formed bone

matrix. By maintaining angiogenic, and osteoblast signalling, PDGF-BB supports vessel stabilisation, bone matrix turnover, and the establishment of long-term integrity (Li *et al,* 2025). Comparatively, the reduced and shorter release duration of PDGF-BB observed in FPRF limits the biomaterial's ability to sustain prolonged anabolic signalling, potentially compromising its regenerative efficacy in defects requiring extended healing timeframes or substantial vascularisation.

The prolonged kinetic release pattern of PDGF-BB from LyPRF is associated with the structural preservation and stabilisation caused by the lyophilisation process, enhancing growth factor entrapment within the fibrin network and reduces degradation rate (Liu *et al,* 2022b). The preserved structural integrity of LyPRF enables it to function as a bioreservoir that regulates the sustained release of growth factors, thereby synchronising their availability with the physiological stages of tissue regeneration. This is supported by findings from Jia et al., who reported that the slow, physiologically relevant release of these growth factors enhances bone regeneration by promoting vascular formation as well as cell proliferation and migration (Jia *et al,* 2024). In contrast, the comparatively reduced and shorter release from FPRF may limit prolonged signalling, diminishing its regenerative efficacy in defects requiring extended healing.

Therefore, the analysis conducted using ELISA assay establish PDGF-BB as a key growth factor to facilitate bone regeneration and strengthen LyPRF's potential as a beneficial biomaterial for BTE applications. By providing both rapid and sustained release phases, LyPRF ensures continuous cellular stimulation across all stages of healing including inflammation to remodelling phases, thereby optimising the regenerative microenvironment. These characteristics reinforce LyPRF as an advanced autologous biomaterial for clinical use in maxillofacial and craniofacial bone regeneration, facilitating angiogenesis and osteogenesis for successful tissue regeneration.

5.7.3 Transforming Growth Factor-pi (TGF- pi)

Transforming growth factor-β 1 (TGF-β1) is a multifunctional growth factor that facilitate cell proliferation, differentiation, and ECM synthesis during tissue regeneration (Deng *et al,* 2024). The kinetic release analysis demonstrates that LyPRF exhibited a sharp initial peak of TGF-β1 on day 1, followed by a gradual and sustained

decline until day 7, without a secondary biphasic peak. In contrast, FPRF demonstrated a rapid drop after day 1, indicating a less stable release profile. Both materials showed no detectable TGF-β1 release beyond day 7 for LyPRF and day 1 for FPRF. This short yet sustained early release from LyPRF highlights its contribution during the initial stages of tissue regeneration, ensuring timely growth factor availability necessary for early healing processes. These findings are partially consistent with the slower release reported by Ehrenfest et al (Ehrenfest *et al.*, 2009). However, differences in sampling intervals may explain the discrepancies. In the current study, data could not be collected consistently at all time points due to limitations in sample volume and assay sensitivity, as well as the rapid depletion of detectable growth factor in FPRF. Consequently, these constraints may have limited the ability to fully capture the complete kinetic release pattern, particularly any later-phase or biphasic release events.

During the inflammatory phase, TGF-β1 have demonstrated that it is able to facilitate immune dynamics by stimulating fibril recruitment, directing immune cell chemotaxis, and initiating ECM synthesis (Massagué & Sheppard, 2023). These coordinated activities establish a favourable microenvironment that complements the chemotactic and mitogenic effects of PDGF. The coordination between TGF-β1 and PDGF ensures effective bioactivity between inflammation resolution and the reparative tissue regeneration, essential for stable BTE applications (Deng *et al.*, 2024).

In the proliferative phase, previous studies revealed that TGF-β1 facilitates MSC migration and differentiation into osteoblasts, enhances collagen synthesis, and supports ECM organisation (Irma *et al.*, 2025). These effects collectively strengthen the structural integrity of newly formed bone tissue. As regeneration progresses into the remodelling phase, TGF-β1 activity diminishes more rapidly than that of PDGF; however, its residual presence contributes to stabilising the ECM and facilitating the subsequent actions of PDGF-AB and PDGF-BB.

In contrast, the limited and short-lived TGF-β1 release observed in FPRF diminishes its capacity to support early immune modulation and extracellular matrix organisation, which can ultimately compromise osteogenic progression. These findings highlight TGF-β1 as a crucial growth factor for early remodelling. The sustained release of TGF-β1 from LyPRF further reinforces its potential as an improved autologous biomaterial for craniofacial regeneration in BTE applications.

5.8 Biocompatibility of LyPRF and FPRF Analysed using MTT Assay

The biocompatibility analysis of LyPRF and FPRF was assessed using an indirect MTT assay in accordance with ISO 10993-5, ensuring standardised, reliable evaluation of the biocompatibility of the biomaterials for BTE applications (Garcia *et al.*, 2024). Biocompatibility is a fundamental characteristic for biomaterials intended for clinical application, as it ensures safe interaction with host tissues without eliciting adverse cellular or systemic effects. The MTT assay, a widely accepted method, enables quantitative assessment of cell viability, metabolic activity, proliferation, and morphological integrity, offering critical insight into the safety and regenerative potential of LyPRF and FPRF for bone tissue engineering applications (Khalef *et al.*, 2024). Human gingival fibroblasts (HGFs) were selected as the representative cell line for the MTT assay to evaluate the biocompatibility of LyPRF and FPRF. This is because HGFs has been used widely in craniofacial studies due to its compatibility and cellular responses relevant to tissue regeneration applications (Savabi *et al.*, 2024). The results indicate that both LyPRF and FPRF exhibit excellent biocompatibility with host cells, supporting their application in craniofacial BTE. The absence of structural alterations or adverse cellular responses suggests that these biomaterials can maintain cellular viability and function, which is essential for effective tissue regeneration (Li *et al.*, 2024b; Vyas *et al.*, 2023). This finding is consistent with previous studies demonstrating that PRF-based materials provide a favourable microenvironment that promotes cell proliferation and osteogenic activity. The strong biocompatibility observed in LyPRF further highlights its potential as a stable, clinically translatable alternative to conventional FPRF.

The observed biocompatibility of HGF cells in this study is consistent with the autologous nature of PRF, which inherently minimizes the risk of immune incompatibility (Vahabi *et al.*, 2019). This biocompatibility is further enhanced by the fabrication protocol, which excludes exogenous additives such as anticoagulants or crosslinking agents that are known to influence biocompatibility. Collectively, these factors indicate that PRF provides a biologically favourable microenvironment that supports cell viability and function, reinforcing its suitability for craniofacial bone tissue engineering applications. As a natural fibrin matrix, PRF entraps platelets,

leukocytes, and various growth factors, creating a microenvironment that promotes cell adhesion, metabolic activity, and tissue regeneration (Jia *et al.*, 2024).

Fresh PRF is widely utilised as a biologically active scaffold for cell preservation and tissue repair in craniofacial regeneration. However, its clinical applicability is constrained by its inherently short half-life, as the material rapidly degrades, loses structural integrity, and cannot be stored after preparation (Jia *et al.*, 2024; Park *et al.*, 2024). This temporal limitation poses challenges for handling, storage, and standardisation, thus restricting its broader use in clinical settings. The MTT assay in this study revealed subtle differences in the temporal biocompatibility profiles of LyPRF and FPRF. FPRF demonstrated a stronger stimulatory effect during early incubation, reflecting its higher initial release of growth factors such as PDGF-AB, PDGF-BB, and TGF-β1. This rapid release of bioactive molecules enhances fibroblast metabolic activity and proliferation, supporting the early cellular responses necessary for tissue regeneration (Ashour *et al.*, 2023). However, this effect was temporary, reflecting the faster degradation and limited growth factor retention of FPRF. In contrast, LyPRF demonstrated more stable and sustained metabolic activity, maintaining higher cell viability at later time points. This prolonged activity is attributed to the preserved fibrin matrix, which enables controlled degradation and gradual release of entrapped growth factors, thereby providing a supportive microenvironment for continued cellular function and tissue regenerative processes. (Wong *et al.*, 2021b).

CHAPTER 6
CONCLUSION

This study comprehensively characterised the physicochemical properties and biocompatibility of LyPRF in comparison to FPRF for potential application in craniofacial bone regeneration. The findings demonstrate that LyPRF preserves the essential structural and biochemical integrity of conventional PRF while offering additional advantages in terms of stability, handling, and long-term storage. Microstructural, elemental, and crystallographic analyses demonstrated that LyPRF retained a porous, sponge-like fibrin architecture with a favourable pore size distribution and enhanced cellular entrapment, while preserving key elemental composition, functional protein groups, and mineral-associated phases associated with osteoconduction and biomimetic mineralisation. In addition, the release profiles of PDGF-AB, PDGF-BB, and TGF-β1 indicated that LyPRF functioned as an effective autologous reservoir, exhibiting higher and more sustained growth factor release in accordance with the sequential inflammatory, proliferative, and remodelling phases of tissue regeneration. Biocompatibility assessment further confirmed that LyPRF supported prolonged fibroblast viability and metabolic activity, with no evidence of cytotoxic effects. Collectively, these findings indicate that LyPRF exhibits structural and biological properties superior to FPRF, attributable to its biomimetic resemblance to native craniofacial bone, and support its potential application as a biomaterial for craniofacial bone tissue engineering.

6.1 Strength and Contribution of The Study

This study presents a systematic and comprehensive evaluation of the physicochemical properties and biocompatibility of LyPRF in comparison FPRF, thereby advancing current understanding of platelet concentrate optimisation for BTE applications. A key strength of this work is the integration of multiple complementary analytical techniques, including XRD, FESEM, EDX, and FTIR, which collectively enabled a detailed assessment of the structural integrity, compositional stability, and mineral-associated characteristics of LyPRF. Additionally, the correlation of these

physicochemical parameters with biological outcomes derived from MTT assays established a coherent structure–function relationship linking material properties to biocompatibility and regenerative potential.

Moreover, the inclusion of growth factor kinetic release analysis provided critical insight into the preservation and sustained bioavailability of key growth factors essential for effective tissue regeneration. The findings demonstrate that LyPRF retains the fundamental fibrin architecture, elemental composition, and biological activity of native PRF while offering enhanced storage stability and improved handling characteristics. By addressing the inherent limitation of conventional PRF related to its short shelf life, this study positions LyPRF as a more practical and versatile biomaterial for potential clinical translation. Overall, this work contributes novel and foundational evidence supporting LyPRF as an advancement over conventional PRF and provides a robust scientific basis to inform future preclinical, translational, and clinical investigations in craniofacial bone regeneration.

6.2 Limitations of The Study

While this study provides valuable insights into the physicochemical and biological characteristics of LyPRF, several limitations should be acknowledged. The experimental investigations were conducted exclusively under in vitro conditions, which do not fully replicate the complex physiological environment associated with bone healing and tissue regeneration in vivo. Consequently, critical factors such as immune responses, vascularisation, and mechanical loading were not accounted for, which may influence the translational relevance of the findings. In addition, the scope of biological evaluation of the LyPRF was limited. Although the MTT assay offered important information regarding cellular viability and biocompatibility, it does not comprehensively reflect other essential biological processes, including osteogenic differentiation, angiogenic potential, or long-term cell–material interactions. Collectively, these limitations underscore the necessity for further in-depth biological assessments and in vivo studies to more fully establish the regenerative capacity and clinical applicability of LyPRF.

6.3 Future Studies

Future research should aim to build upon these findings through in vivo preclinical studies using animal models of craniofacial bone defects to evaluate the regenerative efficacy, degradation behaviour, and host tissue response of LyPRF. Investigating the mechanical properties and degradation kinetics of LyPRF under physiological conditions were provide a deeper understanding of its functional performance. Additionally, the combination of LyPRF with other biomaterials, such as bioglass, hydroxyapatite, or chitosan should be explored to create composite scaffolds that enhance mechanical strength, bioactivity, and controlled growth factor release. Ultimately, translational research involving clinical trials were be essential to validate the safety, reliability, and therapeutic benefits of LyPRF-based constructs, paving the way for their integration into next-generation regenerative therapies for craniofacial reconstruction.

REFERENCES

Aazmi, A., Zhang, D., Mazzaglia, C., Yu, M., Wang, Z., Yang, H., Huang, Y. Y. S., & Ma, L. (2024). Biofabrication methods for reconstructing extracellular matrix mimetics. *Bioactive Materials*, *31*, 475-496. https://doi.org/https://doi.org/10.1016/j.bioactmat.2023.08.018

Abbasi, N., Hamlet, S., Love, R. M., & Nguyen, N.-T. (2020). Porous scaffolds for bone regeneration. *Journal of Science: Advanced Materials and Devices*, *5*(1), 1-9. https://doi.org/https://doi.org/10.1016/j.jsamd.2020.01.007

Aghali, A. (2021). Craniofacial Bone Tissue Engineering: Current Approaches and Potential Therapy. *Cells*, *10*(11). https://doi.org/10.3390/cells10112993

Aizawa, H., Tsujino, T., Watanabe, T., Isobe, K., Kitamura, Y., Sato, A., Yamaguchi, S., Okudera, H., Okuda, K., & Kawase, T. (2020). Quantitative near-infrared imaging of platelets in platelet-rich fibrin (PRF) matrices: comparative analysis of bio-PRF, leukocyte-rich PRF, advanced-PRF and concentrated growth factors. *International Journal of Molecular Sciences*, *21*(12), 4426.

Ali, A., Chiang, Y. W., & Santos, R. M. (2022). X-ray diffraction techniques for mineral characterization: A review for engineers of the fundamentals, applications, and research directions. *Minerals*, *12*(2), 205.

Alizadeh, M., Salehi, S., Tavakoli, M., Mirhaj, M., Varshosaz, J., Kazemi, N., Salehi, S., Mehrjoo, M., & Abadi, S. A. M. (2023). PDGF and VEGF-releasing bi-layer wound dressing made of sodium tripolyphosphate crosslinked gelatin-sponge layer and a carrageenan nanofiber layer [Article]. *International journal of biological macromolecules*, *233*, Article 123491. https://doi.org/10.1016/j.ijbiomac.2023.123491

Almouemen, N., Kelly, H. M., & O'Leary, C. (2019). Tissue Engineering: Understanding the Role of Biomaterials and Biophysical Forces on Cell Functionality Through Computational and Structural Biotechnology Analytical Methods. *Comput Struct Biotechnol J*, *17*, 591-598. https://doi.org/10.1016/j.csbj.2019.04.008

Alonzo, M., Primo, F. A., Kumar, S. A., Mudloff, J. A., Dominguez, E., Fregoso, G., Ortiz, N., Weiss, W. M., & Joddar, B. (2021). Bone tissue engineering techniques, advances, and scaffolds for treatment of bone defects. *Current opinion in biomedical engineering*, *17*, 100248.

Altalbawy, F. M. A., Mukhlif, B. A. M., Hussen, A., Mohammed, J. S., S, R. J., Singh, A., Mishra, S. B., Chauhan, A. S., Astaneh, M. E., & Fereydouni, N. (2025). Regenerative potential of PRP-based scaffolds in chronic wound healing: Mechanisms, advances, and therapeutic insights. *Regen Ther*, *30*, 278-298. https://doi.org/10.1016/j.reth.2025.06.008

Anaya-Sampayo, L. M., García-Robayo, D. A., Roa, N. S., Rodriguez-Lorenzo, L. M., & Martínez-Cardozo, C. (2024). Platelet-rich fibrin (PRF) modified nano-hydroxyapatite/chitosan/gelatin/alginate scaffolds increase adhesion and viability of human dental pulp stem cells (DPSC) and osteoblasts derived from DPSC. *International journal of biological macromolecules*, 133064.

Andia, I., Perez valle, A., Amo, C. D., & Maffulli, N. (2020). Freeze drying of platelet rich plasma: The quest for standardization [Review]. *International Journal of Molecular Sciences*, *21*(18), 1-20, Article 6904. https://doi.org/10.3390/ijms21186904

Ansarizadeh, M., Mashayekhan, S., & Saadatmand, M. (2019). Fabrication, modeling

and optimization of lyophilized advanced platelet rich fibrin in combination with collagen-chitosan as a guided bone regeneration membrane. *International journal of biological macromolecules*, *125*, 383-391.

Ashour, S. H., Mudalal, M., Al-Aroomi, O., Al-Attab, R., Li, W., & Yin, L. (2023). The Effects of Injectable Platelet-Rich Fibrin and Advanced-Platelet Rich Fibrin on Gingival Fibroblast Cell Vitality, Proliferation, Differentiation. *Tissue Engineering and Regenerative Medicine*, *20*. https://doi.org/10.1007/s13770-023-00586-1

Asmundo, M. G., Durukan, E., von Rohden, E., Thy, S. A., Jensen, C. F. S., & Fode, M. (2024). Platelet-rich plasma therapy in erectile dysfunction and Peyronie's disease: a systematic review of the literature. *World Journal of Urology*, *42*(1), 359.

Bakhshandeh, B., Ranjbar, N., Abbasi, A., Amiri, E., Abedi, A., Mehrabi, M. R., Dehghani, Z., & Pennisi, C. P. (2023). Recent progress in the manipulation of biochemical and biophysical cues for engineering functional tissues. *Bioeng Transl Med*, *8*(2), e10383. https://doi.org/10.1002/btm2.10383

Banyatworakul, P., Osathanon, T., Chumprasert, S., Pavasant, P., & Pirarat, N. (2021). Responses of canine periodontal ligament cells to bubaline blood derived platelet rich fibrin in vitro. *Scientific Reports*, *11*. https://doi.org/10.1038/s41598-021-90906-z

Baronio, C. M., & Barth, A. (2020). The Amide I Spectrum of Proteins-Optimization of Transition Dipole Coupling Parameters Using Density Functional Theory Calculations. *J Phys Chem B*, *124*(9), 1703-1714. https://doi.org/10.1021/acs.jpcb.9b11793

Bayer, I. S. (2022). Advances in Fibrin-Based Materials in Wound Repair: A Review. *Molecules*, *27*(14). https://doi.org/10.3390/molecules27144504

Bhambere, D., Gaidhani, K., Harwalkar, M., & Nirgude, P. (2015). LYOPHILIZATION / FREEZE DRYING – A REVIEW. *World Journal of Pharmaceutical Research*, *4*, 516-543.

Bhushan, S., Singh, S., Maiti, T. K., Sharma, C., Dutt, D., Sharma, S., Li, C., & Tag Eldin, E. M. (2022). Scaffold fabrication techniques of biomaterials for bone tissue engineering: a critical review. *Bioengineering*, *9*(12), 728.

Biswas, S., Sarojini, S., Jayaram, S., Philip, I., Umesh, M., Mascarenhas, R., Pappuswamy, M., Balasubramanian, B., & Arokiyaraj, S. (2023). Understanding the Role of Antimicrobial Peptides in Neutrophil Extracellular Traps Promoting Autoimmune Disorders. *Life (Basel)*, *13*(6). https://doi.org/10.3390/life13061307

Boskey, A., & Pleshko Camacho, N. (2007). FT-IR imaging of native and tissue-engineered bone and cartilage. *Biomaterials*, *28*(15), 2465-2478. https://doi.org/10.1016/j.biomaterials.2006.11.043

Calciolari, E., Dourou, M., Akcali, A., & Donos, N. (2025). Differences between first and second generation autologous platelet concentrates. *Periodontology 2000*, *97*(1), 52-73.

Chatterley, A. S., Laity, P., Holland, C., Weidner, T., Woutersen, S., & Giubertoni, G. (2022). Broadband Multidimensional Spectroscopy Identifies the Amide II Vibrations in Silkworm Films. *Molecules*, *27*(19). https://doi.org/10.3390/molecules27196275

Choukroun, J., Aalam, A. A., & Miron, R. J. (2017). Platelet Rich Fibrin "PRF" and Regenerative Medicine:'The Low-Speed Concept'. *MSCs and innovative biomaterials in dentistry*, 21-42.

Choukroun, J., Diss, A., Simonpieri, A., Girard, M.-O., Schoeffler, C., Dohan, S. L., Dohan, A. J., Mouhyi, J., & Dohan, D. M. (2006). Platelet-rich fibrin (PRF): a second-generation platelet concentrate. Part IV: clinical effects on tissue healing. *Oral Surgery, Oral Medicine, Oral Pathology, Oral Radiology, and Endodontology*, *101*(3), e56-e60.

Chuang, E. Y., Lin, Y. C., Huang, Y. M., Chen, C. H., Yeh, Y. Y., Rethi, L., Chou, Y. J., Jheng, P. R., Lai, J. M., Chiang, C. J., & Wong, C. C. (2024). Biofunctionalized hydrogel composed of genipin-crosslinked gelatin/ hyaluronic acid incorporated with lyophilized platelet-rich fibrin for segmental bone defect repair. *Carbohydrate Polymers*, *339*, Article 122174. https://doi.org/10.1016/j.carbpol.2024.122174

Dang, M., Saunders, L., Niu, X., Fan, Y., & Ma, P. X. (2018). Biomimetic delivery of signals for bone tissue engineering. *Bone Research*, *6*(1), 25. https://doi.org/10.1038/s41413-018-0025-8

Dao, H. M., Sahakijpijarn, S., Chrostowski, R., Peng, H. H., Moon, C., Xu, H., Mangolini, F., Do, H. H., Cui, Z., & Williams, R. O., 3rd. (2022). Entrapment of air microbubbles by ice crystals during freezing exacerbates freeze-induced denaturation of proteins. *Int J Pharm*, *628*, 122306. https://doi.org/10.1016/j.ijpharm.2022.122306

Dashore, S., Chouhan, K., Nanda, S., & Sharma, A. (2021). Platelet-Rich Fibrin, Preparation and Use in Dermatology. *Indian Dermatol Online J*, *12*(Suppl 1), S55-s65. https://doi.org/10.4103/idoj.idoj_282_21

de Lima Barbosa, R., Stellet Lourenço, E., de Azevedo dos Santos, J. V., Rodrigues Santiago Rocha, N., Mourão, C. F., & Alves, G. G. (2023). The Effects of Platelet-Rich Fibrin in the Behavior of Mineralizing Cells Related to Bone Tissue Regeneration—A Scoping Review of In Vitro Evidence. *Journal of Functional Biomaterials*, *14*(10), 503. https://www.mdpi.com/2079-4983/14/10/503

Deng, Z., Fan, T., Xiao, C., Tian, H., Zheng, Y., Li, C., & He, J. (2024). TGF-β signaling in health, disease, and therapeutics. *Signal Transduct Target Ther*, *9*(1), 61. https://doi.org/10.1038/s41392-024-01764-w

Diao, W., Li, P., Jiang, X., Zhou, J., & Yang, S. (2024). Progress in copper-based materials for wound healing. *Wound repair and regeneration*, *32*(3), 314-322. https://doi.org/https://doi.org/10.1111/wrr.13122

Dias, F. J., Venegas, C., Borie, E., Arias, A., Watanabe, I. S., & Fuentes, R. (2020). A new insight of Platelet-Rich Fibrin clots morphology and their elemental composition. *Tissue Cell*, *65*, 101362. https://doi.org/10.1016/j.tice.2020.101362

Ehrenfest, D., de Peppo, G. M., Doglioli, P., & Sammartino, G. (2009). Slow release of growth factors and thrombospondin-1 in Choukroun's platelet-rich fibrin (PRF): A gold standard to achieve for all surgical platelet concentrates technologies. *Growth factors (Chur, Switzerland)*, *27*, 63-69. https://doi.org/10.1080/08977190802636713

Farag, A., Ngeun, S. K., Kaneda, M., Aboubakr, M., Elhaieg, A., Hendawy, H., & Tanaka, R. (2024). Exploring the Potential Effects of Cryopreservation on the Biological Characteristics and Cardiomyogenic Differentiation of Rat Adipose-Derived Mesenchymal Stem Cells. *Int J Mol Sci*, *25*(18). https://doi.org/10.3390/ijms25189908

Feng, J., Liu, J., Wang, Y., Diao, J., Kuang, Y., & Zhao, N. (2023). Beta-TCP scaffolds with rationally designed macro-micro hierarchical structure improved

angio/osteo-genesis capability for bone regeneration. *Journal of Materials Science: Materials in Medicine*, *34*(7), 36. https://doi.org/10.1007/s10856-023-06733-3

Feng, M., Wang, Y., Zhang, P., Zhao, Q., Yu, S., Shen, K., Miron, R. J., & Zhang, Y. (2020). Antibacterial effects of platelet-rich fibrin produced by horizontal centrifugation. *International Journal of Oral Science*, *12*(1), 32. https://doi.org/10.1038/s41368-020-00099-w

Ferraz, M. P. (2023). Bone Grafts in Dental Medicine: An Overview of Autografts, Allografts and Synthetic Materials. *Materials (Basel)*, *16*(11). https://doi.org/10.3390/ma16114117

Gan, S., Zheng, Z., Zhang, M., Long, L., Zhang, X., Tan, B., Zhu, Z., Liao, J., & Chen, W. (2023a). Lyophilized Platelet-Rich Fibrin Exudate-Loaded Carboxymethyl Chitosan/GelMA Hydrogel for Efficient Bone Defect Repair [Article]. *ACS Applied Materials and Interfaces*, *15*(22), 26349-26362. https://doi.org/10.1021/acsami.3c02528

Gan, S. Q., Zheng, Z., Zhang, M., Long, L., Zhang, X., Tan, B. W., Zhu, Z. M., Liao, J. F., & Chen, W. C. (2023b). Lyophilized Platelet-Rich Fibrin Exudate-Loaded Carboxymethyl Chitosan/GelMA Hydrogel for Efficient Bone Defect Repair. *Acs Applied Materials & Interfaces*, *15*(22), 26349-26362. https://doi.org/10.1021/acsami.3c02528

Garcia, C., Garcia, P., Santos, O., Steffens, D., Martins, S., Pranke, P., Crespo, J., Henriques, J. A., & Roesch-Ely, M. (2024). Red propolis extract associated to platelet- rich plasma and stromal cells with focus in cell therapy and functional tissue regeneration. *Anais da Academia Brasileira de Ciências*, *96*. https://doi.org/10.1590/0001-3765202420240100

Gaßling, V., Douglas, T., Purcz, N., Schaubroeck, D., Balcaen, L., Bliznuk, V., Declercq, H., Vanhaecke, F., & Dubruel, P. (2013). Magnesium-enhanced enzymatically mineralized platelet-rich fibrin for bone regeneration applications. *Biomedical materials (Bristol, England)*, *8*, 055001. https://doi.org/10.1088/1748-6041/8/5/055001

Georgeanu, V. A., Gingu, O., Antoniac, I. V., & Manolea, H. O. (2023). Current Options and Future Perspectives on Bone Graft and Biomaterials Substitutes for Bone Repair, from Clinical Needs to Advanced Biomaterials Research. *Applied Sciences*, *13*(14), 8471. https://www.mdpi.com/2076-3417/13/14/8471

Götz, W., Tobiasch, E., Witzleben, S., & Schulze, M. (2019). Effects of Silicon Compounds on Biomineralization, Osteogenesis, and Hard Tissue Formation. *Pharmaceutics*, *11*(3). https://doi.org/10.3390/pharmaceutics11030117

Grzelak, A., Hnydka, A., Higuchi, J., Michalak, A., Tarczynska, M., Gaweda, K., & Klimek, K. (2024). Recent Achievements in the Development of Biomaterials Improved with Platelet Concentrates for Soft and Hard Tissue Engineering Applications. *International Journal of Molecular Sciences*, *25*(3), 1525.

Haghparast-Kenarsari, T., Abdouss, M., Heidari Keshel, S., Heshmatipour, Z., Rahimi, A., & Biazar, E. (2024). Improving properties of platelet-rich fibrin scaffold with tannic acid for wound healing [Article]. *International Wound Journal*, *21*(4), Article e14571. https://doi.org/10.1111/iwj.14571

Hamraoui, A. (2025). Cell adhesion and surface interactions: A comprehensive review of surface energy, wettability, and topography effects. *AIP Advances*, *15*. https://doi.org/10.1063/5.0280399

Handtke, S., & Thiele, T. (2020). Large and small platelets—(When) do they differ? *Journal of Thrombosis and Haemostasis*, *18*(6), 1256-1267.

https://doi.org/https://doi.org/10.1111/jth.14788
Hasan, S. M., Sen, P., Anik, H., Islam, M., Roy, M., Ahmed, T., & Haque, A. N. M. A. (2025). Recent progress in polymeric ultrafine fibrous scaffolds for enabling cell infiltration in tissue engineering. *Journal of Biomaterials Applications*, 8853282251380622. https://doi.org/10.1177/08853282251380622
He, Z., Zhang, H., Li, H., Wang, Y., Qian, J., Cai, X., Sun, L., & Huang, J. (2020). Preparation, Biosafety, and Cytotoxicity Studies of a Newly Tumor-Microenvironment-Responsive Biodegradable Mesoporous Silica Nanosystem Based on Multimodal and Synergistic Treatment. *Oxid Med Cell Longev*, *2020*, 7152173. https://doi.org/10.1155/2020/7152173
Heydari, M.-H., Sadeghian, A., Khadivi, G., Mustafa, H. J., Javinani, A., Nadjmi, N., & Khojasteh, A. (2024). Prevalence, trend, and associated risk factors for cleft lip with/without cleft palate: a national study on live births from 2016 to 2021. *BMC Oral Health*, *24*(1), 36. https://doi.org/10.1186/s12903-023-03797-z
Huang, D., Li, Z., Li, G., Zhou, F., Wang, G., Ren, X., & Su, J. (2025a). Biomimetic structural design in 3D-printed scaffolds for bone tissue engineering. *Materials Today Bio*, *32*, 101664. https://doi.org/https://doi.org/10.1016/j.mtbio.2025.101664
Huang, J., Ratnayake, J., Ramesh, N., & Dias, G. J. (2020). Development and Characterization of a Biocomposite Material from Chitosan and New Zealand-Sourced Bovine-Derived Hydroxyapatite for Bone Regeneration. *ACS Omega*, *5*(27), 16537-16546. https://doi.org/10.1021/acsomega.0c01168
Huang, S., Li, Q., Li, X., Ye, H., Zhang, L., & Zhu, X. (2025b). Recent Research Progress of Wound Healing Biomaterials Containing Platelet-Rich Plasma. *Int J Nanomedicine*, *20*, 3961-3976. https://doi.org/10.2147/ijn.S506677
Hughes, E. A., Robinson, T. E., Bassett, D. B., Cox, S. C., & Grover, L. M. (2019). Critical and diverse roles of phosphates in human bone formation. *Journal of Materials Chemistry B*, *7*(47), 7460-7470.
Irma, J., Kartasasmita, A. S., Kartiwa, A., Irfani, I., Rizki, S. A., & Onasis, S. (2025). From Growth Factors to Structure: PDGF and TGF-β in Granulation Tissue Formation. A Literature Review. *J Cell Mol Med*, *29*(11), e70374. https://doi.org/10.1111/jcmm.70374
Izumiya, M., Haniu, M., Ueda, K., Ishida, H., Ma, C., Ideta, H., Sobajima, A., Ueshiba, K., Uemura, T., Saito, N., & Haniu, H. (2021). Evaluation of MC3T3-E1 Cell Osteogenesis in Different Cell Culture Media. *Int J Mol Sci*, *22*(14). https://doi.org/10.3390/ijms22147752
Jarvis, M. C. (2023). Hydrogen bonding and other non-covalent interactions at the surfaces of cellulose microfibrils. *Cellulose*, *30*(2), 667-687.
Jasmine, S., Thangavelu, A., Krishnamoorthy, R., Alzahrani, K., & Alshuniaber, M. (2021). Architectural and ultrastructural variations of human leukocyte-rich platelet-rich fibrin and injectable platelet-rich fibrin [Article]. *Journal of Microscopy and Ultrastructure*, *9*(2), 76-80. https://doi.org/10.4103/JMAU.JMAU_7_20
Jeong, J., Kim, J. H., Shim, J. H., Hwang, N. S., & Heo, C. Y. (2019). Bioactive calcium phosphate materials and applications in bone regeneration. *Biomater Res*, *23*, 4. https://doi.org/10.1186/s40824-018-0149-3
Jia, K., You, J., Zhu, Y., Li, M., Chen, S., Ren, S., Chen, S., Zhang, J., Wang, H., & Zhou, Y. (2024). Platelet-rich fibrin as an autologous biomaterial for bone regeneration: mechanisms, applications, optimization. *Front Bioeng Biotechnol*, *12*, 1286035. https://doi.org/10.3389/fbioe.2024.1286035

Karageorgiou, V., & Kaplan, D. (2005). Porosity of 3D Biomaterial Scaffolds and Osteogenesis. *Biomaterials*, *26*, 5474-5491. https://doi.org/10.1016/j.biomaterials.2005.02.002

Kardos, D., Hornyák, I., Simon, M., Hinsenkamp, A., Marschall, B., Várdai, R., Kállay-Menyhárd, A., Pinke, B., Mészáros, L., Kuten, O., Nehrer, S., & Lacza, Z. (2018). Biological and Mechanical Properties of Platelet-Rich Fibrin Membranes after Thermal Manipulation and Preparation in a Single-Syringe Closed System. *International Journal of Molecular Sciences*, *19*(11), 3433. https://www.mdpi.com/1422-0067/19/11/3433

Kargozar, S., Mozafari, M., Hamzehlou, S., Brouki Milan, P., Kim, H.-W., & Baino, F. (2019). Bone Tissue Engineering Using Human Cells: A Comprehensive Review on Recent Trends, Current Prospects, and Recommendations. *Applied Sciences*, *9*(1), 174. https://www.mdpi.com/2076-3417/9/1/174

Khalef, L., Lydia, R., Filicia, K., & Moussa, B. (2024). Cell viability and cytotoxicity assays: Biochemical elements and cellular compartments. *Cell biochemistry and function*, *42*(3), e4007.

Khan, A. R., Gholap, A. D., Grewal, N. S., Jun, Z., Khalid, M., & Zhang, H.-J. (2025). Advances in smart hybrid scaffolds: A strategic approach for regenerative clinical applications. *Engineered Regeneration*, *6*, 85-110. https://doi.org/https://doi.org/10.1016/j.engreg.2025.02.002

Khan, U. M., Sameen, A., Decker, E. A., Shabbir, M. A., Hussain, S., Latif, A., Abdi, G., & Aadil, R. M. (2024). Implementation of plant extracts for cheddar-type cheese production in conjunction with FTIR and Raman spectroscopy comparison. *Food Chemistry: X*, *22*, 101256. https://doi.org/https://doi.org/10.1016/j.fochx.2024.101256

Kim, H., Kumbar, S. G., & Nukavarapu, S. P. (2021). Biomaterial-directed cell behavior for tissue engineering. *Curr Opin Biomed Eng*, *17*. https://doi.org/10.1016/j.cobme.2020.100260

Krishani, M., Shin, W. Y., Suhaimi, H., & Sambudi, N. S. (2023). Development of Scaffolds from Bio-Based Natural Materials for Tissue Regeneration Applications: A Review [Review]. *Gels*, *9*(2), Article 100. https://doi.org/10.3390/gels9020100

Li, S., Cai, X., Guo, J., Li, X., Li, W., Liu, Y., & Qi, M. (2025). Cell communication and relevant signaling pathways in osteogenesis–angiogenesis coupling. *Bone Research*, *13*(1), 45.

Li, S., Dan, X., Chen, H., Li, T., Liu, B., Ju, Y., Li, Y., Lei, L., & Fan, X. (2024a). Developing fibrin-based biomaterials/scaffolds in tissue engineering [Review]. *Bioactive Materials*, *40*, 597-623. https://doi.org/10.1016/j.bioactmat.2024.08.006

Li, S., Dan, X., Chen, H., Li, T., Liu, B., Ju, Y., Li, Y., Lei, L., & Fan, X. (2024b). Developing fibrin-based biomaterials/scaffolds in tissue engineering. *Bioact Mater*, *40*, 597-623. https://doi.org/10.1016/j.bioactmat.2024.08.006

Liu, Q., Zhou, Y., & Li, Z. (2018). PDGF BB promotes the differentiation and proliferation of MC3T3 E1 cells through the Src/JAK2 signaling pathway. *Mol Med Rep*, *18*(4), 3719-3726. https://doi.org/10.3892/mmr.2018.9351

Liu, W., Liu, Y., Li, T., Liu, L., Du, M., Du, J., Qi, Y., & Xiang, G. (2024a). Long-term stability of frozen platelet-rich plasma under -80 °C storage condition. *Regen Ther*, *26*, 826-830. https://doi.org/10.1016/j.reth.2024.09.006

Liu, X., Yin, M., Li, Y., Wang, J., Da, J., Liu, Z., Zhang, K., Liu, L., Zhang, W., & Wang, P. (2022a). Genipin modified lyophilized platelet-rich fibrin scaffold for

sustained release of growth factors to promote bone regeneration. *Frontiers in Physiology, 13*, 1007692.

Liu, X., Yin, M., Li, Y., Wang, J., Da, J., Liu, Z., Zhang, K., Liu, L., Zhang, W., Wang, P., Jin, H., & Zhang, B. (2022b). Genipin modified lyophilized platelet-rich fibrin scaffold for sustained release of growth factors to promote bone regeneration [Article]. *Frontiers in Physiology*, *13*, Article 1007692. https://doi.org/10.3389/fphys.2022.1007692

Liu, X., Zhou, J., Chen, M., Chen, S., You, J., Li, Y., Lv, H., Zhang, Y., & Zhou, Y. (2024b). 3D-printed biomimetic bone scaffold loaded with lyophilized concentrated growth factors promotes bone defect repair by regulation the VEGFR2/PI3K/AKT signaling pathway [Article]. *International journal of biological macromolecules*, *282*, Article 136938. https://doi.org/10.1016/j.ijbiomac.2024.136938

Liu, Z., Jin, H., Xie, Q., Jiang, Z., Guo, S., Li, Y., & Zhang, B. (2019a). Controlled Release Strategies for the Combination of Fresh and Lyophilized Platelet-Rich Fibrin on Bone Tissue Regeneration [Article]. *BioMed Research International*, *2019*, Article 4923767. https://doi.org/10.1155/2019/4923767

Liu, Z., Jin, H., Xie, Q., Jiang, Z., Guo, S., Li, Y., & Zhang, B. (2019b). Controlled release strategies for the combination of fresh and lyophilized platelet rich fibrin on bone tissue regeneration. *BioMed Research International*, *2019*(1), 4923767.

Lutzweiler, G., Ndreu Halili, A., & Engin Vrana, N. (2020). The Overview of Porous, Bioactive Scaffolds as Instructive Biomaterials for Tissue Regeneration and Their Clinical Translation. *Pharmaceutics*, *12*(7). https://doi.org/10.3390/pharmaceutics12070602

Mahmoodabadi, R. A., Golafshan, H. A., Pezeshkian, F., Shahriarirad, R., & Namazi, M. R. (2023). Evaluation of the Effect of Platelet-Rich Fibrin Matrix in the Correction of Periorbital Wrinkles: An Experimental Clinical Trial. *Dermatol Pract Concept, 13*(1). https://doi.org/10.5826/dpc.1301a50

Mariano, L. C., Fernandes, M. H. R., & Gomes, P. S. (2022). Antimicrobial Biomaterials for the Healing of Infected Bone Tissue: A Systematic Review of Microtomographic Data on Experimental Animal Models. *Journal of Functional Biomaterials*, *13*(4), 193. https://www.mdpi.com/2079-4983/13/4/193

Martineau, I., Lacoste, E., & Gagnon, G. (2004). Effects of calcium and thrombin on growth factor release from platelet concentrates: kinetics and regulation of endothelial cell proliferation. *Biomaterials*, *25*(18), 4489-4502.

Marx, R. E., Carlson, E. R., Eichstaedt, R. M., Schimmele, S. R., Strauss, J. E., & Georgeff, K. R. (1998). Platelet-rich plasma: Growth factor enhancement for bone grafts. *Oral Surg Oral Med Oral Pathol Oral Radiol Endod*, *85*(6), 638-646. https://doi.org/10.1016/s1079-2104(98)90029-4

Massagué, J., & Sheppard, D. (2023). TGF-β signaling in health and disease. *Cell*, *186*(19), 4007-4037.

Mihaylova, Z., Tsikandelova, R., Sanimirov, P., Gateva, N., Mitev, V., & Ishkitiev, N. (2018). Role of PDGF-BB in proliferation, differentiation and maintaining stem cell properties of PDL cells in vitro. *Archives of Oral Biology*, *85*, 1-9. https://doi.org/https://doi.org/10.1016/j.archoralbio.2017.09.019

Milano, F., Chevrier, A., De Crescenzo, G., & Lavertu, M. (2023). Injectable Lyophilized Chitosan-Thrombin-Platelet-Rich Plasma (CS-FIIa-PRP) Implant to Promote Tissue Regeneration: In Vitro and Ex Vivo Solidification Properties [Article]. *Polymers*, *15*(13), Article 2919.

https://doi.org/10.3390/polym15132919
Molenda, M., & Kolmas, J. (2023). The Role of Zinc in Bone Tissue Health and Regeneration-a Review. *Biol Trace Elem Res*, *201*(12), 5640-5651. https://doi.org/10.1007/s12011-023-03631-1
Monaghan, J. F., Cullen, D., Wynne, C., Lyng, F. M., & Meade, A. D. (2023). Effect of pre-analytical variables on Raman and FTIR spectral content of lymphocytes [Article]. *Analyst*, *148*(21), 5422-5434. https://doi.org/10.1039/d3an00686g
Moon, S., Hong, J., Go, S., & Kim, B. S. (2023). Immunomodulation for Tissue Repair and Regeneration. *Tissue Eng Regen Med*, *20*(3), 389-409. https://doi.org/10.1007/s13770-023-00525-0
Mościcka, P., & Przylipiak, A. (2021). History of autologous platelet-rich plasma: A short review. *J Cosmet Dermatol*, *20*(9), 2712-2714. https://doi.org/10.1111/jocd.14326
Nakajima, R., Saita, Y., Kobayashi, Y., Wakayama, T., Uchino, S., Momoi, Y., Yamamoto, N., & Ishijima, M. (2024). Comparison of bioactive substances in novel-developed freeze-dried platelet-rich plasma (PRP) and activated normal PRP, and investigation of bioactive substance levels after long-term storage. *Regenerative Therapy*, *27*, 200-206. https://doi.org/https://doi.org/10.1016/j.reth.2024.03.021
Narayanaswamy, R., Patro, B. P., Jeyaraman, N., Gangadaran, P., Rajendran, R. L., Nallakumarasamy, A., Jeyaraman, M., Ramani, P., & Ahn, B. C. (2023). Evolution and Clinical Advances of Platelet-Rich Fibrin in Musculoskeletal Regeneration [Review]. *Bioengineering*, *10*(1), Article 58. https://doi.org/10.3390/bioengineering10010058
Ngah, N. A., Dias, G. J., Tong, D. C., Mohd Noor, S. N. F., Ratnayake, J., Cooper, P. R., & Hussaini, H. M. (2021a). Lyophilised Platelet-Rich Fibrin: Physical and Biological Characterisation. *Molecules*, *26*(23). https://doi.org/10.3390/molecules26237131
Ngah, N. A., Ratnayake, J., Cooper, P. R., Dias, G. J., Tong, D. C., Noor, S., & Hussaini, H. M. (2021b). Potential of Lyophilized Platelet Concentrates for Craniofacial Tissue Regenerative Therapies. *Molecules*, *26*(3), Article 517. https://doi.org/10.3390/molecules26030517
Ngah, N. A., Ratnayake, J., Dias, G. J., Tong, D. C., Noor, S. N. F. M., Cooper, P. R., & Hussaini, H. M. (2024). Physicochemical and biocompatibility characterisation of a 3D lyophilised platelet-rich fibrin scaffold for cleft lip and palate repair [Article]. *Journal of Applied Biomaterials and Functional Materials*, *22*. https://doi.org/10.1177/22808000241289208
Nie, J., Zhang, S., Wu, P., Liu, Y., & Su, Y. (2020a). Electrospinning with lyophilized platelet-rich fibrin has the potential to enhance the proliferation and osteogenesis of MC3T3-E1 cells. *Frontiers in Bioengineering and Biotechnology*, *8*, 595579.
Nie, J., Zhang, S. M., Wu, P., Liu, Y. G., & Su, Y. J. (2020b). Electrospinning With Lyophilized Platelet-Rich Fibrin Has the Potential to Enhance the Proliferation and Osteogenesis of MC3T3-E1 Cells. *Frontiers in Bioengineering and Biotechnology*, *8*, Article 595579. https://doi.org/10.3389/fbioe.2020.595579
Obeagu, E. I. (2025a). Iron homeostasis and health: understanding its role beyond blood health - a narrative review. *Ann Med Surg (Lond)*, *87*(6), 3362-3371. https://doi.org/10.1097/ms9.0000000000003100
Obeagu, E. I. (2025b). Platelet-derived growth factor (PDGF) and its impact in fibroid pathogenesis: A narrative review. *Medicine*, *104*(25), e42995.

https://doi.org/10.1097/md.0000000000042995
Oliveira É, R., Nie, L., Podstawczyk, D., Allahbakhsh, A., Ratnayake, J., Brasil, D. L., & Shavandi, A. (2021). Advances in Growth Factor Delivery for Bone Tissue Engineering. *Int J Mol Sci*, *22*(2). https://doi.org/10.3390/ijms22020903
Orasugh, J. T., Ghosh, S. K., & Chattopadhyay, D. (2020). Chapter 10 - Nanofiber-reinforced biocomposites. In B. Han, S. Sharma, T. A. Nguyen, L. Longbiao, & K. S. Bhat (Eds.), *Fiber-Reinforced Nanocomposites: Fundamentals and Applications* (pp. 199-233). Elsevier. https://doi.org/https://doi.org/10.1016/B978-0-12-819904-6.00010-4
Paek, S. C., Min, S. K., & Park, J. B. (2020). Effects of platelet-derived growth factor-BB on cellular morphology and cellular viability of stem cell spheroids composed of bone-marrow-derived stem cells. *Biomed Rep*, *13*(6), 59. https://doi.org/10.3892/br.2020.1366
Palanques-Pastor, T., Gallardo, C. E. A., Megías-Vericat, J. E., Bonora-Centelles, A., Merlos-Juan, A., Bonete-Lluch, D., Ruiz-Dueñas, T., García-Pellicer, J., & Poveda-Andrés, J. L. (2025). Standardization and Comparative Characterization of Platelet-Rich Plasma Preparation Systems: A Methodological Study with Clinical Applicability Assessment.
Pandey, G., Dhakal, K., Singh, A., Dhungel, S. K., & Adhikari, R. (2021). Facile methods of preparing pure hydroxyapatite nanoparticles in ordinary laboratories. *BIBECHANA*, *18*, 83-90. https://doi.org/10.3126/bibechana.v18i1.29600
Paradowska-Stolarz, A., Mikulewicz, M., & Duś-Ilnicka, I. (2022). Current concepts and challenges in the treatment of cleft lip and palate patients—A comprehensive review. *Journal of Personalized Medicine*, *12*(12), 2089.
Pardeshi, S. R., Deshmukh, N. S., Telange, D. R., Nangare, S. N., Sonar, Y. Y., Lakade, S. H., Harde, M. T., Pardeshi, C. V., Gholap, A., Deshmukh, P. K., & More, M. P. (2023). Process development and quality attributes for the freeze-drying process in pharmaceuticals, biopharmaceuticals and nanomedicine delivery: a state-of-the-art review. *Future Journal of Pharmaceutical Sciences*, *9*(1), 99. https://doi.org/10.1186/s43094-023-00551-8
Park, W. J., Han, S. H., Kim, N. J., & Park, J. B. (2024). The Efficacy of Utilizing Platelet-Rich Fibrin for Managing Periodontal Intrabony Defects in Conjunction with Graft Material: A Systematic Review and Meta-Analysis [Article]. *Applied Sciences (Switzerland)*, *14*(8), Article 3371. https://doi.org/10.3390/app14083371
Patel, H., Pundkar, A., Shrivastava, S., Chandanwale, R., & Jaiswal, A. M. (2023). A Comprehensive Review on Platelet-Rich Plasma Activation: A Key Player in Accelerating Skin Wound Healing. *Cureus*, *15*(11), e48943. https://doi.org/10.7759/cureus.48943
Piplani, C., Gosselin, A., Bargoud, C., Macor, M., Choron, R. L., Hanna, J. S., Tutwiler, V., & Goswami, J. (2025). Effect of Aging and Sex on Clot Formation, Structure, and Lysis in Trauma Patients. *J Am Coll Surg*, *241*(2), 160-169. https://doi.org/10.1097/xcs.0000000000001347
Qian, B., Yang, Q., Wang, M., Huang, S., Jiang, C., Shi, H., Long, Q., Zhou, M., Zhao, Q., & Ye, X. (2022). Encapsulation of lyophilized platelet-rich fibrin in alginate-hyaluronic acid hydrogel as a novel vascularized substitution for myocardial infarction. *Bioactive Materials*, *7*, 401-411. https://doi.org/https://doi.org/10.1016/j.bioactmat.2021.05.042
Risman, R. A., Abdelhamid, A., Weisel, J. W., Bannish, B. E., & Tutwiler, V. (2022).

Effects of clot contraction on clot degradation: A mathematical and experimental approach. *Biophys J*, *121*(17), 3271-3285. https://doi.org/10.1016/j.bpj.2022.07.023

Romero-López, M., Li, Z., Rhee, C., Maruyama, M., Pajarinen, J., O'Donnell, B., Lin, T. H., Lo, C. W., Hanlon, J., Dubowitz, R., Yao, Z., Bunnell, B. A., Lin, H., Tuan, R. S., & Goodman, S. B. (2020). Macrophage Effects on Mesenchymal Stem Cell Osteogenesis in a Three-Dimensional In Vitro Bone Model. *Tissue Eng Part A*, *26*(19-20), 1099-1111. https://doi.org/10.1089/ten.TEA.2020.0041

Roshan, S., Thomas, D., K, S., D, A., & Radhakrishnan, R. (2024). A periodontist's favourite: The platelet concentrates. *International Dental Journal of Student's Research*, *11*, 158-162. https://doi.org/10.18231/j.idjsr.2023.034

Savabi, O., Nejatidanesh, F., Sharifi, M., Shirani, M., Valanezhad, A., Watanabe, I., Beni, B. H., & Khodaei, M. (2024). Cytotoxicity of dental ceramic materials on human gingival fibroblasts. *Dent Res J (Isfahan)*, *21*, 53.

Scimeca, M., Bischetti, S., Lamsira, H. K., Bonfiglio, R., & Bonanno, E. (2018). Energy Dispersive X-ray (EDX) microanalysis: A powerful tool in biomedical research and diagnosis. *Eur J Histochem*, *62*(1), 2841. https://doi.org/10.4081/ejh.2018.2841

Serna, J., & Bergwitz, C. (2020). Importance of Dietary Phosphorus for Bone Metabolism and Healthy Aging. *Nutrients*, *12*(10), 3001. https://www.mdpi.com/2072-6643/12/10/3001

Shokouhinejad, N., Tahun, I. A., Tahan, S. S., Mohandes, F., Nekoofar, M. H., & Dummer, P. M. (2023). Microstructure and color stability of calcium silicate-based dental materials exposed to blood or platelet-rich fibrin. *Clinical Oral Investigations*, *27*(3), 1193-1206.

Sindhi, K., Pingili, R. B., Beldar, V., Bhattacharya, S., Rahaman, J., & Mukherjee, D. (2025). The role of biomaterials-based scaffolds in advancing skin tissue construct [Review]. *Journal of Tissue Viability*, *34*(2), Article 100858. https://doi.org/10.1016/j.jtv.2025.100858

Sindhusha, V. B., & Ramamurthy, J. (2023). Comparison of Antimicrobial Activity of Injectable Platelet-Rich Fibrin (i-PRF) and Leukocyte and Platelet-Rich Fibrin (l-PRF) Against Oral Microbes: An In Vitro Study. *Cureus*, *15*(9), e46196. https://doi.org/10.7759/cureus.46196

Siqueira, A. S., Braga, N. F., Muñoz, P. A. R., de Freitas, L. F., Ferreira, A. H., & Fechine, G. J. M. (2024). Biodegradable scaffold: integration of polylactic acid, hydroxyapatite, and graphene oxide via FDM 3D printing [Article]. *Express Polymer Letters*, *18*(6), 656-672. https://doi.org/10.3144/expresspolymlett.2024.48

Srirangarajan, S., Sindhu, V., Prabhu, S., Rao, R. J., & Rudresh, V. (2021). Does Cigarette Smoking Induce Changes in Biologic and Mechanical Properties of Platelet-Rich Fibrin Membranes? *Int J Periodontics Restorative Dent*, *41*(6), e213-e221. https://doi.org/10.11607/prd.4573

Stamnitz, S., & Klimczak, A. (2021). Mesenchymal Stem Cells, Bioactive Factors, and Scaffolds in Bone Repair: From Research Perspectives to Clinical Practice. *Cells*, *10*(8). https://doi.org/10.3390/cells10081925

Stanbouly, D., Lee, K. C., & Chuang, S.-K. (2022). A narrative review of craniofacial deformities. *Frontiers of Oral and Maxillofacial Medicine*, *6*. https://fomm.amegroups.org/article/view/69149

Stone, W. L., Leavitt, L., & Varacallo, M. (2024). Physiology, Growth Factor. In *StatPearls*. StatPearls Publishing

Copyright © 2024, StatPearls Publishing LLC.
Sui, X., Zhang, H., Yao, J., Yang, L., Zhang, X., Li, L., Wang, J., Li, M., & Liu, Z. (2023a). 3D printing of 'green' thermo-sensitive chitosan-hydroxyapatite bone scaffold based on lyophilized platelet-rich fibrin [Article]. *Biomedical Materials (Bristol)*, *18*(2), Article 025022. https://doi.org/10.1088/1748-605X/acbad5

Sui, X., Zhang, H., Yao, J., Yang, L., Zhang, X., Li, L., Wang, J., Li, M., & Liu, Z. (2023b). 3D printing of 'green' thermo-sensitive chitosan-hydroxyapatite bone scaffold based on lyophilized platelet-rich fibrin. *Biomedical Materials*, *18*(2), 025022. https://doi.org/10.1088/1748-605X/acbad5

Sun, J., Han, L., Liu, C., Ma, J., Li, X., Sun, S., & Wang, Z. (2023a). Effect of autologous lyophilized platelet rich fibrin on the reconstruction of osteochondral defects in rabbits. *Experimental and Therapeutic Medicine*, *26*(6), 1-11.

Sun, J., Jiang, X., Luo, J., Zhao, L., Xu, Z., & Xiao, W. (2020). Effect of platelet-derived growth factor (PDGF-BB) and bone morphogenic protein 2 (BMP-2) transfection of rBMSCs compounded with platelet-rich plasma on adipogenic differentiation. *Braz J Med Biol Res*, *54*(2), e9944. https://doi.org/10.1590/1414-431x20209944

Sun, J., Li, G., Wu, S., Zou, Y., Weng, W., Gai, T., Chen, X., Zhang, K., Zhou, F., Wang, X., & Su, J. (2023b). Engineering preparation and sustained delivery of bone functional exosomes-laden biodegradable hydrogel for in situ bone regeneration [Article]. *Composites Part B: Engineering*, *261*, Article 110803. https://doi.org/10.1016/j.compositesb.2023.110803

Sun, S. H., Fan, H. H., Wang, X. W., Bing, B. D., & Hu, Y. J. (2025). Platelet-rich fibrin attenuates inflammation and fibrosis in vulvar lichen sclerosus via the TGF-β/SMAD3 pathway [Article]. *Archives of Dermatological Research*, *317*(1), Article 360. https://doi.org/10.1007/s00403-025-03811-0

Sun., Han, L., Liu, C. D., Ma, J. L., Li, X., Sun, S. H., & Wang, Z. F. (2023). Effect of autologous lyophilized platelet-rich fibrin on the reconstruction of osteochondral defects in rabbits. *Experimental and Therapeutic Medicine*, *26*(6), Article 569. https://doi.org/10.3892/etm.2023.12268

Tonk, G., Yadav, P. K., Agarwal, S., & Jamoh, K. (2022). Donor site morbidity in autologous bone grafting—a comparison between different techniques of anterior iliac crest bone harvesting: a prospective study. *Journal of Orthopaedics, Trauma and Rehabilitation*, *29*(1), 22104917221092163.

Usoltsev, D., Sitnikova, V., Kajava, A., & Uspenskaya, M. (2019). Systematic FTIR Spectroscopy Study of the Secondary Structure Changes in Human Serum Albumin under Various Denaturation Conditions. *Biomolecules*, *9*(8). https://doi.org/10.3390/biom9080359

Vahabi, S., Yadegary, Z., & Karamshahi, M. (2019). Evaluating the adhesion of human gingival fibroblasts and MG-63 osteoblast-like cells to activated PRP-coated membranes [Article]. *Cell and Tissue Banking*, *20*(3), 339-349. https://doi.org/10.1007/s10561-019-09772-9

Vijayan, S., Merlin, T., & Jisha, M. (2023). Biocompatibility and cytotoxicity of polymer sutures. In *Advanced Technologies and Polymer Materials for Surgical Sutures* (pp. 249-264). Elsevier.

Vuletić, M., Knežević, P., Jokić, D., Rebić, J., Žabarović, D., & Macan, D. (2014). Alveolar Bone Grafting in Cleft Patients from Bone Defect to Dental Implants. *Acta Stomatol Croat*, *48*(4), 250-257. https://doi.org/10.15644/asc47/4/2

Vyas, J., Shah, I., Singh, S., & Prajapati, B. G. (2023). Biomaterials-based additive

manufacturing for customized bioengineering in management of otolaryngology: a comprehensive review [Review]. *Frontiers in Bioengineering and Biotechnology*, *11*, Article 1234340. https://doi.org/10.3389/fbioe.2023.1234340

Vyas, T., Gupta, P., Kumar, S., Gupta, R., Gupta, T., & Singh, H. P. (2020). Cleft of lip and palate: A review. *J Family Med Prim Care*, *9*(6), 2621-2625. https://doi.org/10.4103/jfmpc.jfmpc_472_20

Wang, X., Gong, W., Li, R., Li, L., & Wang, J. (2024). Preparation of genetically or chemically engineered exosomes and their therapeutic effects in bone regeneration and anti-inflammation [Review]. *Frontiers in Bioengineering and Biotechnology*, *12*, Article 1329388. https://doi.org/10.3389/fbioe.2024.1329388

Wang, Z., Han, L., Sun, T., Wang, W., Li, X., & Wu, B. (2019a). Preparation and effect of lyophilized platelet-rich fibrin on the osteogenic potential of bone marrow mesenchymal stem cells in vitro and in vivo. *Heliyon*, *5*(10).

Wang, Z., Wang, Z., Lu, W. W., Zhen, W., Yang, D., & Peng, S. (2017). Novel biomaterial strategies for controlled growth factor delivery for biomedical applications. *NPG Asia Materials*, *9*(10), e435-e435. https://doi.org/10.1038/am.2017.171

Wang, Z. F., Han, L., Sun, T. Y., Wang, W. J., Li, X., & Wu, B. L. (2019b). Preparation and effect of lyophilized platelet-rich fibrin on the osteogenic potential of bone marrow mesenchymal stem cells in vitro and in vivo. *Heliyon*, *5*(10), Article e02739. https://doi.org/10.1016/j.heliyon.2019.e02739

Warin, R., Vongchan, P., Suriyasathaporn, W., Boripun, R., & Suriyasathaporn, W. (2022). In vitro assessment of lyophilized advanced platelet-rich fibrin from dogs in promotion of growth factor release and wound healing. *Veterinary Sciences*, *9*(10), 566.

Warin, R., Vongchan, P., Suriyasathaporn, W., Hall, D. C., Boripun, R., & Suriyasathaporn, W. (2023). In Vitro Antimicrobial Properties and Their Mechanisms in Relation to Reactive Oxygen Species of Canine Platelet-Rich Fibrin [Article]. *Animals*, *13*(24), Article 3786. https://doi.org/10.3390/ani13243786

Wijayanti, D. A., Wirajaya, G. N. K. A., Pratiwi, N. H., Karina, V. M., & Murdiastuti, K. (2025). Combination of Collagen-Chitosan Hydrogel and Injectable Platelet-Rich Fibrin as a Biomaterial for Bone Regeneration: Characterization and Growth Factor Release Pattern. *European Journal of Dentistry*.

Wong, C.-C., Chen, C.-H., Chan, W. P., Chiu, L.-H., Ho, W.-P., Hsieh, F.-J., Chen, Y.-T., & Yang, T.-L. (2017). Single-stage cartilage repair using platelet-rich fibrin scaffolds with autologous cartilaginous grafts. *The American journal of sports medicine*, *45*(13), 3128-3142.

Wong, P.-C., Wang, C.-Y., Jang, J. S.-C., Lee, C.-H., & Wu, J.-L. (2021a). Large-pore platelet-rich fibrin with a mg ring to allow mc3t3-e1 preosteoblast migration and to improve osteogenic ability for bone defect repair. *International Journal of Molecular Sciences*, *22*(8), 4022.

Wong, P. C., Wang, C. Y., Jang, J. S. C., Lee, C. H., & Wu, J. L. (2021b). Large-Pore Platelet-Rich Fibrin with a Mg Ring to Allow MC3T3-E1 Preosteoblast Migration and to Improve Osteogenic Ability for Bone Defect Repair. *International Journal of Molecular Sciences*, *22*(8), Article 4022. https://doi.org/10.3390/ijms22084022

Wong, S. K., Yee, M. M. F., Chin, K. Y., & Ima-Nirwana, S. (2023). A Review of the

Application of Natural and Synthetic Scaffolds in Bone Regeneration. *J Funct Biomater*, *14*(5). https://doi.org/10.3390/jfb14050286

Wu, S., Guo, W., Li, R., Zhang, X., & Qu, W. (2022). Progress of platelet derivatives for cartilage tissue engineering. *Frontiers in Bioengineering and Biotechnology*, *10*, 907356.

Xie, H., Xie, Y. F., Liu, Q., Shang, L. Y., & Chen, M. Z. (2019). Bone regeneration effect of injectable-platelet rich fibrin (I-PRF) in lateral sinus lift: a pilot study [Article]. *Shanghai Kou Qiang Yi Xue / Shanghai Journal of Stomatology*, *28*(1), 71-75. https://doi.org/10.19439/j.sjos.2019.01.014

Xu, F., Zou, D., Dai, T., Xu, H., An, R., Liu, Y., & Liu, B. (2018a). Effects of incorporation of granule-lyophilised platelet-rich fibrin into polyvinyl alcohol hydrogel on wound healing. *Scientific Reports*, *8*(1), 14042. https://doi.org/10.1038/s41598-018-32208-5

Xu, X., Zheng, L., Yuan, Q., Zhen, G., Crane, J. L., Zhou, X., & Cao, X. (2018b). Transforming growth factor-β in stem cells and tissue homeostasis. *Bone Res*, *6*, 2. https://doi.org/10.1038/s41413-017-0005-4

Yajamanya, S. R., Chatterjee, A., Babu, C. N., & Karunanithi, D. (2016). Fibrin network pattern changes of platelet-rich fibrin in young versus old age group of individuals: A cell block cytology study. *Journal of Indian Society of Periodontology*, *20*(2), 151-156. https://doi.org/10.4103/0972-124x.176390

Zapata-Sifuentes, M., Quispe-Salcedo, A., Watanabe, T., Kawase, T., & Ohshima, H. (2024). Effect of leukocyte and platelet-rich plasma on osseointegration after implant placement in mouse maxilla. *Regen Ther*, *26*, 741-748. https://doi.org/10.1016/j.reth.2024.08.019

Zhang, J.-Y., Xiang, X.-N., Yu, X., Liu, Y., Jiang, H.-Y., Peng, J.-L., He, C.-Q., & He, H.-C. (2024). Mechanisms and applications of the regenerative capacity of platelets-based therapy in knee osteoarthritis. *Biomedicine & Pharmacotherapy*, *178*, 117226. https://doi.org/https://doi.org/10.1016/j.biopha.2024.117226

Zhang, M., Yu, W., Niibe, K., Zhang, W., Egusa, H., Tang, T., & Jiang, X. (2018). The Effects of Platelet-Derived Growth Factor-BB on Bone Marrow Stromal Cell-Mediated Vascularized Bone Regeneration. *Stem Cells Int*, *2018*, 3272098. https://doi.org/10.1155/2018/3272098

Zhang, Y., Wang, Z.-L., Deng, Z.-P., Wang, Z.-L., Song, F., & Zhu, L.-L. (2022). Emerging Delivery Strategies of Platelet Rich Plasma with Hydrogels for Wound Healing. *Advances in Polymer Technology*, *2022*(1), 5446291.

Zhao, J., Zhou, C., Xiao, Y., Zhang, K., Zhang, Q., Xia, L., Jiang, B., Jiang, C., Ming, W., Zhang, H., Long, H., & Liang, W. (2024). Oxygen generating biomaterials at the forefront of regenerative medicine: advances in bone regeneration. *Front Bioeng Biotechnol*, *12*, 1292171. https://doi.org/10.3389/fbioe.2024.1292171

APPENDICES

APPENDIX 1

PHYSICOCHEMICAL AND BIOLOGICAL PROPERTIES OF LYOPHILISED PLATELET-RICH FIBRIN: A SCOPING REVIEW

H) Check t<x updates

TISSUE ENGINEERING: Part B
Volume 00, Number 00, 2025
© Mary Ann Liebert, (NY) LLC.
DOI: 10.1177/19373368251397947

©termis
Tissue Engineering
& Regenerative Medicine
International Society

REVIEW ARTICLE

Physicochemical and Biological Properties of Lyophilized Platelet-Rich Fibrin: A Scoping Review

Wan Nur Irdina Rusman, BSc,[1] Siti Noor Fazliah Mohd Noor, BDS, MClindent, PhD,[2] Tin Wui Wong, BSc, PhD,[3,4] and Nurul Aida Ngah, DDS, MClinDent, PhD[1]

Multiple studies have been conducted recendy to fabricate lyophilized platelet-rich fibrin (LyPRF) as a biological agent. These analyses have also encompassed the integration of LyPRF into various biomaterials for the objective of bone tissue engineering (BTE). However, a definitive manufacturing procedure has not yet been established, and precise data regarding the characterization of LyPRF are still lacking. This systematic literature review aimed to compile existing evidence on the physicochemical and biological properties of this biomaterial as a scaffold for BTE. A comprehensive literature search was performed in SCOPUS, ScienceDirect, PubMed, and Web of Science to identify eligible articles published related to the various *in vitro* analyses conducted on the biomaterial for its characterization. The inclusion criteria allowed us to concentrate on papers published in English between 2019 and 2025. The study excluded review papers, meta-analyses, editorials, conference pieces, theses, methodological articles, and research that conducted clinical trials or exclusively *in vivo* analyses. This classification also includes literature with no open access. The preliminary database search produced 3,047 publications, of which only 15 were selected following the application of inclusion and exclusion criteria. LyPRF is beneficial to lengthen the shelf life of the product and can be incorporated into other biomaterials to improve compatibility and reduce degradation time. Therefore, based on the compiled analysis of the included studies, it is found that the surface morphology of LyPRF is irregular, porous, densely populated with fibrin network, and exhibits a uniform aggregation of cells. Furthermore, it is shown that LyPRF demonstrates elements that are analogous to craniofacial bone properties, thereby enhancing its utility in BTE. Additionally, the lyophilization process preserves growth factors present in LyPRF, leading to its consistent and gradual release, increasing the cell proliferation potential of this biomaterial. Existing evidence indicates that LyPRF is a promising candidate for BTE. Future research should prioritize comparative evaluations of fabrication protocols and rigorous biocompatibility testing to establish its suitability as a biomaterial for bioscaffold production in BTE.

Keywords: lyophilized platelet-rich fibrin, tissue engineering, bioscaffold, tissue regeneration, hard tissue

Impact Statement

This systematic review highlights current evidence on the physicochemical and biological properties of lyophilized platelet-rich fibrin (LyPRF), emphasizing its potential as a bioactive scaffold for bone tissue engineering. This study addresses a critical gap in the LyPRF fabrication protocol by demonstrating structural similarity to craniofacial bone, sustained growth factor release, and compatibility with other biomaterials, thereby underscoring its potential for clinical translation in regenerative medicine.

Introduction

Bone is a dynamic and highly vascularized living tissue composed of a complex matrix of collagen fibers and mineral deposits, primarily hydroxyapatites. Defects on the structure and function of bones, specifically craniofacial such as congenital anomalies, trauma, oncological surgery, degenerative conditions, infections, tumor excision, or accidents, can lead to various craniofacial abnormalities.[1] Therefore, to treat bone deformities, a variety of clinical

'Faculty of Dentistry, Universiti Teknologi MARA (UiTM), Selangor Branch, Sungai Buloh, Malaysia.
Craniofacial and Biomaterials Group, Oral Cancer Research Program, Advanced Medical and Dental Institute, Universiti Sains Malaysia, Pulau Pinang, Malaysia.
[3]Non-Destructive Biomedical and Pharmaceutical Research Centre, Smart Manufacturing Research Institute, Universiti Teknologi MARA, Puncak Alam Campus, Selangor, Malaysia.
[4]Faculty of Pharmacy, UiTM Puncak Alam Campus, Selangor, Malaysia.

APPENDIX 2

STANDARDIZING LYOPHILIZED PLATELET-RICH FIBRIN PROTOCOLS FOR BONE TISSUE ENGINEERING: A SYSTEMATIC REVIEW

STANDARDIZING LYOPHILIZED PLATELET-RICH FD3RIN PROTOCOLS FOR BONE TISSUE ENGINEERING: A SYSTEMATIC REVIEW

Wan Nur Irdina Rusman ', Siti Noor Fazliah Mohd Noor [2], Nurul Aida Ngah '

1. Faculty of Dentistry, Universiti Teknologi MARA (UiTM), Sungai Buloh Campus, Selangor, Malaysia
2. Craniofacial and Biomaterials Group, Advanced Medical and Dental Institute, Universiti Sains Malaysia, Kepala Batas, Pulau Pinang, Malaysia

Abstract

Background: The application of lyophilized platelet-rich fibrin (LyPRF) as a bioactive material in bone tissue engineering (BTE) particularly for craniofacial regeneration, has gained increasing interest in recent years. While multiple studies have demonstrated the integration of LyPRF into scaffolds for BTE applications, the lack of a standardized fabrication protocol remains a significant hurdle. **Objectives:** This systematic review aimed to identify and compile the current evidence regarding the fabrication protocol for LyPRF, intended as a potential growth factor reservoir and bioscaffold for bone regeneration. **Methods:** A comprehensive literature search was conducted across SCOPUS, ScienceDirect, PubMed, and Web of Science databases for eligible articles published related to LyPRF fabrication protocol published between 2019 and 2025 following PRISMA 2020 Guidelines. **Results:** Fifteen (15) articles were found eligible and included from the 3047 initial records identified and assessed. The review revealed that LyPRF offers better clinical shelf-life and can be combined with other biomaterials to enhance scaffold compatibility and bone regeneration properties. An optimal fabrication protocol involved centrifugation at 3,000 rpm for 10 minutes followed by lyophilization at -80°C for 24 hours. **Conclusion:** The aforementioned results identified the most effective methodology for fabricating LyPRF that preserved its physicochemical, biological, and biocompatible properties as a promising biomaterial for BTE.

Keywords: Platelet-rich Fibrin, Tissue Engineering, Bioscaffold, Tissue Regeneration

APPENDIX 3

The 6th International Invention & Innovation in Dentistry Exhibition (IIIDentEx) 2024

CERTIFICATE

Of Attendance

4 CPD POINTS

This Certificate is Presented To

Wan Nur Irdina Rusman

For attending

The 6th International Invention & Innovation in Dentistry Exhibition 2024
held at Noble Resort Hotel, Melaka
On 19th October 2024

Professor Dr. Aida Nur Ashikin Abd Rahman
DEAN
FACULTY OF DENTISTRY
UNIVERSITITEKNOLOGI MARA

2£ k,2 JICD

APPENDIX 4

26th Annual General Meeting of IADR Malaysian Section

#*IADR INTERNATIONAL ASSOCIATION FOR DENTAL, ORAL, AND CRANIOFACIAL RESEARCH MALAVSIAN SECTION

CERTIFICATE

OF APPRECIATION

This certificate is proudly presented to

MS. WAN NUR IRDINA RUSMAN

In recognition of your participation as presenter in the 23rd Annual Scientific Meeting and 26th Annual General Meeting of the **IADR** Malaysian Section, held on 6 September 2025 at The Everly Hotel Putrajaya.

Prof Dr Nctpf *ApHi* **Yahya**
President (2024-2026)
IADR Malaysian Section

APPENDIX 5

EuroPerioll Vienna 2025

EFP **EuroPerio**
MAY 14-1712025
VIENNA

MAY 14-1712025
VIENNA

Certificate of Attendance

EuroPerioll

from May 14-17, 2025

Vienna, Austria

EuroPeriol 1 is eligible for a maximum of 25.75 hours of continuing education.

Wan Nur Irdina Rusman

has attended a total of 25.75 hours of continuing education

hours within scientific sessions: 19.75

within sponsor sessions: 6

Lior Shapira	**Anton Sculean**	**Elena Figuero**
EP11 Scientific Chair	EP11 Congress Chair	EP11 Treasurer

EFP European coordinator: Monica Guinea - Cink Coworking - EFP office n'17, Calle Henri Dunant 15-17. 28036 Madrid. Spain E-mail monica(5?efp ora

Congress Management Office Mondial Congress & Events. Operngasse 20b 1040 Vienna. Austria
E-mail europerio<5>mondial-congress com

APPENDIX 6

Certificate of copyright

COPYRIGHT ACT 1987

COPYRIGHT (VOLUNTARY NOTIFICATION) REGULATIONS 2012

CERTIFICATE OF COPYRIGHT NOTIFICATION
[Subregulation 8(2)]

Notification Number	**CRLY2025W09911**
Title of Work	**PHYSICOCHEMICAL AND BIOCOMPATIBILITY CHARACTERISATION OF LYOPHILISED PLATELET-RICH FIBRIN FOR CRANIOFACIAL REGENERATION**
Category of Work	**LITERARY**
Date of Notification	**08 OCTOBER 2025**
Date of Creation	**10 DECEMBER 2024**

This is **to** certify, under the Copyright Act 1987 [Act 332] and the Copyright (Voluntary Notification) Regulations 2012 that the copyrighted work bearing the Notification No. above for the applicant **NURUL AIDA BINTI NGAH (800406115306), WAN NUR IRDINA BINTI RUSMAN (010405030240), SITI NOOR FAZLIAH BINTI MOHD NOOR (730102015014) as** the **OWNER** and **NURUL AIDA BINTI NGAH (800406115306), WAN NUR IRDINA BINTI RUSMAN (010405030240), SITI NOOR FAZLIAH BINTI MOHD NOOR (730102015014) as** the **AUTHOR** have been recorded in the Register of Copyright, in accordance with section 26B of the Copyright Act 1987 [Act 332].

YUSNIEZA SYARMILA BINTI YUSOFF
CONTROLLER OF COPYRIGHT
MALAYSIA

(Agency under the Ministry of Domestic Trade and Cost of Living)

AUTHOR'S PROFILE

Wan Nur Irdina Binti Rusman obtained her Bachelor of Science (Hons.) in Bio-Molecular Science from Universiti Teknologi MARA (UiTM), Shah Alam, in 2023. She is currently pursuing a Master of Dental Science at Universiti Teknologi MARA (UiTM), Sungai Buloh. Her research interests lie in bone tissue engineering, regenerative medicine, and platelet concentrate-based biomaterials, with particular emphasis on the development of lyophilised platelet-rich fibrin for craniofacial bone regeneration.

She has published a review article entitled "Physicochemical and Biological Properties of Lyophilised Platelet-Rich Fibrin: A Scoping Review" in *Tissue Engineering: Part B* and has submitted another manuscript entitled "Standardizing Lyophilized Platelet-Rich Fibrin Protocols for Bone Tissue Engineering: A Systematic Review" to *Sains Malaysiana*.

She has presented her research at the 6th International Invention & Innovation in Dentistry Exhibition (IIIDentEx) 2024, the 26th Annual General Meeting of IADR Malaysian Section, and EuroPerio11 Vienna 2025. In recognition of her research contributions, she obtained copyright registration for her work entitled "Physicochemical and Biocompatibility Characterisation of Lyophilised Platelet-Rich Fibrin for Craniofacial Regeneration."

Her broader academic interests include bioengineering, biotechnology, and biomolecular sciences. She aspires to further her academic career by pursuing a Doctor of Philosophy (Dentistry) and contributing to translational research in regenerative biomaterials.

LIST OF PUBLICATION:

Rusman WNI, Mohd Noor SNF, Wong TW, Ngah NA. Physicochemical and Biological Properties of Lyophilized Platelet-Rich Fibrin: A Scoping Review. Tissue Engineering Part B: Reviews. 2025;0(0). doi:10.1177/19373368251397947

No	Title	Hardcopy	Softcopy
1	PHYSICOCHEMICAL AND BIOCOMPATIBILITY CHARACTERISATION OF LYOPHILISED PLATELET-RICH FIBRIN FOR BONE TISSUE ENGINEERING		/